AMRL-TR-65-156

AD624996

STUDY AND DEVELOPMENT OF MATERIALS AND TECHNIQUES FOR PASSIVE THERMAL CONTROL OF FLEXIBLE EXTRAVEHICULAR SPACE GARMENTS

DAVID L. RICHARDSON

ARTHUR D. LITTLE, INC.

SEPTEMBER 1965

AEROSPACE MEDICAL RESEARCH LABORATORIES
AEROSPACE MEDICAL DIVISION
AIR FORCE SYSTEMS COMMAND
WRIGHT-PATTERSON AIR FORCE BASE, OHIO

STUDY AND DEVELOPMENT OF MA[illegible] AND TECHNIQUES FOR PASSIVE THERMAL CONTROL OF FLEXIBLE EXTRAVEHICULAR SPACE GARMENTS

DAVID L. RICHARDSON

PAGES ______

ARE

MISSING

IN

ORIGINAL

DOCUMENT

FOREWORD

This final report was prepared by Arthur D. Little, Inc., Cambridge, Massachusetts, under Contract No. AF 33(615)-1904, and covers the period from July 1964 through June 1965. The work was performed under the direction of the Aerospace Medical Research Laboratories, in support of Project 6373, "Equipment for Life Support in Aerospace," Task 637302, "Respiratory Support Equipment," with Mr. D. A. Keating as project director, and Mr. K. R. Cramer, of the Aerospace Research Laboratories, Office of Aerospace Research, as project advisor.

The author acknowledges the assistance of Mr. J. A. Ruseckas, Mr. F. DiStefano, and Mr. R. Sears of the David Clark Co. for assistance in providing sections of the thermal control space suit; and Mr. C. Mook of National Aeronautics and Space Administration, Washington, D.C., Mr. D. Gates of National Aeronautics and Space Administration, Marshall Space Flight Center, Mr. G. A. Zerlaut of IIT Research Institute, and Dr. N. Searle of American Cyanamid for assistance with low absorptance coatings.

The author acknowledges the assistance of Arthur D. Little, Inc., personnel: Dr. P. E. Glaser for technical guidance of the project; Mr. F. Gabron and R. Buckles for the thermal analysis; Dr. I. Simon and Dr. E. Stone for the space hazards; T. R. A. Davis, M.D., for physiological considerations; Dr. A. E. Wechsler for over-all review of the project; and Mr. E. J. Boudreau, Mr. R. Carroll and Mr. J. Cleary for the experimental work performed.

The guidance of Mr. D. A. Keating and Mr. K. R. Cramer in this study is gratefully acknowledged.

This technical report has been reviewed and is approved.

WAYNE H. McCANDLESS
Technical Director
Biomedical Laboratory
Aerospace Medical Research Laboratories

ABSTRACT

This program encompassed an analytical and experimental investigation of the application of passive thermal control techniques to extravehicular flexible space garments in 300 nautical mile earth orbits. Results indicate that passive thermal control by varying the absorptance and emittance of the outer surface of the garment is not possible when internal heat generated is in excess of 1500 Btu/hr. For all conditions, the suit's solar absorptance should be as small as possible and its emittance as large as possible. By controlling the conductance of the space suit wall, internal heating rates to 2000 Btu/hr are achievable when the space suit has an absorptance of 0.17 and an emittance of 0.85. A solar parasol with selected radiating properties on each side allows for higher internal heating rates. Experiments were made in a simulated noon orbit with a cylindrical section of a space suit which was first tested with an evacuated insulation and then with a helium-fillable insulation. The range of average conductance for these insulations was 0.3 to 4.0 Btu/sq ft hr ^{o}F. A range of internal heat generation from 600 to 2100 Btu/hr was achieved when the evacuated insulation was filled with helium.

TABLE OF CONTENTS

TABLE OF CONTENTS (cont'd)

LIST OF FIGURES

LIST OF FIGURES (cont'd)

LIST OF TABLES

LIST OF SYMBOLS

Symbol	Definition
A	area, ft^2
C	conductance, $Btu/ft^2\ hr\ ^oF$
D	diameter, ft
F	radiant exchange view factor
L	length, ft
Q	heat generated in the space suit, Btu/hr
T	temperature, ^oR
k	thermal conductivity, $Btu\ in/ft^2\ hr\ ^oF$
n	number of spaces between radiating surfaces in an insulation
p	pressure, psi
q	heat flux per unit area, $Btu/ft^2\ hr$
q_a	earth-reflected solar radiation (albedo), $Btu/ft^2\ hr$
q_e	earth thermal radiation (earthshine), $Btu/ft^2\ hr$
q_s	solar radiant flux, $Btu/ft^2\ hr$
t	temperature, ^oF
w	water flow rate, lbs/hr
α	absorptance
δ	insulation thickness, in
ϵ	emittance
γ	angle between axis of cylinder or normal to a flat plate and the earth-astronaut line, degrees
θ_s	angle between earth-astronaut line and earth-sun line
ϕ_c	angle of rotation of the cylinder axis or normal to a flat plate about the earth-astronaut line

<u>Subscripts</u>

a	albedo
e	earth, earthshine
i	inner wall
o	astronaut, outer surface
p	parasol
s	sun, solar
1	parasol side facing the sun
2	parasol side facing the astronaut

SECTION I
INTRODUCTION

With the advent of a manned orbiting laboratory program, the development of flexible garments for space operations has taken on new importance in light of the prospective increases in extravehicular mission duration.

The design of full-pressure space suits with built-in comfort conditioning capabilities is already to the point where prototype models are being tested under simulated space conditions. Although the protection afforded by such suits permits work to be done independent of the external environment, the work effectiveness of the astronaut is directly related to the performance of the temperature control system. Present garments are designed as a kind of flexible anthropoform thermos bottle, from which all the heat generated internally by man and his equipment is extracted by a pure gas or a liquid-gas heat transport system to a heat exchanger and finally ejected into space by evaporation of an expendable coolant. This cooling system requires a rather complex heat transport mechanism and the complete dependence on the expendable coolant may become restrictive with increasing mission durations. Such systems must not only produce the proper temperatures within the suit, but they must also be extremely reliable and of minimum complexity. Ideally, the suit should enable the astronaut to carry out his mission without the use of time-limited power sources or materials which restrict duration of a mission.

From the experience already obtained in temperature control in spacecraft, it appears feasible to provide for the interchange of heat between the astronaut and his surroundings by means of passive temperature controls which might either eliminate or supplement cooling systems. It has been shown theoretically that a thermal balance between the astronaut and his surroundings can be achieved through the use of correctly chosen surface emissivity-absorptivity and insulation characteristics which permit a steady-state condition to be approached while maintaining a habitable thermal environment within the protective extravehicular garment. Such techniques have been successfully applied for the temperature control of spacecraft and satellites, and there are now available extensive studies, computer programs, and a vast amount of practical experience in radiant heat control by judicious choice of spectrally selective surface coatings and variable thermal insulation.

The chief problem in achieving thermal balance of an astronaut in his extravehicular garment is the severe changes in temperature which may occur due to an increase in his metabolic rate or in variations in the radiant heat input to the space suit, depending upon the astronaut's position relative to the external radiant heat sources (the sun and the earth) and to his space vehicle. This problem is aggravated by critical heat short circuits such as helmet, foot wear, gloves, seams, and zippers; these will increase the thermal control requirements because the heat flow through them may be greater than that through the insulated portions of the flexible garment.

The purpose of this investigation was to provide the necessary research and development for techniques and materials which provide passive thermal control for various portions or all portions of flexible extravehicular space garments. Thermal control techniques which have been successfully applied for temperature control of spacecraft and satellites were analyzed to determine if they are applicable to maintaining a thermal balance between the astronaut and his surroundings.

This investigation was carried out in two phases:

A. PHASE I

In Phase I, we analyzed the problem of maintaining an astronaut in 300 nautical mile earth orbits from the point of view of his thermal environment. Two orbits were considered: the twilight orbit and the noon orbit. Heat generated by the astronaut and by various subsystems ranged from 1000 to 2500 Btu/hr. Techniques considered for controlling the temperature in the space suit were (1) variation of surface absorptance and emittance, (2) variation of suit insulation conductance, (3) time dependent heat storage, and (4) directional radiation shielding. For each technique we established the metabolic and subsystem heat inputs beyond which the astronaut's comfort limit is exceeded.

Materials with inherent variable thermal characteristics were selected and screening tests were performed to determine the range of possible thermal control. Screening tests consisted of:

1. Measurement of apparent thermal conductivity of variable conductance space suit insulation schemes.

2. Measurement of room temperature emittance of insulation components and space suit exterior thermal control surfaces and coatings.

3. Determination of solar absorptance characteristics of space suit exterior thermal control surfaces and coatings.

A helium-fillable insulation and a suit with an exterior thermal control surface of low absorptance and high emittance was selected as the most practical combination for providing thermal control of the astronaut's environment. Alternately evacuating and filling the insulation with helium provides a wide range of insulation conductance.

B. PHASE II

In Phase II, a cylindrical model of an astronaut's space suit with an evacuated insulation and then with a helium-fillable insulation was tested in a simulated 300 nautical mile noon orbit. Equilibrium environment temperatures were determined for a range of metabolic and subsystem heat inputs. Azimuthal temperature distributions on the suit inner and outer walls were determined for selected orbit conditions and metabolic and subsystem heat inputs. Orbit conditions simulated were in the earth umbra and on the earth-sun line.

The model was tested in an Arthur D. Little, Inc., space simulation chamber. Included in the chamber are a solar simulator and an earthshine-albedo simulation panel. With the space suit section, this chamber is capable of providing a vacuum of less than 10^{-4} torr, space background temperature of 140°R, simulated solar heating rate of one solar constant in a 10 in. diameter beam, earthshine, and simulated albedo.

SECTION II
CONCLUSIONS

As a result of the analytical and experimental phases of this program, we have formulated the following conclusions about thermal control for flexible space garments:

1. For passive thermal control to be possible, α_o/ϵ_o must be as small as possible and ϵ_o as large as possible. Thermal control by variation of the α_o/ϵ_o of the space suit external surface is not effective unless α_o/ϵ_o can be varied in the range from 0.01 to 1.0 while ϵ_o remains constant at greater than 0.8.

2. Passive thermal control can be maintained by variable conductance techniques. Suit conductance should be as high as possible for periods of high metabolic rate and then be decreased by a factor of about 50 for periods of low metabolic rate.

3. Azimuthal heat distribution on the inside wall of the space suit is helpful in maintaining comfortable interior temperature distributions. It also allows transfer of heat in areas where the external surface of the suit faces space.

4. Space chamber tests with a section of a space suit is an effective means for measuring suit performance. A five-fold increase in metabolic rate was achieved for a space suit section in the earth umbra when evacuated insulation was filled with helium and a three-fold increase in metabolic rate was achieved for the space suit section on the earth-sun line when evacuated insulation was filled with helium.

It is to be noted that the conclusions drawn from work on this program are applicable not only to flexible space garments but are generally applicable to both hard space suits and manned space vehicles.

SECTION III
RECOMMENDATIONS

A continuing effort in studies of thermal control for extravehicular space garments should include:

1. Expansion of the scope to include hard suits and total encapsulation.

2. Analysis of thermal control techniques applicable to rigid surfaces but not readily applicable to flexible surfaces.

3. Analysis of the three-body thermal equilibrium problem which arises when an extravehicular astronaut remains in proximity to his space vehicle.

4. Development of techniques for controlling the insulation conductance by increasing or decreasing mechanical loading on the insulation.

SECTION IV
ANALYSIS

A. DEFINITION OF ORBIT RADIANT ENVIRONMENT

In the analysis of space suit performance, a 300 nautical mile earth orbit was assumed. Two orbits were selected which would provide the limits of the radiant heat input environment for the astronaut. In the noon orbit, the astronaut travels in a plane which includes the earth-sun vector. The astronaut therefore alternately is in the sun and in the shade of the earth. For a 300 nautical mile orbit, the period of orbit is approximately 88 minutes. In the twilight earth orbit, the astronaut travels in a plane which is normal to the earth-sun vector and therefore one side of the astronaut is always in the sun. One side of the astronaut which is normal to the earth-sun line is exposed to reflected sunlight (albedo) and long wavelength radiant energy from the earth (earthshine) and the opposite side faces space. Figure 1 shows the orientation of the astronaut with respect to the earth and the radiant input conditions for the two orbit conditions. Summarized in table I are the magnitudes of the radiant thermal energy incident on the astronaut. For the actual heat absorbed by the astronaut's space suit, account must be taken of the angular view factors (astronaut-to-earth and astronaut-to-sun) and the spectral properties, absorptance (α) and emittance (ϵ), of the astronaut's external surface.

Radiant energy from the sun has a spectral distribution in the range of approximately 0.2 to 3.5 microns with a peak intensity at 0.5 micron and can be approximated by a 5800°K black-body source. The radiant energy from earth-reflected solar energy (albedo) has the same spectral distribution as solar energy but with reduced intensity corresponding to an average earth reflectance of 0.4. The earth radiation spectral range extends from 5 to 50 microns with peak radiation at a wavelength of 12 microns and is represented by a 240°K black-body source.

B. THERMAL ENVIRONMENT OF THE ASTRONAUT

The astronaut was assumed to have a cylindrical shape with an external area of 25.5 sq ft and a length-to-diameter ratio of 5.5. The external area of the 50th percentile man is approximately 21 sq ft.

From physical measurements of pilots, both nude and suited in a full pressure suit,[1] we estimated that the external area of an astronaut's space suit is at least 20% greater than his body area. While at rest, the minimum metabolic rate is 500 Btu/hr, and at peak work load the maximum metabolic rate is 2000 Btu/hr. In addition, there is a thermal input of 500 Btu/hr from various subsystems. Therefore, the total heat load on the space suit is in the range from 1000 to 2500 Btu/hr. In terms of the average heat flux per unit area at the external surface of the suit, these rates correspond to a range of 39 to 98 Btu/sq ft hr.

TABLE I

ORBIT RADIANT ENVIRONMENT

Type of Radiant Energy	Twilight Orbit	Noon Orbit Earth Umbra	Noon Orbit Earth-Sun Line
Solar (Btu/ft^2 hr)	442	0	442
Albedo (Btu/ft^2 hr)	177	0	177
Earthshine (Btu/ft^2 hr)	66.4	66.4	66.4

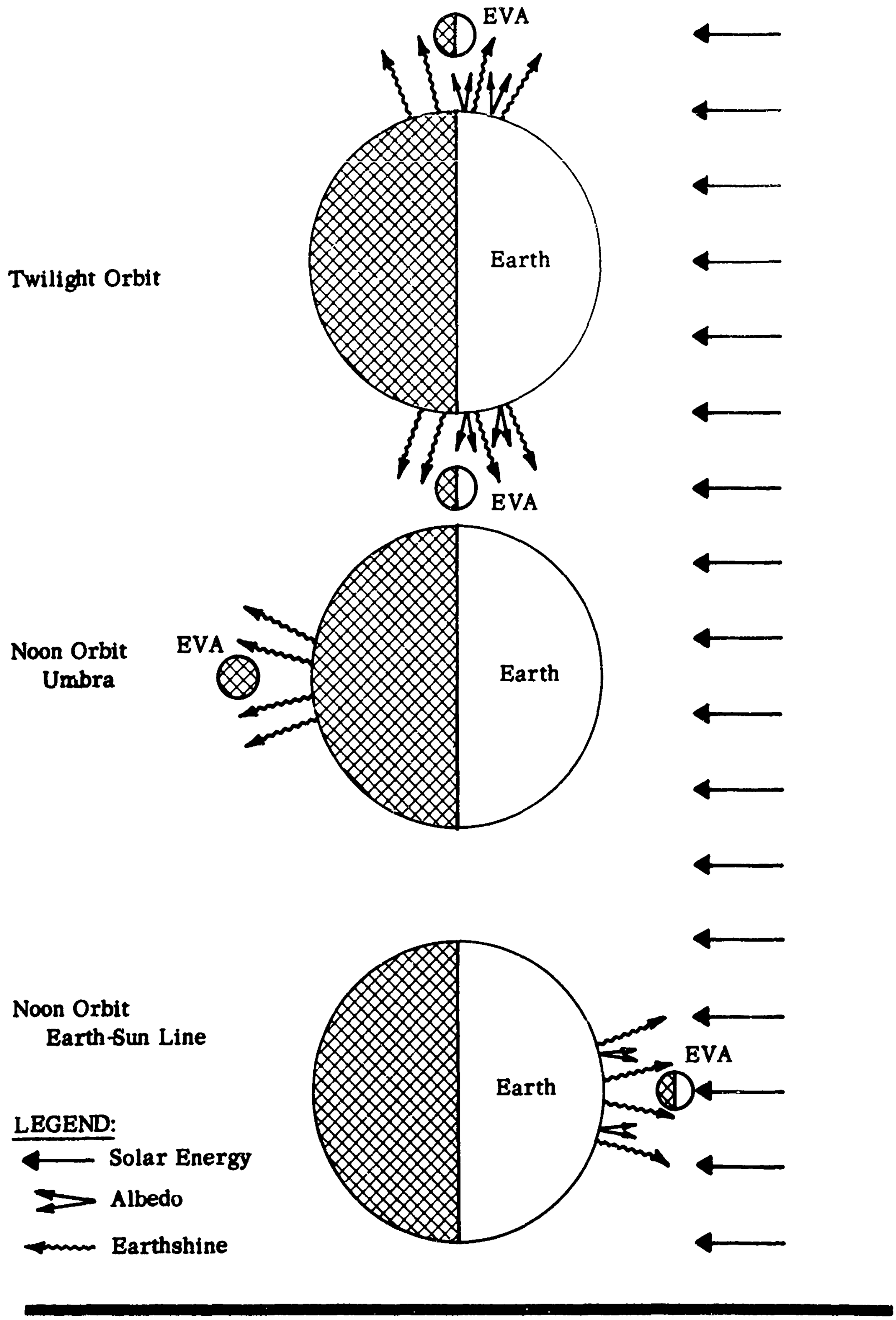

FIGURE 1. ORBIT RADIANT ENVIRONMENTS

An upper limit of 2500 Btu/hr is probably unrealistic for prolonged effort in zero-gravity extravehicular missions and a more reasonable upper limit (including 500 Btu/hr of subsystem input) might be 1500 Btu/hr. Recent studies(2,3) with garmented subjects on a treadmill indicate that a large portion of an astronaut's energy is used in overcoming the "stiffness" of flexible space suits when inflated to 3.5 psi and that further developments in space suits will aid in reducing the energy requirements.

The comfort range of habitable space suit environment was assumed to be when the astronaut's skin temperature is in the range of 82.4 to 89.6°F. It was further assumed that heat transfer from the astronaut would be primarily by radiation, convection, and gas conduction, and that a no-sweating condition exists.

C. THERMAL CONTROL PERFORMANCE REQUIREMENTS FOR AVERAGE ORBIT CONDITIONS

The analytical approach in our study of the noon and twilight orbits was the same and is outlined in detail in the appendix. The orientation of the cylinder (astronaut) to the earth-sun vector for the noon orbit is shown in figure 2, for the twilight orbit in figure 3. In both orbits, the cylinder axis was aligned normal to the earth-sun line and was parallel with the polar axis.

At various angular positions in the orbit the view factors, earth-to-cylinder, were used in conjunction with corresponding solar, albedo, and earthshine radiant fields to compute the incident radiant energies on the astronaut. Average incident heat fluxes to the cylinder were then computed for the orbit and used in a parametric analysis of the equilibrium external temperature of the astronaut for a range of surface absorptance-to-emittance and a range of internal heating from 0 to 2500 Btu/hr.

1. Noon Orbit Calculations

The calculated equilibrium external temperatures shown in figure 4 indicate that external temperatures at less than 50°F cannot be maintained by α_o/ϵ_o surface coatings ($\alpha_o/\epsilon_o > 0.2$) when internal heat generation rates are in excess of about 1800 Btu/hr. Figure 5 shows the range of insulation conductance required for a fixed value of the external surface α_o/ϵ_o for internal wall temperature of 75°F. For an α_o/ϵ_o of 0.2 (the approximate lower limit of α_o/ϵ_o for available space suit coating materials), the range of insulation conductance extends from 0.3 Btu/sq ft hr °F at 1000 Btu/hr to 20 Btu/sq ft hr °F at about 2300 Btu/hr. It is to be noted that the conductance approaches infinity for internal heat generations in excess of 2300 Btu/hr. This indicates that the external surface α_o/ϵ_o limits the heat flow. Shown on figure 5 are some hypothetical surface properties $\alpha_o/\epsilon_o = 0.1$ and zero which indicate that to approach the highest internal heat generation of 2500 Btu/hr, it is necessary to go to unrealizable surface coatings.

Figure 6 shows the range of α_o/ϵ_o of surface coatings required to maintain the internal wall temperature at 75°F when the insulation conductance is

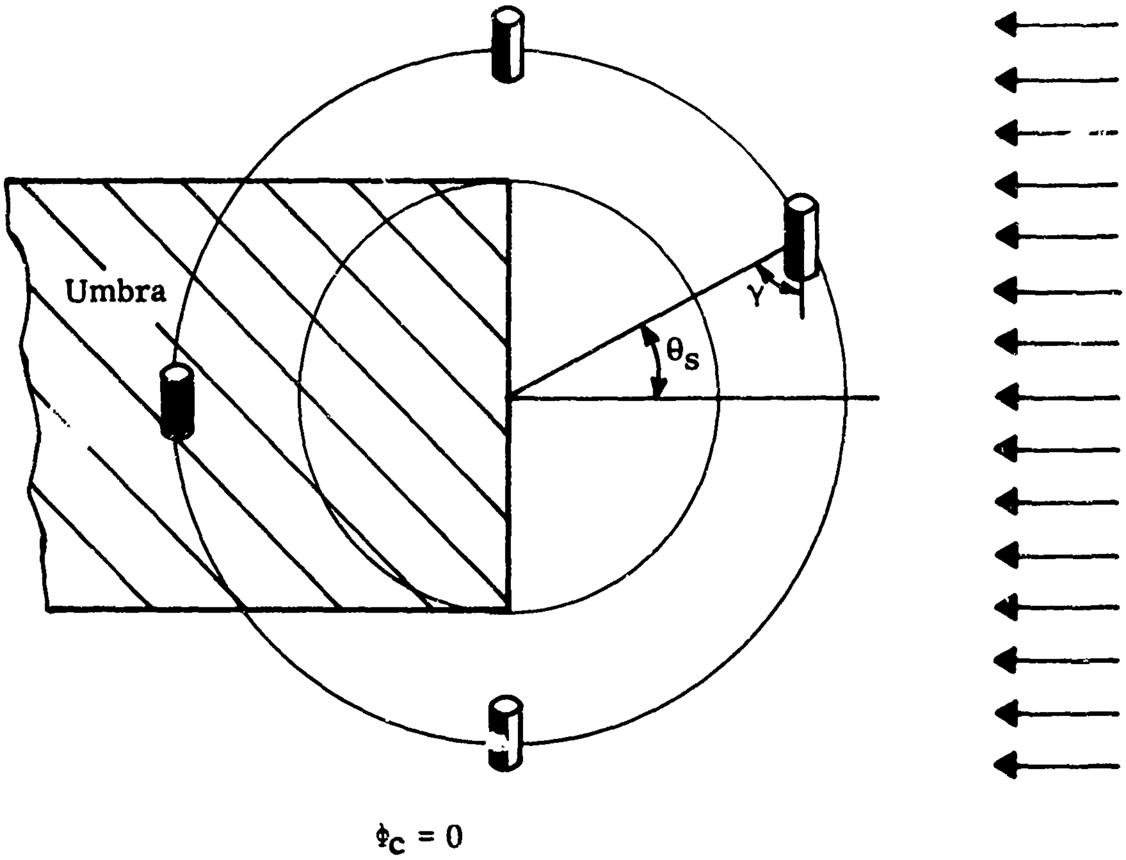

FIGURE 2. ASTRONAUT ORIENTATION IN A NOON ORBIT

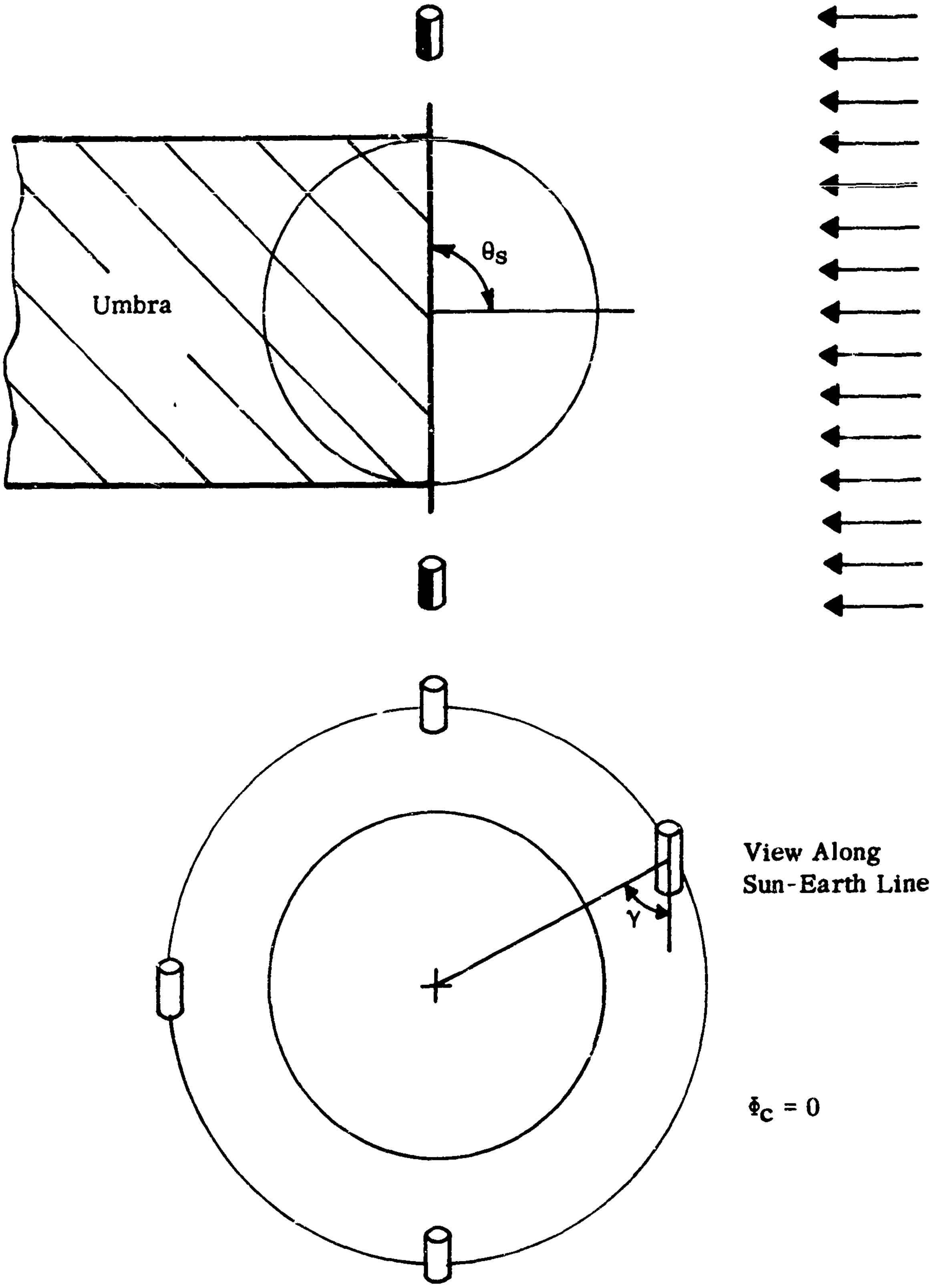

FIGURE 3. ASTRONAUT ORIENTATION IN TWILIGHT ORBIT

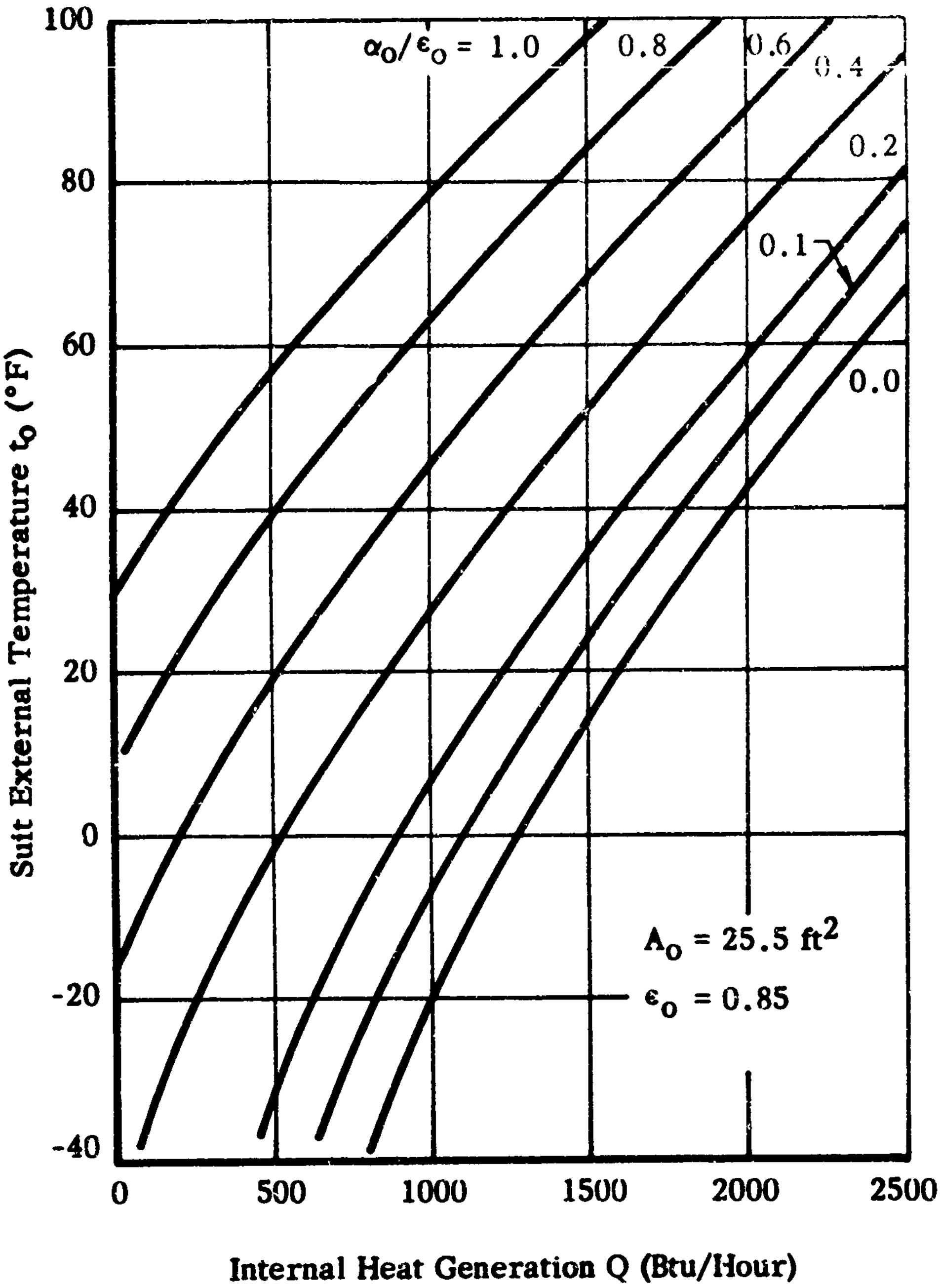

FIGURE 4. AVERAGE EXTERNAL WALL TEMPERATURE FOR A SPACE SUIT IN A NOON ORBIT

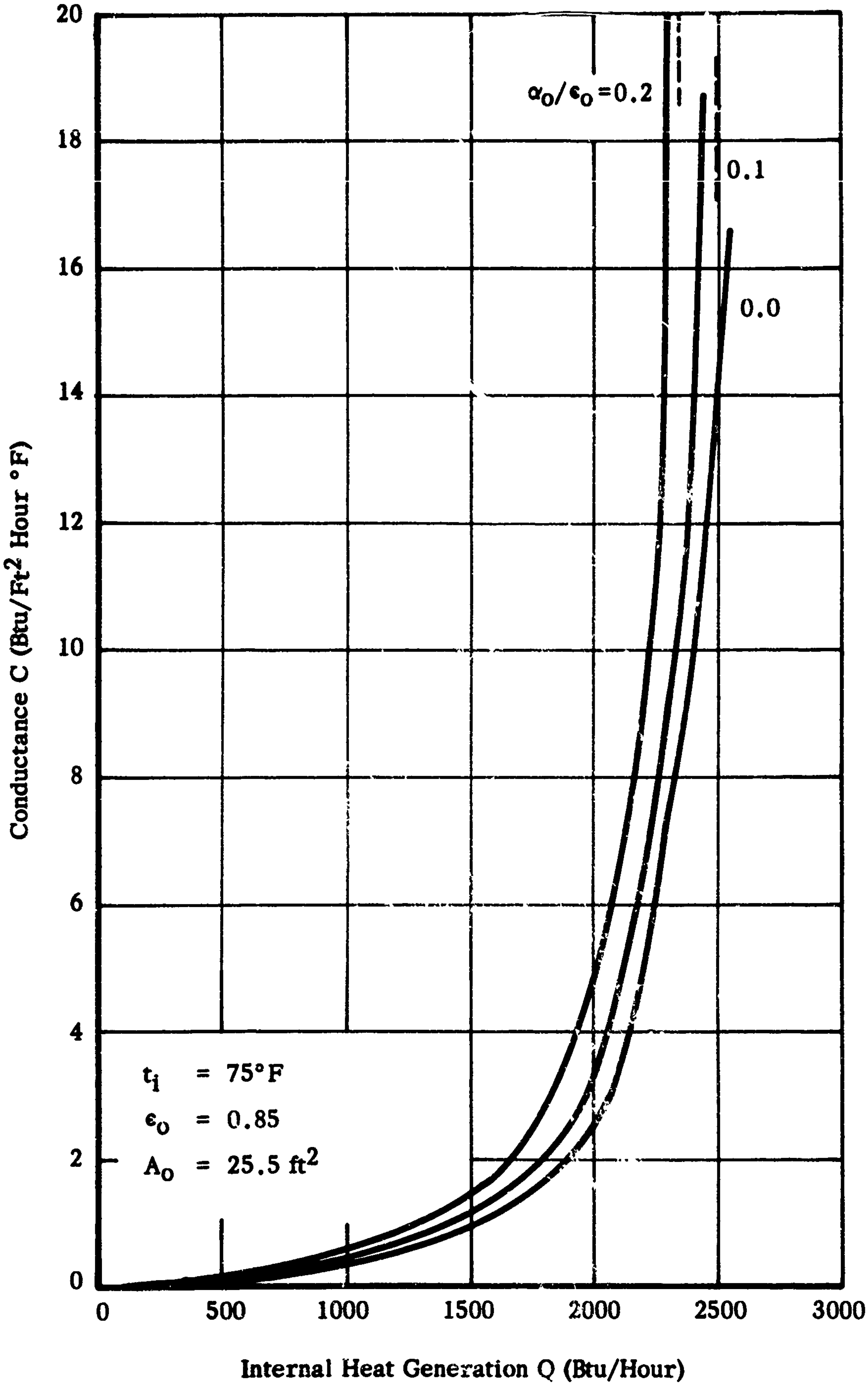

FIGURE 5 . INSULATION CONDUCTANCE REQUIREMENTS FOR A SPACE SUIT IN A NOON ORBIT

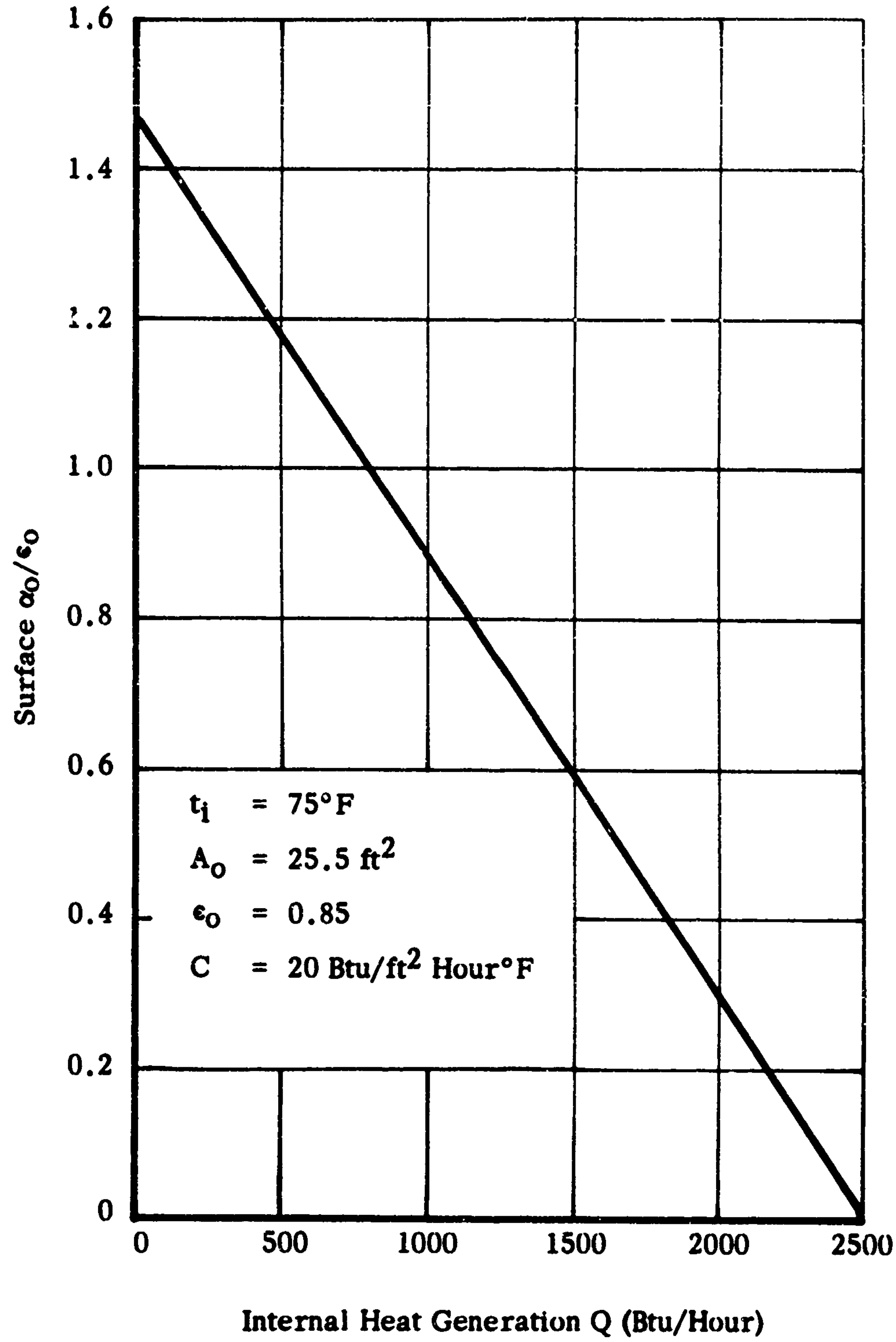

FIGURE 6. SURFACE α_o/ϵ_o REQUIREMENTS FOR A SPACE SUIT IN A NOON ORBIT

20 Btu/sq ft hr $^{\circ}$F. For this case, the external surface α_o/ϵ_o decreases from 0.9 at 1000 Btu/hr to zero for 2500 Btu/hr internal heat generation. Such a range of external surface α_o/ϵ_o ratios is outside the capability of present day spacecraft coating technology. From the results summarized in figures 4 through 6, we conclude that for typical materials (ϵ_o = 0.85 and $\alpha_o/\epsilon_o \doteq 0.2$) comfortable skin temperatures cannot be achieved for the highest internal heat generation rate of 2500 Btu/hr. For the lowest internal heat generation rate, 1000 Btu/hr, control is possible by varying α_o/ϵ_o, by varying the insulation conductance or by varying both.

2. Twilight Orbit Calculations

Inasmuch as the astronaut is always located in the sun in the twilight orbit, the total radiant energy incident upon the astronaut is greater than it is in the noon orbit.

Equilibrium temperatures shown in figure 7 indicate that it is again difficult to achieve high internal heat generation rates with available space suit external coatings. Figure 8 shows the insulation conductance requirements for the space suit in a twilight orbit. Figure 9 shows the surface α_o/ϵ_o requirements for the space suit in twilight orbit.

D. TIME-DEPENDENT HEAT ABSORPTION AND REJECTION

Predicted passive thermal control performance requirements for average orbit conditions indicate that for the highest metabolic rate input (2500 Btu/hr) variation of the α_o/ϵ_o characteristics and thermal conductance may be insufficient to provide thermal control for the space suit. Under a high metabolic rate input, time-dependent techniques may be utilized to maintain thermal balance by heat absorption or rejection. Several of these techniques were considered, including heat capacity and phase change of water and chemical and physical desiccants. Of primary interest in the analysis were heat capacity and phase change of water. Desiccants for removal of water from an evaporative cooling system of a space suit were eliminated because of the weight of active material required for removal of each pound of water and the difficulties in regenerating these active materials. It was considered more practical to use the cooling ability of the phase change of water by evaporating it overboard from the suit. Evaporative cooling by water is practical for short durations and in a 300 nautical mile earth orbit when resupply of the evaporated water is possible. For longer missions where resupply is not feasible, however, water recondensation or removal by desiccants might be practical.

1. Heat Capacity

Of the potentially acceptable heat capacities, water appears to be most attractive because of its high heat capacity in relation to the mass required. In a 300 nautical mile orbit, a water-filled shell, 5/8 inch thick, would meet the minimum temperature requirements for one orbit in the earth's shadow.(4) Similarly, this heat capacity could be used for thermal control heat balance during periods of high metabolic rate. Heat

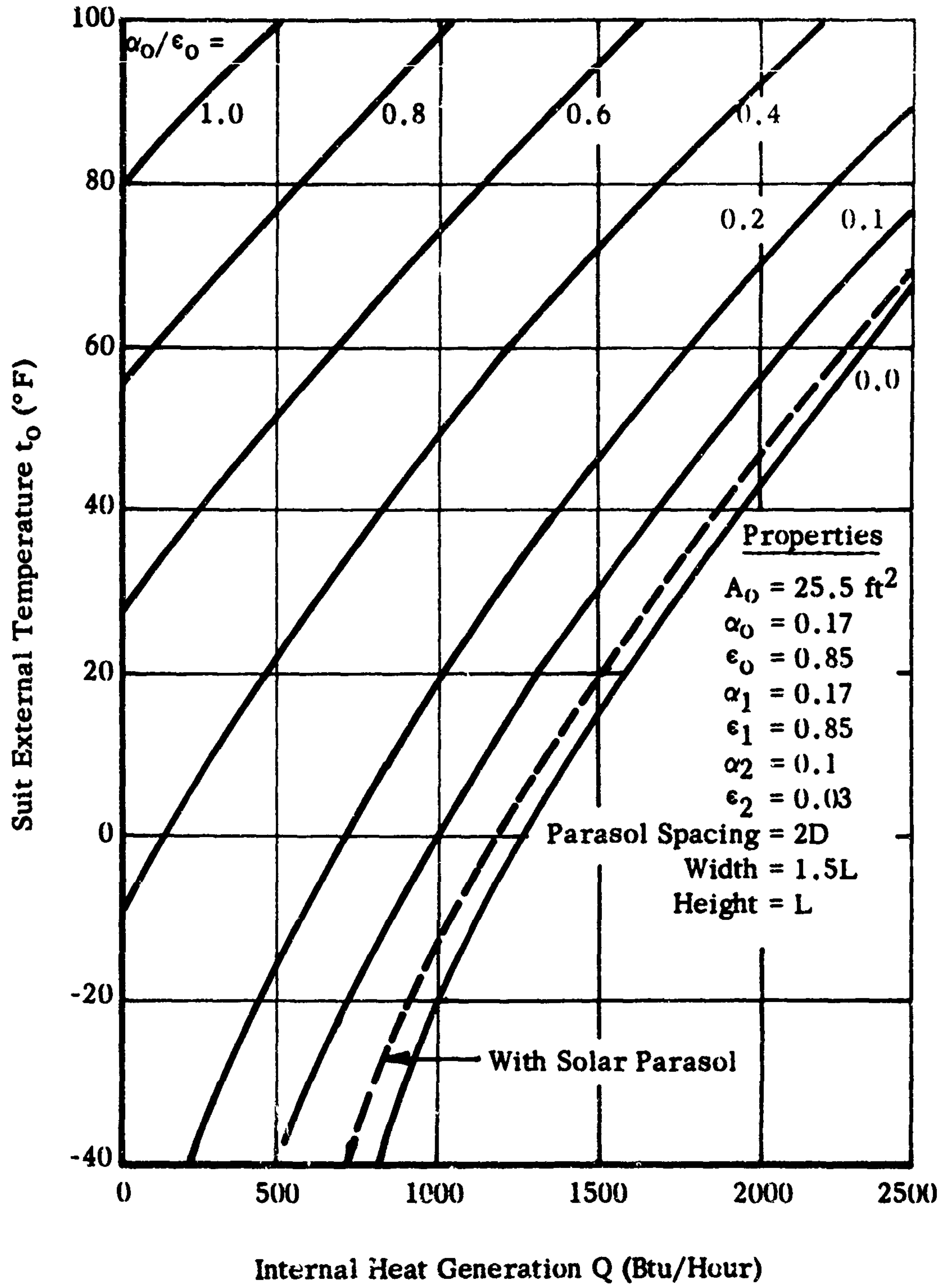

FIGURE 7. AVERAGE EXTERNAL WALL TEMPERATURE FOR A SPACE SUIT IN A TWILIGHT ORBIT

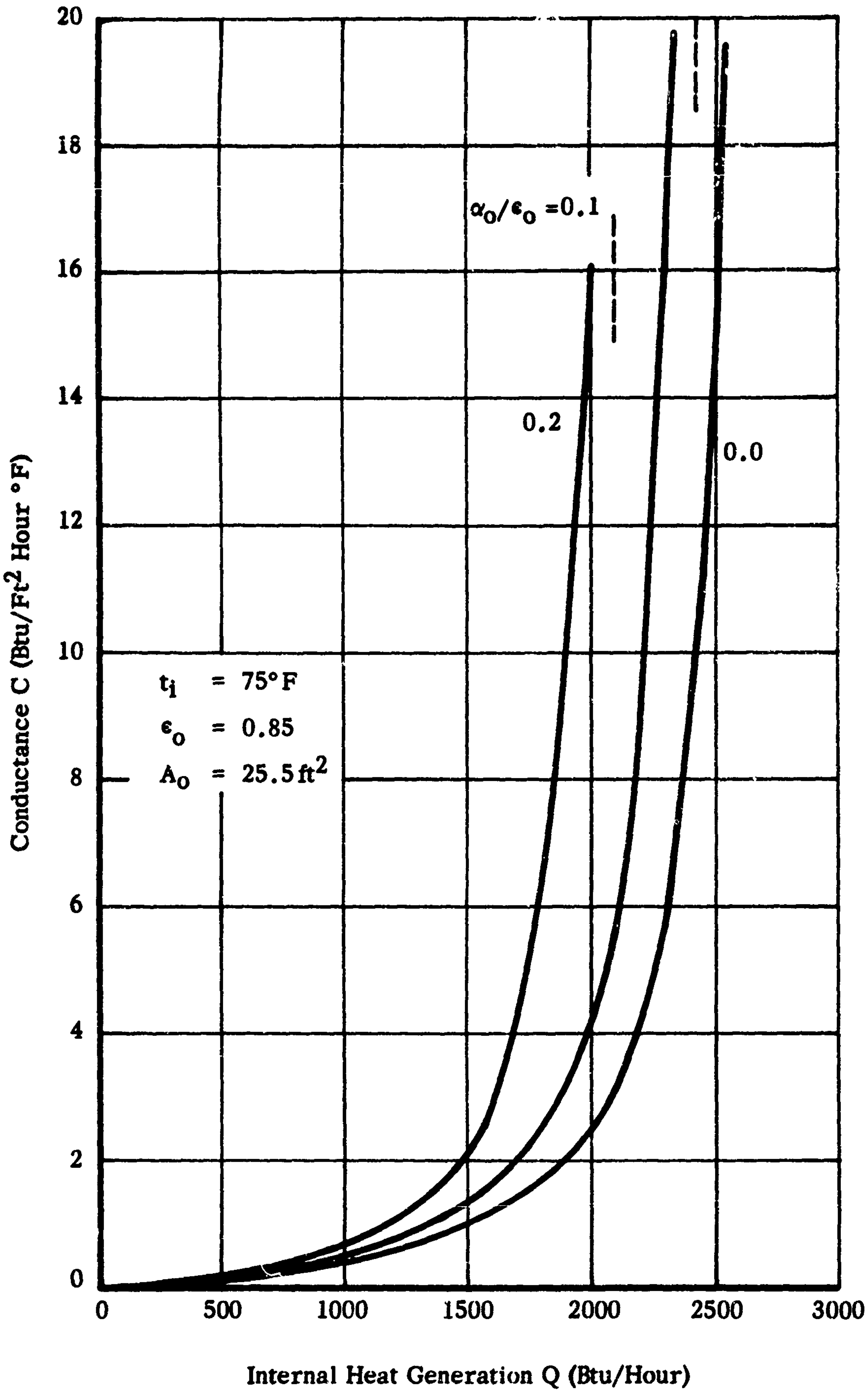

FIGURE 8. INSULATION CONDUCTANCE REQUIREMENTS FOR A SPACE SUIT IN A TWILIGHT ORBIT

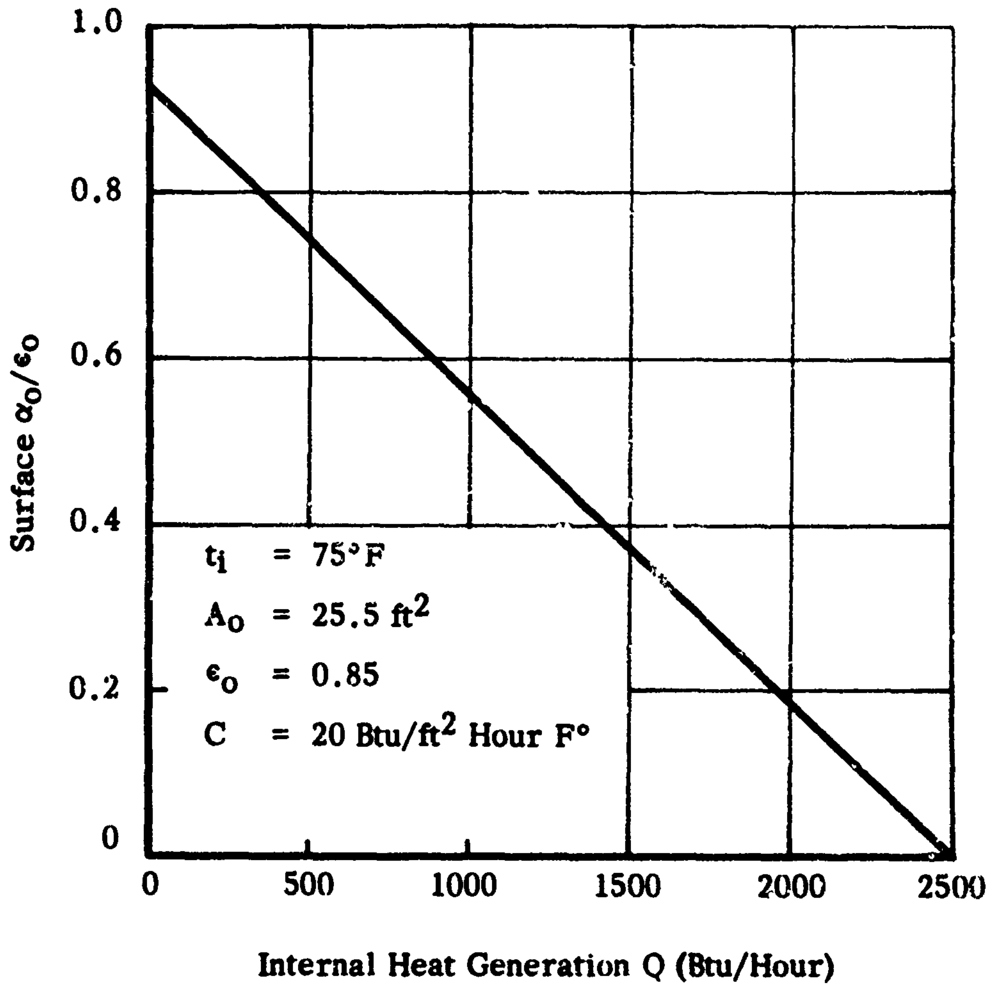

FIGURE 9. SURFACE α_o/ϵ_o REQUIREMENTS FOR A SPACE SUIT IN A TWILIGHT ORBIT

capacity is useful however only for absorbing high metabolic input during periods of activity and rejecting this heat during periods of low metabolic activity. Depending upon the over-all metabolic rate, the radiative characteristics of the space suit system, and the type of orbit, heat capacity alone may be insufficient to smooth out the temperature excursions during the orbit. The data indicated on figures 4 and 7 indicate that for achievably low α_0/ϵ_0 ratios it is difficult to maintain the suit external surface temperature sufficiently low that metabolic energy can be transferred from the inner wall to the outer wall when the astronaut is working at his highest metabolic rates. For instance, if the astronaut is in a noon orbit and it is desirable to maintain the external suit temperature at 50°F, for an α_0/ϵ_0 of 0.2 the maximum metabolic rate which the astronaut can work at is approximately 1800 Btu/hr. In this case, heat storage will do the astronaut no good since what he needs is a heat rejection capability. The same reasoning when applied to the average twilight orbit indicates that a slightly lower metabolic rate is the maximum possible for an external suit temperature of 50°F.

2. Phase Change

Although a number of materials exhibit phase changes at the temperature range of interest, water has the highest heat of vaporization. Heats of fusion are typically an order of magnitude less; in addition, frozen materials may present mechanical problems in achieving suit flexibility. By controlling the vapor pressure of water within the garment, extreme heat can be absorbed for short periods of time by exhausting the water vapor overboard. From the analysis of averaged orbit conditions, we see that internal heat generation rates in excess of about 1500 Btu/hr may have to be rejected by means other than radiation from the space suit surface. During periods of high activity, heat can be rejected by evaporative water cooling.

At 70°F we know that 1050 Btu/lb of water can be absorbed by evaporating at a pressure of 0.36 psia. Shown in figure 10 is the amount of water required, as a function of the excess metabolic activity, to maintain suit internal equilibrium temperature of 70°F. Thus, for prolonged periods of metabolic activity in excess of approximately 1500 Btu/hr (this is an estimated limit that can be achieved with the α_0/ϵ_0 coating on a space suit as a passive thermal control), the excess metabolic energy can be rejected by evaporating water. For a metabolic rate of 2000 Btu/hr, the excess above 1500 is 500 Btu/hr and approximately a half pound of water will be used per hour of activity.

E. SOLAR PARASOL

We analyzed the feasibility of providing a solar parasol for shielding the astronaut during extravehicular operations in the sunlight. The parasol was assumed to have a white paint coating on the side facing the sun and a polished aluminum surface facing the astronaut. Properties of the solar parasol are summarized in table II. In the analysis we accounted for the following radiant interactions:

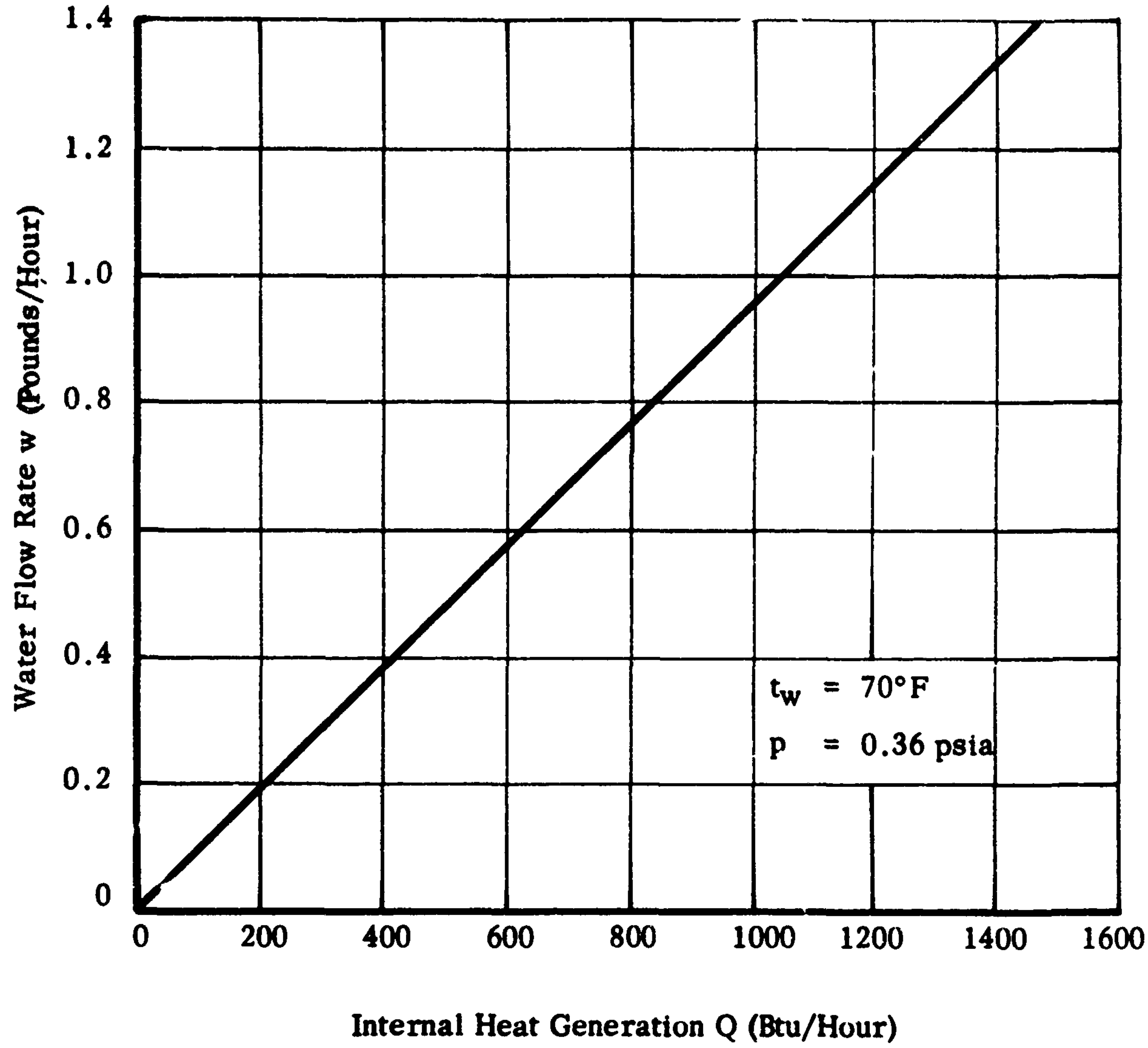

FIGURE 10. WATER REQUIREMENTS FOR EVAPORATIVE COOLING

TABLE II

PROPERTIES OF SOLAR PARASOL

Width	=	1.5 D
Height	=	L
Spacing	=	2 D

Surface Facing Sun	α_1	=	0.17
	ϵ_1	=	0.85
Surface Facing Astronaut	α_2	=	0.1
	ϵ_2	=	0.03

1. Earthshine and albedo on the astronaut and parasol.

2. Solar on the parasol.

3. Earthshine and albedo reflected by the astronaut and parasol onto each other.

4. Direct radiation between the astronaut and the parasol.

5. Back-reflection of direct radiation between the astronaut and the parasol.

6. Internal heat generation in the astronaut.

The effect of this solar parasol upon the equilibrium temperature of an astronaut on the earth-sun line is summarized in figure 11. The effect of the same solar parasol on the average external wall temperature for a space suit in a twilight orbit is summarized on figure 7 as a broken curve. Results show that a solar parasol decreases the suit external temperature and allows higher internal heat generation rates (metabolic) for a given external wall temperature. For the twilight orbit and for the astronaut on the earth-sun line, an increase of 500 Btu/hr in the internal heat generation above the unshaded condition is achieved before the astronaut becomes uncomfortably warm.

F. TEMPERATURE DISTRIBUTIONS FOR SELECTED ORBIT POSITIONS

Equilibrium temperatures for selected points on the astronaut were calculated for three orbit positions: (1) on the earth-sun line, (2) in the earth umbra, and (3) in a twilight orbit. Selected materials properties were used which correspond to the properties of the space suit materials used in the orbit simulation phase of this program. Circumferential temperature distributions on the inside and outside wall of the space suit are presented for heat input rates of 1000, 1500, and 2000 Btu/hr.

The analysis and the method of solution are outlined in detail in the Appendix. The solution, in brief, requires that the albedo, earthshine, and solar view factors (F_a, F_e, and F_s) be specified for each circumferential position on the astronaut, that the suit external surface (α_o and ϵ_o) properties be specified, and that the heat generation term (q_m) be given.

1. Temperature Distributions

Temperature distributions on the outer wall of the space suit for the astronaut on the earth-sun line are given in figure 12. The two temperature peaks correspond to the side facing the sun and the side facing the earth. The magnitude of the sun side peak is proportional to the solar absorptance α_s, and the magnitude of the earth side peak is proportional to a combination of the room temperature absorptance α_o ($\alpha_o = \epsilon_o$) and the albedo absorptance α_s. For the astronaut in the earth umbra, the external temperature distribution is given in figure 13. Here, no solar radiation

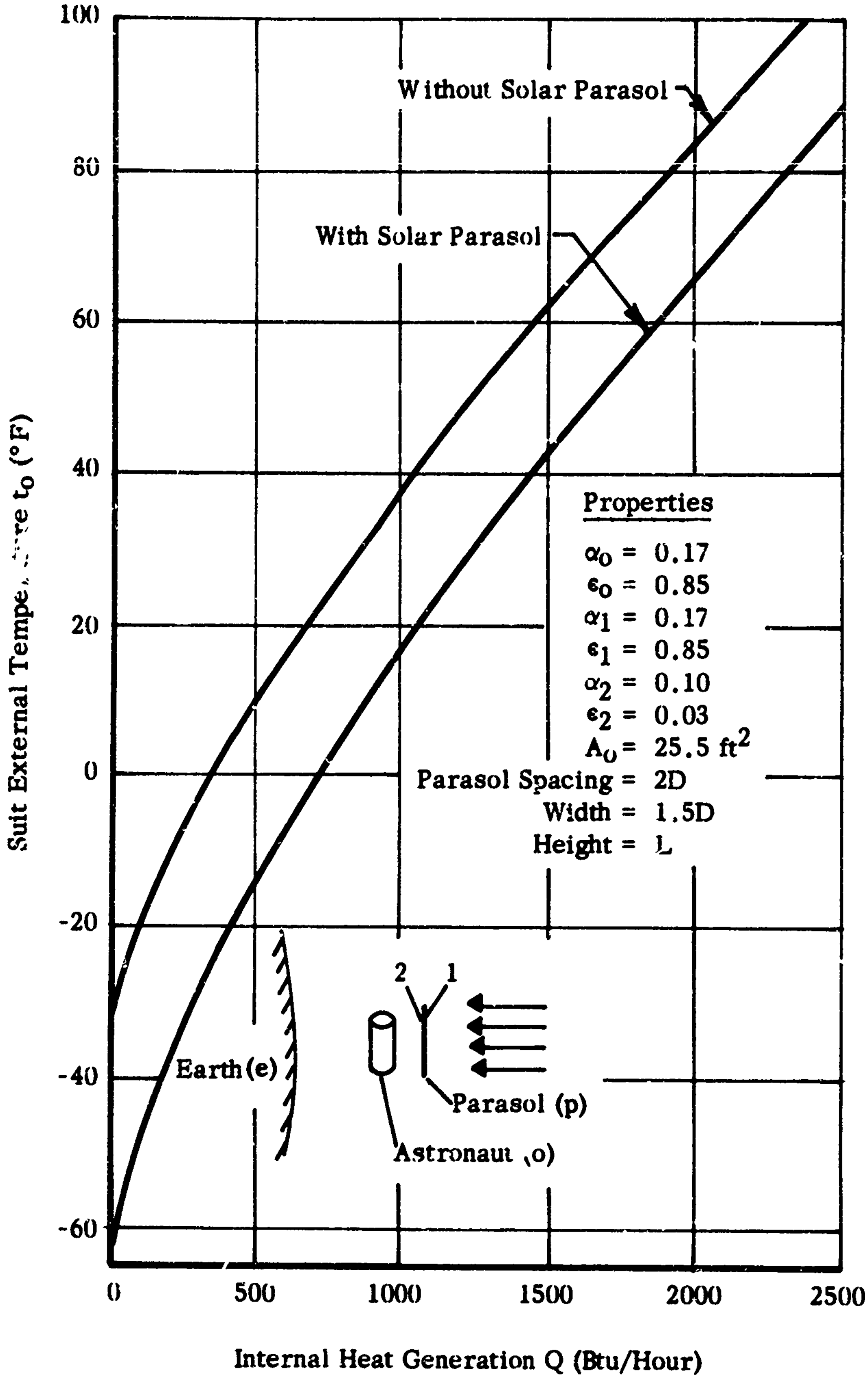

FIGURE 11. THE EFFECT OF A SOLAR PARASOL ON EQUILIBRIUM TEMPERATURE FOR A SPACE SUIT ON THE EARTH-SUN LINE

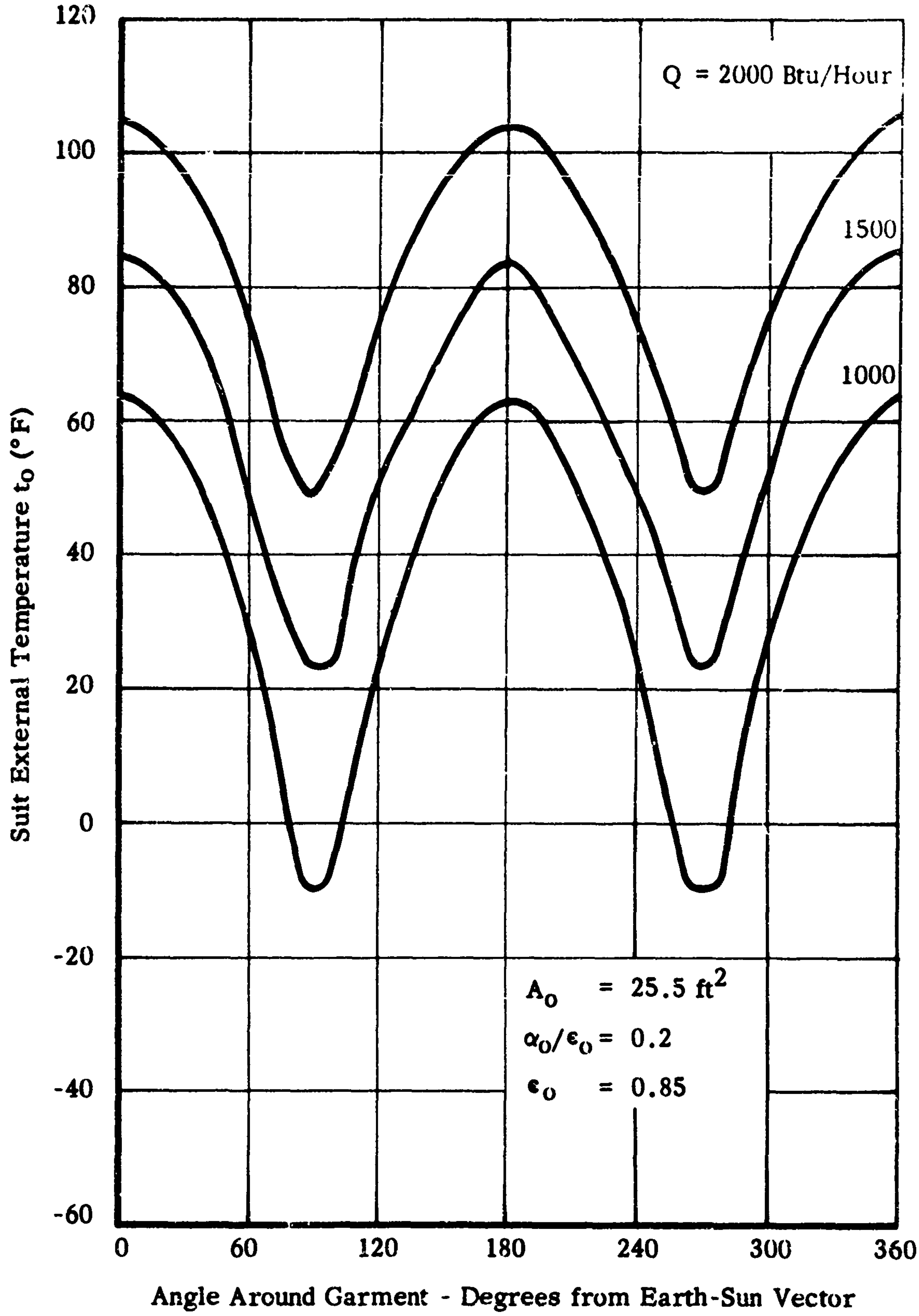

FIGURE 12. EXTERNAL TEMPERATURE DISTRIBUTION FOR A SUIT ON EARTH-SUN LINE

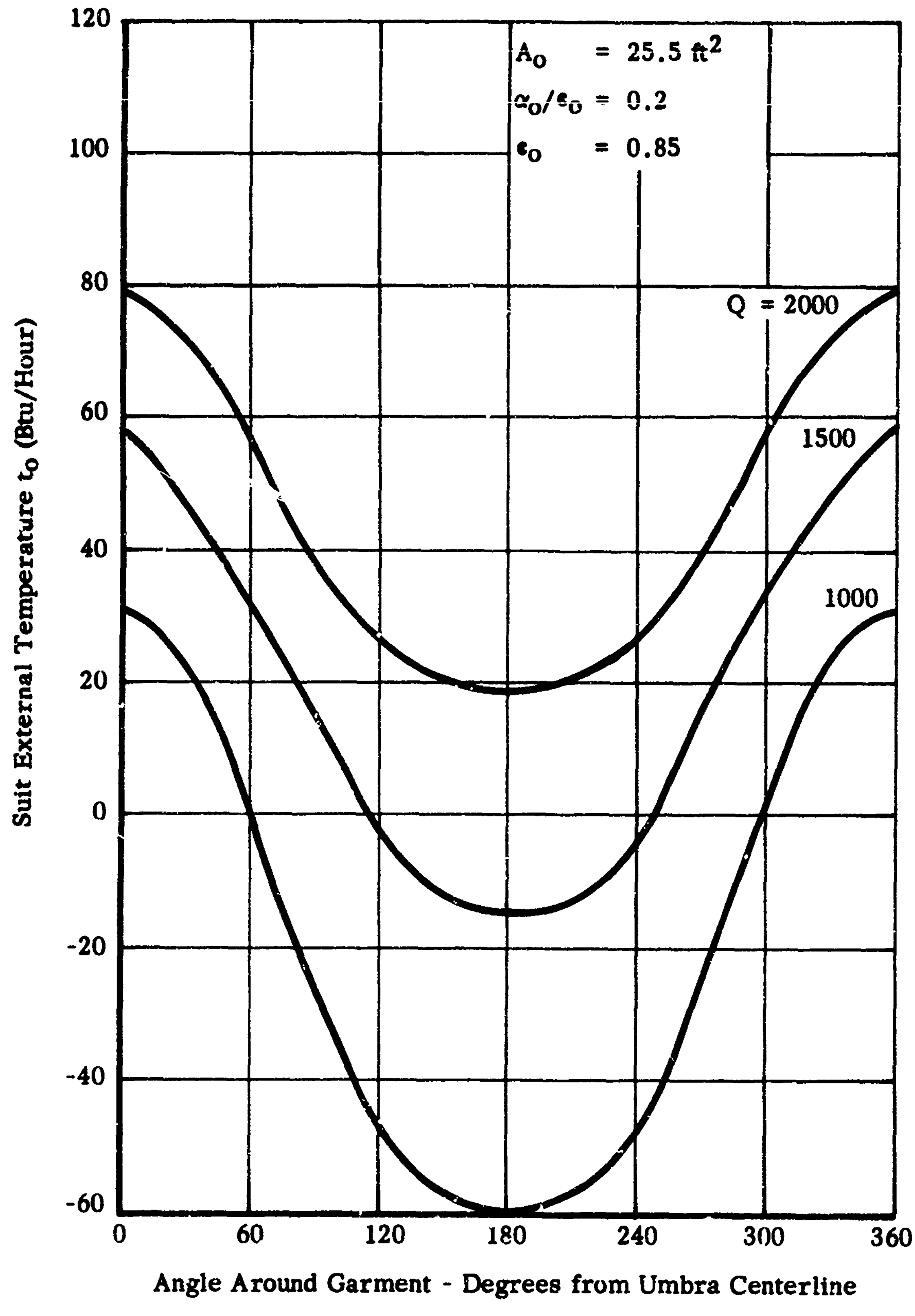

FIGURE 13. EXTERNAL TEMPERATURE DISTRIBUTION FOR A SPACE SUIT IN THE EARTH UMBRA

is present and the single peak corresponds to the side that faces the earth. The opposite side faces space and therefore is at a lower equilibrium temperature. The temperature distribution for an astronaut in a twilight orbit is given in figure 14.

G. DISCUSSION OF ANALYSIS

If we allow for a minimum temperature difference of 20^{o}F across the insulation and assume that 70^{o}F represents a comfortable upper limit on the temperature which should be achieved on the inner wall of the space suit, then 50^{o}F represents the upper limit of the suit external temperature. With this upper limit we can see from figure 4 that for suit properties of $\epsilon_o = 0.85$ and $\alpha_o/\epsilon_o = 0.2$, the upper limit on internal heat generation is 1800 Btu/hr for a noon orbit. For the twilight orbit (figure 7) the limit is 1550 Btu/hr. By the addition of a solar parasol in the twilight orbit (see figure 7), the upper limit on internal heat generation is increased to 2050 Btu/hr. Thus, it can be seen that rejection of the highest internal heat generated in the space suit is the primary problem in protection of an astronaut in 300 nautical mile orbits. At heat generation rates below the upper limit, passive control of an astronaut's environment can be achieved by varying the suit insulation conductance or the suit radiation characteristics.

The analysis of the azimuthal temperature distributions on the external surface for selected orbit positions (see figures 12 through 14) shows that large variations in temperature occur around the astronaut particularly when the astronaut is on the earth-sun line or in a twilight orbit. These large azimuthal temperature gradients indicate that azimuthal heat distribution schemes might allow for transfer of more heat in areas where the external temperature is low and less heat in areas where the temperature is high.

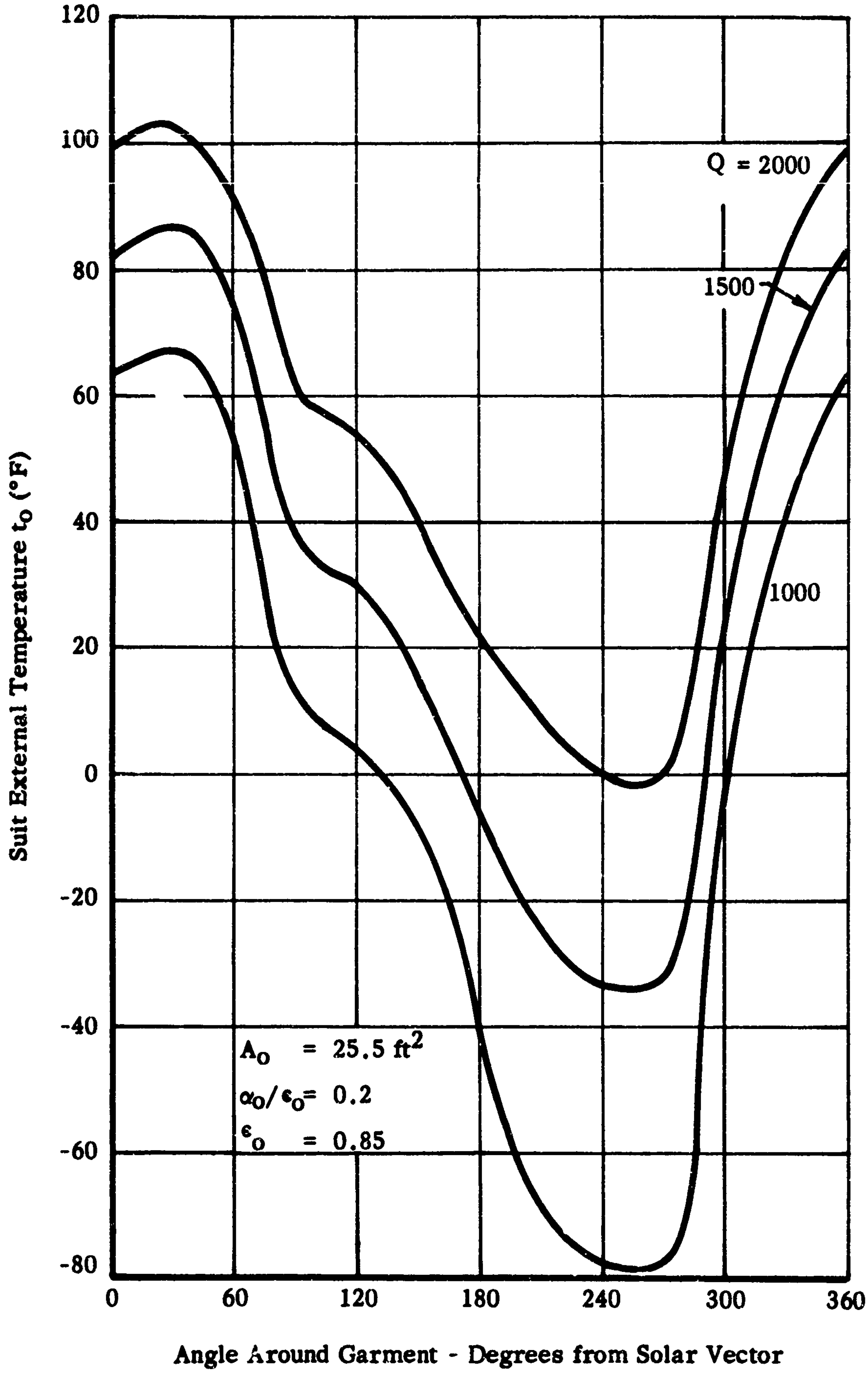

FIGURE 14. EXTERNAL TEMPERATURE DISTRIBUTION FOR A SPACE SUIT IN A TWILIGHT ORBIT

SECTION V
SPACE HAZARDS

To evaluate the damage to space suit materials resulting from their exposure to space radiation at and beyond 300 miles altitude and the effect of this damage on passive thermal control techniques, we compiled data on space radiation from a number of sources.

A. ELECTROMAGNETIC RADIATION

Solar radiation is the only significant component of the electromagnetic radiant flux in the orbit considered. Of the solar flux received outside of the earth's atmosphere, the most active component is that lying in the ultraviolet and far ultraviolet regions of the spectrum. According to the results obtained with rocket-flight spectrometers and ionization chambers,[5] radiant flux from the quiescent sun in the near and far ultraviolet regions consists of three components:

1. Black-body radiation corresponding to an effective temperature of the photosphere of 4200°K.

2. Chromospheric line emissions, principally hydrogen Lyman-alpha at 1216 Å, and weaker lines of CII, NV, OI, SiII, SiIII, and SII.

3. Coronal radiation corresponding to an effective temperature of about 500,000°K.

The black-body radiation of the photosphere drops off rapidly under 3000 Å as shown below:

4000 - 3000 Å	6.00×10^{-3} w/cm^2
3000 - 2000	4.30×10^{-4}
2000 - 1500	4.72×10^{-6}
1500 - 1200	3.56×10^{-8}
1200 - 1000	1.82×10^{-10}
1000 - 500	negligible

The line emissions contribute to most of the energy in the 1000 to 1350 Å range, the Lyman-alpha line alone accounting for over 94% of the energy. Below the Lyman continuum ($\lambda < 900$ Å), there are no chromospheric emission lines of significant intensity and the solar flux reaches a minimum at approximately 500 Å.

In the still shorter wavelength range (soft X-ray range) the coronal emission becomes predominant and reaches a peak at about 50 Å wavelength. The total coronal emission flux integrated from 5 to 500 Å is estimated to be of the order of 1×10^{-7} watts/cm^2. The galactic (cosmic ray) component of the electromagnetic radiation flux, even though highly energetic (10^4 to 10^8 ev photon energy), is insignificant because of the very low flux density. The integrated flux density from 0 to 1 mev is estimated at about 10^{-13} watts/cm^2.(6)

B. PARTICLE RADIATION

1. Spatial Distribution

In contrast to the solar electromagnetic radiation which is uniform everywhere in the vicinity of the earth, particle radiation, mainly protons and electrons, has a highly non-uniform distribution. The earth's magnetic field causes some of the particle flux to become trapped in the Van Allen radiation belts, and it also deflects the trajectories of the less energetic cosmic ray particles so that they can approach the earth's surface only in the circumpolar regions. The geomagnetic cut-off latitude for 100 mev protons is about 65 degrees. For lower energies it becomes higher (e.g., 80 degrees for 0.1 mev protons); electrons of energies less than about 5 mev are incident only at the poles.

The spatial distribution of proton and electron fluxes in the Van Allen belts is well documented.(7) The natural distribution of high energy protons and electrons has been shown to be temporarily disturbed to a distance of about 1.6 earth radii by high-altitude nuclear tests.

2. Proton Flux

The spatial distribution of proton flux results in turn from the fact that the energy of protons arriving in the geomagnetic field is spread over a broad interval covering more than 10 orders of magnitude. The proton flux density generally decreases with increasing energy, and it is customary to plot the integrated flux density N ($>$E) as a function of energy E on a logarithmic scale as shown in figure 15 (these data were compiled from references 8, 9, and 10). The integrated flux N ($>$E) is the total number of protons of energy greater than E per cm^2 sec steradian.

Because of the complexity of the spatial distribution of the flux, figure 15 must be used with due consideration of the regions in which protons of certain energy are likely to be found. Some components of proton flux are present only occasionally during periods of intense solar activity. In the quiescent period of the solar cycle, only a few flare emissions may occur per year while at maximum activity there may be on the average of one or more per month. The flux-energy curves of figure 15 are drawn as fairly wide bands since the experimental data from which they are derived are subject to a high degree of uncertainty. The envelope lines drawn in the diagram seem to represent safe estimates of the maximum flux density to be expected.

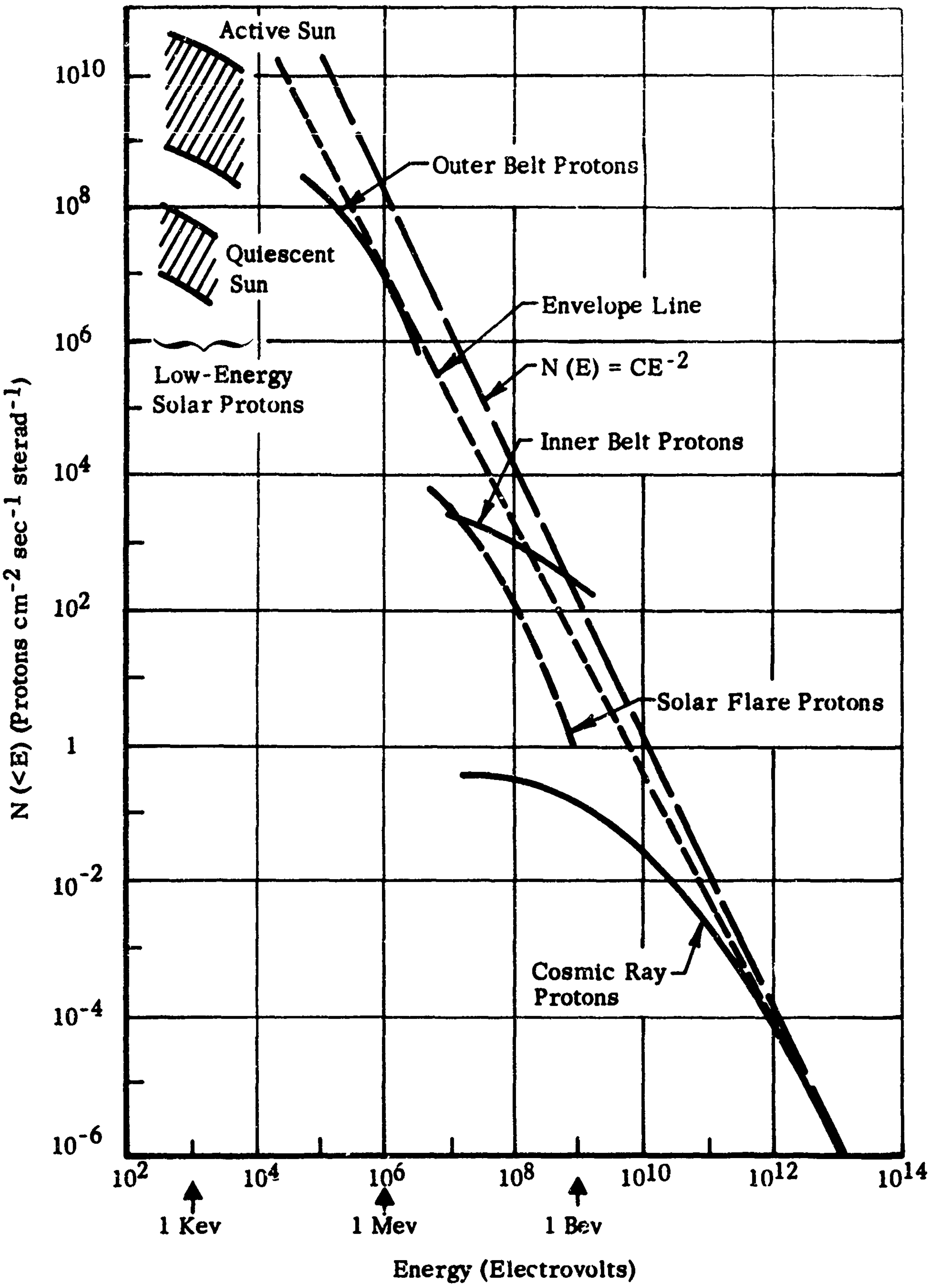

FIGURE 15. INTEGRATED PROTON FLUX DENSITY

3. Electron Flux

The only experimental data available for electrons are those from the Van Allen belt experiments. From these results we see that the maximum flux density of trapped electrons is of the order of 10^7 to 10^9 electrons/ cm^2/sec at altitudes from 600 to 900 nautical miles. Below 300 nautical miles, the electron flux is negligible.

4. Effects of Orbital Inclination on Particle Fluxes

Since particle fluxes are essentially confined to equatorial radiation belts and to circumpolar cones of entry, the time an orbiting object will actually spend in the flux will depend on the orientation of the orbital plane. Depending on orbital altitude and inclination, the satellite may traverse radiation regions in four typical ways:

	Type of Traversal	
Altitude (n.m.)	0-65° lat.	65-90° lat.
200 to 500	none	cones
1000 to 3500	belts	cones and belts

The fraction of time actually spent in the radiation regions under these typical conditions can be estimated to a first approximation by idealizing the belt and cones to simple geometric configurations shown in figures 16 and 17. It can be seen that the fraction of time spent in the radiation zones is almost never 100%, with the exception of high-altitude equatorial orbits. Low polar orbits may be exposed for as little as 12% of the time (at 80 degrees orbital inclination).

C. MICROMETEORITE FLUX

There is a possibility of an astronaut being struck by micrometeorites which, although small in size (10^{-10} gm), are traveling at extremely high velocities (10 to 100 km/sec).(11) Direct hit by a meteorite of a mass greater than approximately 10^{-4} gm would probably be fatal to the astronaut wearing a standard space suit. The energy of a meteorite of one milligram mass impacting with a velocity greater than 20 km/sec is estimated to be sufficient to penetrate a sheet of aluminum 3 mm in thickness. However, the probability of such an event is exceedingly small. The distribution of particle flux density vs. mass for meteorites follows an inverse law which can be very nearly represented by a straight line in a logarithmic plot shown in figure 18. Direct measurements obtained with spacecraft(12) appear to be consistent with the extensive data underlying the statistical distribution such as shown in figure 18.

On the basis of this distribution, we can estimate that the number of micrometeorites of a mass greater than 0.1 mg crossing a one square meter area from all directions is of the order of 10^{-11} particles per second. Hence, the area would be hit, on the average, about three times in 10,000 years by meteorites greater than this size. If we lower the potentially hazardous mass limit, the probability of a hit will increase, but it would seem to be still very low.

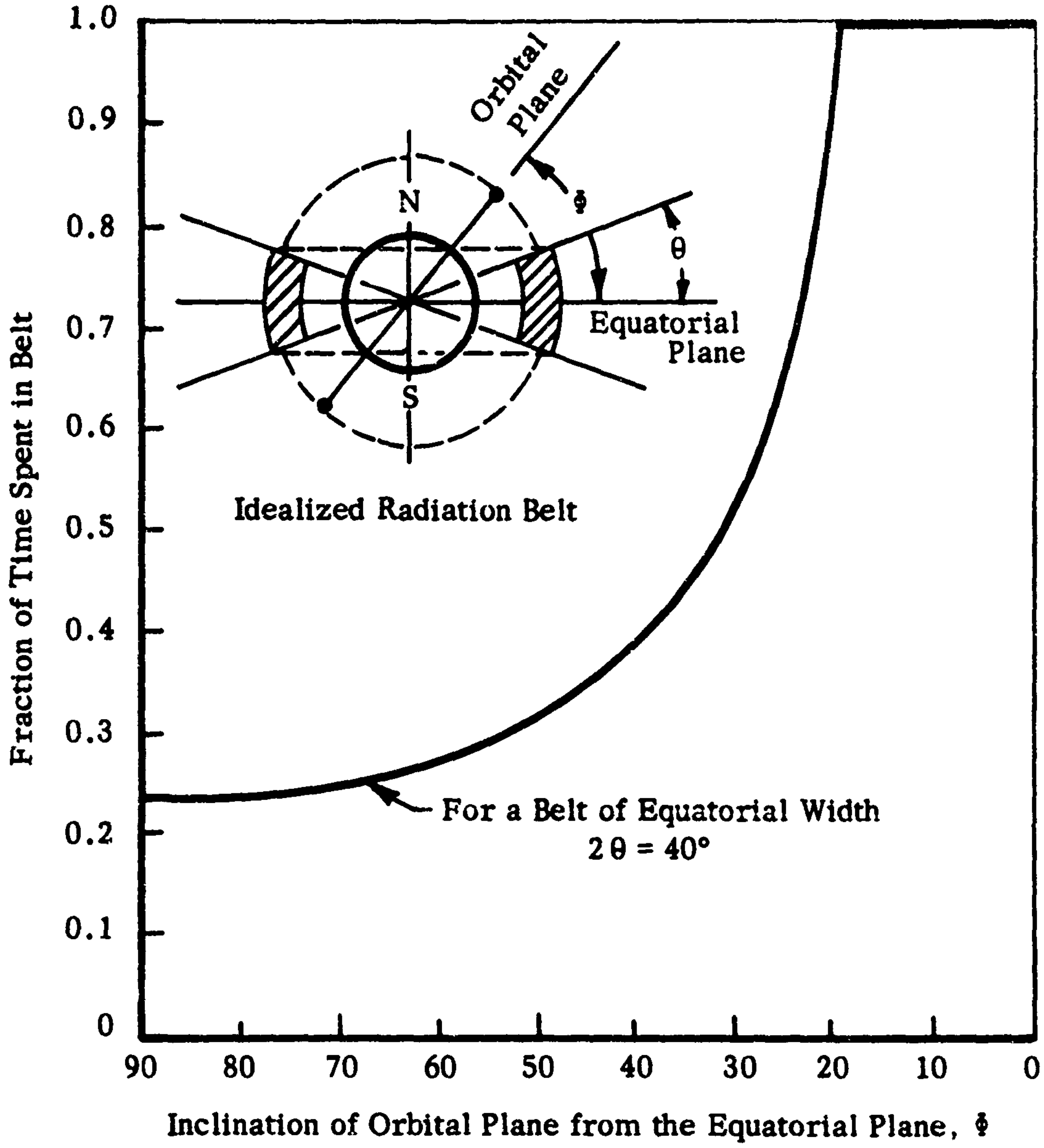

FIGURE 16. FRACTION OF TIME WITHIN AN IDEALIZED RADIATION BELT

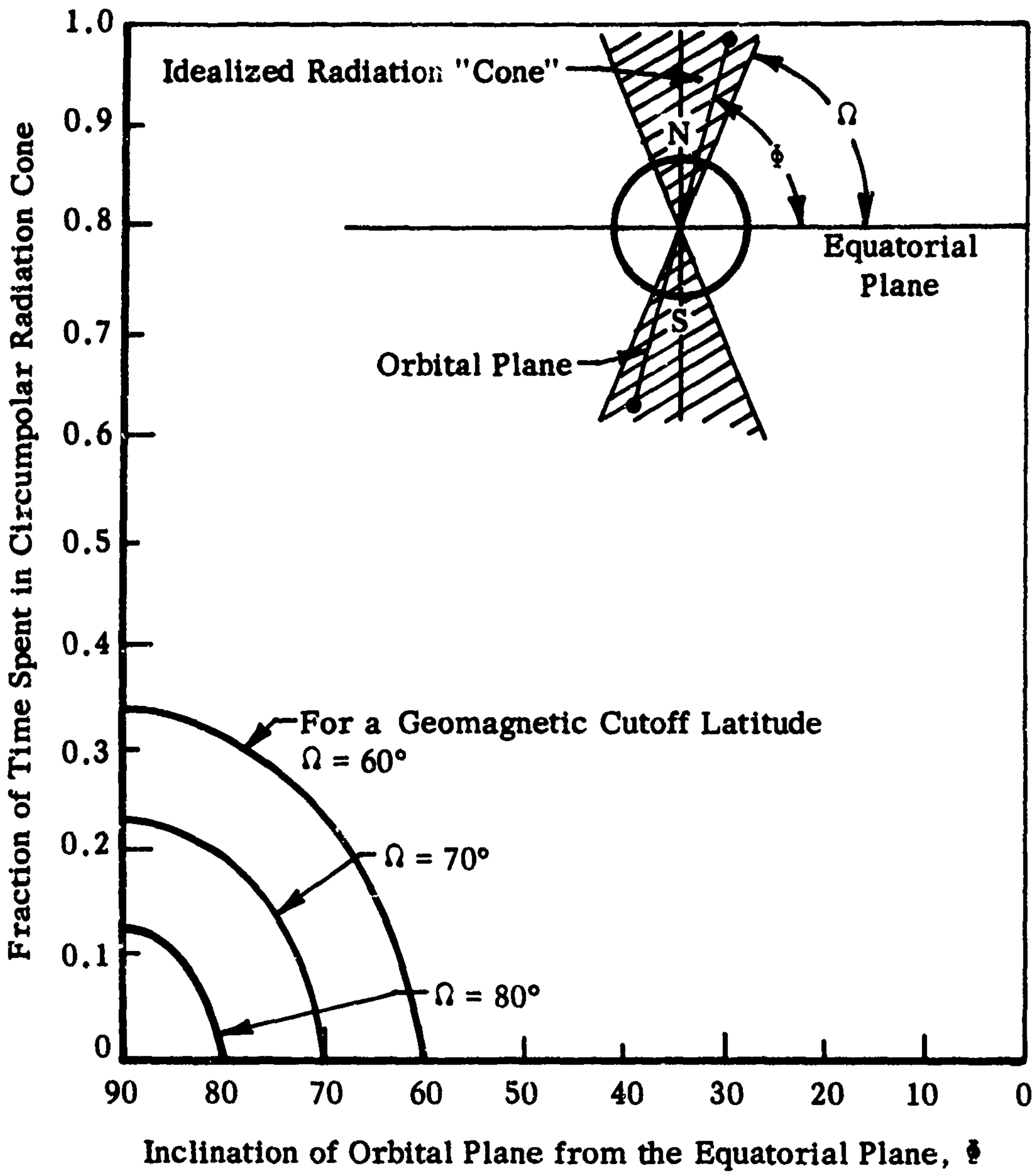

FIGURE 17. FRACTION OF TIME WITHIN AN IDEALIZED CIRCUMPOLAR RADIATION CONE

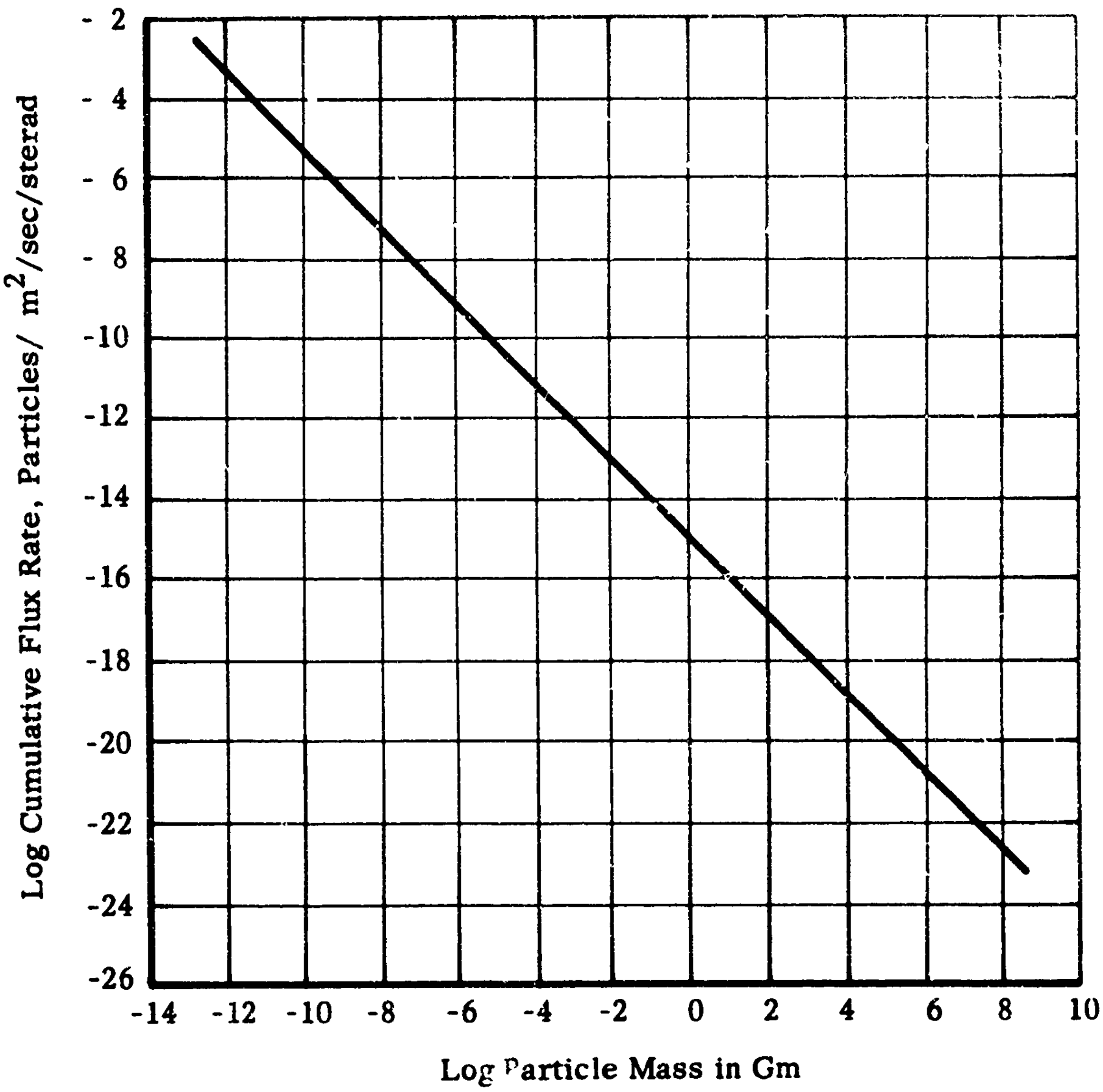

FIGURE 18. METEORITE FLUX IN THE VICINITY OF THE EARTH

SECTION VI
MATERIALS SELECTION

From the analysis of average orbit conditions, we estimated the range of properties of materials necessary to achieve thermal control. We found that to radiate the internally-generated heat from the suit surface, materials for the external surface of the space suit must at all times exhibit high emittance (ϵ) and a low absorptance-to-emittance ratio (α/ϵ). However, review of work on thermal control of space vehicles indicates that it is difficult to find coatings for flexible space suit materials which exhibit a controllable range of α/ϵ of 0.01 to 1.0 and at the same time have a high value of emittance, $\epsilon \geq 0.85$, necessary to achieve passive thermal control. A wide range of absorptance (α) is achievable through the use of louvers; however, such assemblies also exhibit high values of α/ϵ at the same time. Attention was thus focused on selecting materials which exhibit variable conductance.

A. VARIABLE CONDUCTANCE

To achieve thermal control by varying the conductance (C) of the flexible space suit wall, we found that for external suit materials with attainably low α/ϵ and high ϵ the material should have minimum conductance (approximately 0.5 Btu/sq ft hr ^{o}F) for periods of low metabolic activity and maximum conductance (approximately 20 Btu/sq ft hr ^{o}F) for periods of high metabolic activity. There are several ways to obtain this range of conductance. To permit a variation in the insulation characteristics of flexible space suit materials, control can be exercised over the heat transfer mechanisms of gas conduction, solid conduction, and radiation. The degree of variation that can be obtained may extend up to several orders of magnitude of thermal conductance.

1. Gas Conduction

The effect of gas conduction in an insulation can be divided into two regions: (1) a region ranging from atmospheric pressure down to a few millimeters of mercury in which conduction is independent of pressure, and (2) a region at pressures lower than a few millimeters where gas conduction depends on pressure. The transition from one type of conduction to the other depends on the geometry and the arrangement of the material making up the insulators as determined by the pressure required to obtain a specific mean free path of the gas molecules. When this mean free path is greater than the distance between the individual particles, the pressure-dependent region is reached. The thermal conductivity of the gas at this point decreases substantially until a lower limit is obtained when most of the gas molecules have been removed. The larger the particle spacing, the lower the pressure required for the thermal conductivity to approach its limiting value. At this lower limit, the thermal conductivity still has a finite value because heat can be transferred by both solid conduction and by radiation.

A change in insulating effectiveness is obtained when a gas is allowed to enter or leave the insulation during periods when thermal control is desired. Through proper choice of gas, the variation in gas conduction can be maximized.(13) Studies with cryogenic insulations have indicated that a three order of magnitude increase in conductivity (k) is possible when helium gas fills the evacuated layers of multifoil insulation.(14) Unfortunately, such high efficiency insulations, even when filled with helium, are still substantial barriers to heat flow and the maximum attainable conductivity is approximately 0.5 Btu in/sq ft hr $^{\circ}$F when helium filled. For the insulation reported, the range of conductance was from 0.0005 when evacuated to 0.14 Btu/sq ft hr $^{\circ}$F when filled with helium at atmospheric pressure. It is to be noted that the maximum conductance in this insulation is considerably less than the minimum conductance necessary in the proposed space suit insulation system.

For a gas-fillable insulation to provide effective thermal control, it should have good radiant heat transfer characteristics at all times and its total conductance should decrease by a factor of at least 50 when evacuated. Good radiation heat transfer can be achieved with a multilayer insulation which has a minimum number of black radiation shields, each of which has high emittance characteristics.

To estimate the range of conductance which can be achieved through the introduction of helium into an evacuated insulation, we calculated the contribution of the gas and radiation conductances in two hyopthetical insulations.

For convenience we assumed that the conductance consists of two components, the gas conductance and a combination of radiation and solid conductance. Of the latter two we assumed that the radiation conductance was controlling and therefore, total conductance can be represented by

$$C = k/\delta + \frac{1}{\mu} \frac{\sigma T_o^4}{T_o}. \tag{1}$$

The first term represents the gas conductance and the second term represents the radiation conductance. The factor μ is the radiation shielding factor given by

$$\mu = n \left(\frac{2}{\epsilon} - 1\right) \tag{2}$$

and represents the effect of adding radiation shields to an insulation system. The first term of equation 1 becomes negligibly small when the insulation is evacuated and becomes large when helium gas is introduced.

Results of our calculations are presented in table III. Insulation "A" corresponds to the insulation which was tested on the space suit section, and insulation "B" corresponds to the insulation tested in the screening program.

TABLE III

HEAT TRANSFER MODES IN PROPOSED SPACE SUIT INSULATIONS

$\epsilon = 0.9$

$t = 70^{o}F$

$k = 0.08$ Btu/sq ft hr ^{o}F (Helium at $70^{o}F$)

	Gas Conductance $\left(\frac{k}{\delta}\right)$	Radiant Conductance $\left(\frac{\sigma T_o^4}{\mu T_o}\right)$
<u>Insulation A</u>		
3 spacers 2 radiation shields 2 fabric layers Thickness 0.05 in	$19.2 \frac{\text{Btu}}{\text{sq ft hr } ^{o}F}$	$0.07 \frac{\text{Btu}}{\text{sq ft hr } ^{o}F}$
<u>Insulation B</u>		
5 spacers 2 radiation shields 2 fabric layers 2 calorimeter walls Thickness 0.09 in	11.0	0.04

2. Solid Conduction

To reduce the heat transfer by solid conduction, the conduction paths through an insulation must be broken up through the use of either finely-divided particulate materials (powders or fibers) or multilayer composites. In this manner resistances to heat flow are formed at the surface of individual particles or layers depending upon the contact areas between the materials.(15) One approach is to use multilayer composites such as crinkled aluminized polyester film. Studies have shown(14) that a three orders of magnitude increase in heat flux is obtainable when layers of this material are subjected to mechanical loads of up to 3 psi. A similar although less pronounced effect can be obtained by subjecting powders or fibers to mechanical loads. Although this method of increasing the conductance of a multilayer insulation is readily applicable to a space suit, we decided not to use it in our test program in favor of using the helium-fillable insulation.

3. Test Program

Samples of insulation for use in insulating a space suit were tested in the laboratory to determine their thermal conductance. In these tests, we used the double-guarded cold-plate apparatus shown in figure 19.(14) This apparatus consists of the following major components: (a) a measuring vessel enclosed in the ring-shaped guard vessel, (b) an outer guard jacket, (c) a warm plate on which the sample is placed, and (d) a sample chamber which permits the atmosphere and pressure surrounding the sample to be controlled separately from that of the bell jar enclosing the rest of the apparatus.

The apparatus can be used to study insulations whose thermal conductivities are between 10^{-4} and 20 Btu in/sq ft hr ^{o}F. It is designed so that one side of the sample can be exposed over a range of discrete temperatures from 5.9 to 438^{o}R depending upon the boiling point of the specific fluid used. The other side of the sample can be exposed to a range of temperatures from 36 to 900^{o}R by proper choice of circulating fluids. The test sample which is in the form of a disc 12 inches in diameter can be changed in thickness from 0 to 2 inches by applying mechanical compression from 0 to 50 psi while the test is in progress.

Modifications were made to the Model-12 thermal conductivity apparatus to permit measurement of conductivity of insulation samples when surface temperatures are +85^{o}F and -32^{o}F. These modifications were a heater for maintaining the sample inner surface at 85^{o}F, a heat flow meter for measuring the heat flux through the insulation, and a cooling system to maintain the sample outer surface at temperatures as low as -40^{o}F. Provision was made for testing 12-inch diameter samples, either evacuated or filled with helium, at low pressure. The apparatus arrangement is shown in figure 20.

Space suit insulation models which were tested in the thermal conductivity apparatus are summarized in table IV. Included for comparison is a typical

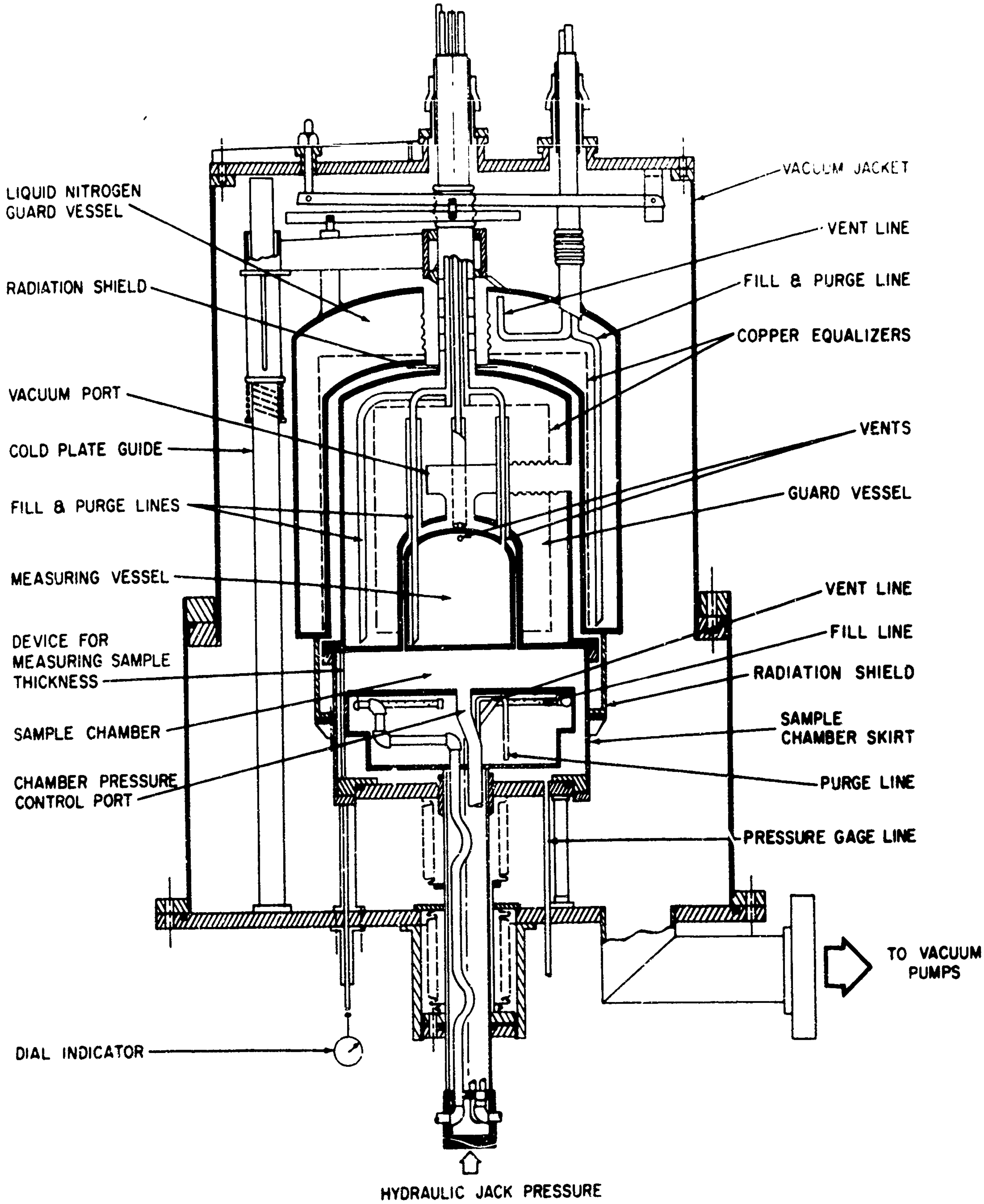

FIGURE 19. THERMAL CONDUCTIVITY APPARATUS

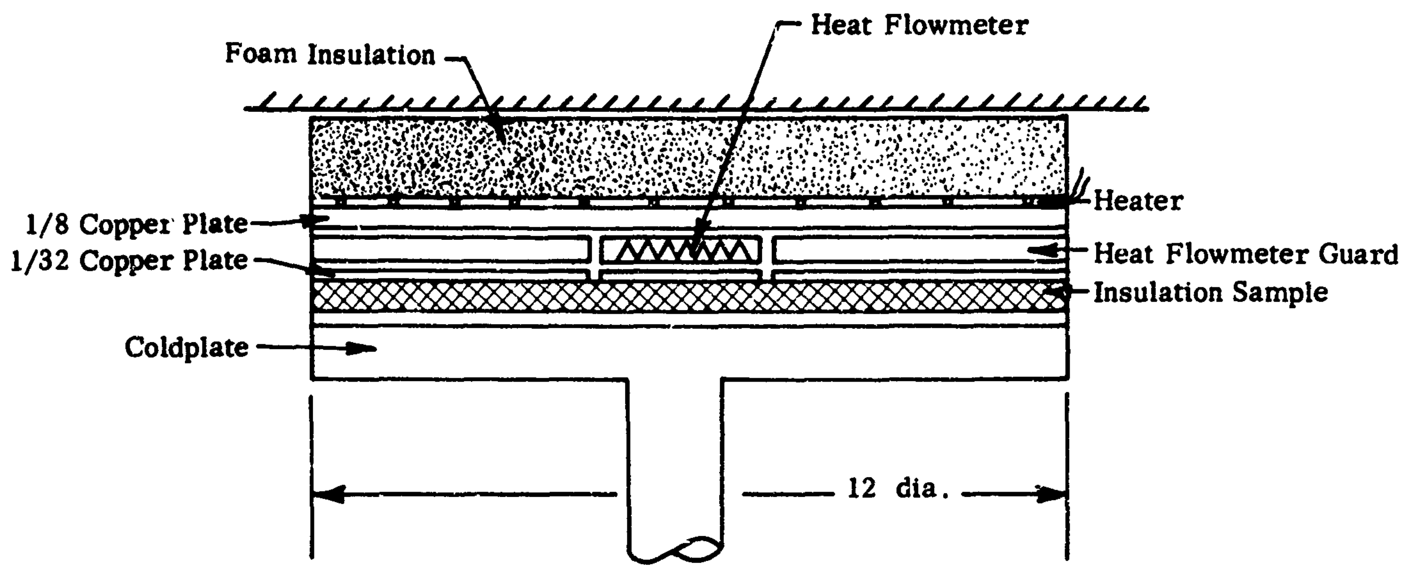

FIGURE 20. MODIFICATIONS OF THERMAL CONDUCTIVITY APPARATUS

TABLE IV

SPACE SUIT INSULATIONS TESTED

Sample No. 1

6 layers of nylon net - mesh, 1/16 x 1/16 in
5 layers of 0.00025-in mylar film, aluminized on both sides

Sample No. 2

3 oz Nomex HT-1 fabric
0.003-in nylon net - mesh, 1/16 x 1/16 in
0.004-in black polyethylene film
0.003-in nylon net
0.004-in black polyethylene film
0.003-in nylon net
3 oz Nomex HT-1 fabric

Sample No. 3

3 oz Nomex HT-1 fabric
0.003-in nylon net - mesh, 1/16 x 1/16 in
P-1807A neoprene coated rip-stop nylon fabric (black side facing the center of the insulation)
0.003-in nylon net
CAT 323 black dacron with polyurethane coating
P-1807A (black side facing the center of the insulation)
0.003-in nylon net
3 oz Nomex HT-1 fabric

Sample No. 4

3 oz Nomex HT-1 fabric
0.003-in nylon net - mesh, 1/16 x 1/16 in
P-1807A neoprene coated rip-stop nylon fabric (black side facing the center of the insulation)
0.003-in nylon net
P-1807A (black side facing the center of the insulation)
0.003-in nylon net
3 oz Nomex HT-1 fabric

Sample No. 3005

11 layers of nylon net - mesh, 1/8 x 1/8 in
10 layers of 0.002-in tempered minum

cryogenic insulation which is designed for low thermal radiation under all operating conditions (Sample No. 3005); it was tested during another program. The first sample tested in this present program (Sample No. 1) is similar to a multifoil insulation scheme which was originally proposed for the Gemini extravehicular space suit. Sample No. 2 was designed to have good radiant transmission characteristics under all conditions, good conduction characteristics when filled with helium at atmospheric pressure, and poor conduction characteristics when evacuated. Samples Nos. 3 and 4 are similar to the final configuration of space suit insulation tested in our space chamber under simulated 300 nautical mile orbit conditions.

In each test, optimum spacing of the calorimeter hot and cold plates was determined by measuring the heat flux for various spacings and using the spacing for minimum heat flow. Measurements of heat flow were made under vacuum conditions and for various pressures of helium gas in the insulation. There was some difficulty in maintaining the desired cold plate temperature for conditions of high conductivity encountered when helium filled the insulation at near atmospheric pressure. Results of these tests are summarized in table V. The range of conductance for the type of insulation used in tests with the space suit section was from about 0.1 Btu/sq ft hr ^{o}F when evacuated to 14 Btu/sq ft hr ^{o}F when helium filled.

The effect of helium gas pressure on thermal conductivity of the various samples is summarized in figure 21. For those samples (Samples 2, 3, and 4) which were designed to have good radiant transmission characteristics under all conditions, the maximum thermal conductivity was in excess of 1.0 Btu in/sq ft hr ^{o}F at atmospheric pressure. These insulations exhibited greater than a two orders of magnitude decrease in thermal conductivity when evacuated.

B. SURFACE COATINGS FOR LOW α/ϵ

The analytical phases of the program indicated that to achieve thermal control of the space suit its surface coating must have maximum emissive power at room temperature and minimum solar absorptance. Such materials exhibit high values of ϵ and low values of α/ϵ and are characteristic of the white-pigmented paints which have been used successfully for thermal control of orbiting space vehicles.

Several extensive studies on the effect of ultraviolet irradiation in vacuum on white spacecraft coatings have indicated that no materials are completely unaffected by ultraviolet irradiation in vacuum.(16,17) Ultraviolet radiation from the sun is the primary cause of damage to thermal control surfaces in an orbital environment. Although low values of α/ϵ can be achieved, the solar absorptance is degraded by ultraviolet attacking the pigments and pigment binders. Zinc oxide and, to a lesser extent, zinc sulphide were found to be unusually stable white pigments and formed relatively stable coatings when dispersed in pure potassium silicate or in certain methyl silicone polymers. Results of tests indicate that for long periods of exposure (approximately 2000 equivalent sun hours of ultraviolet

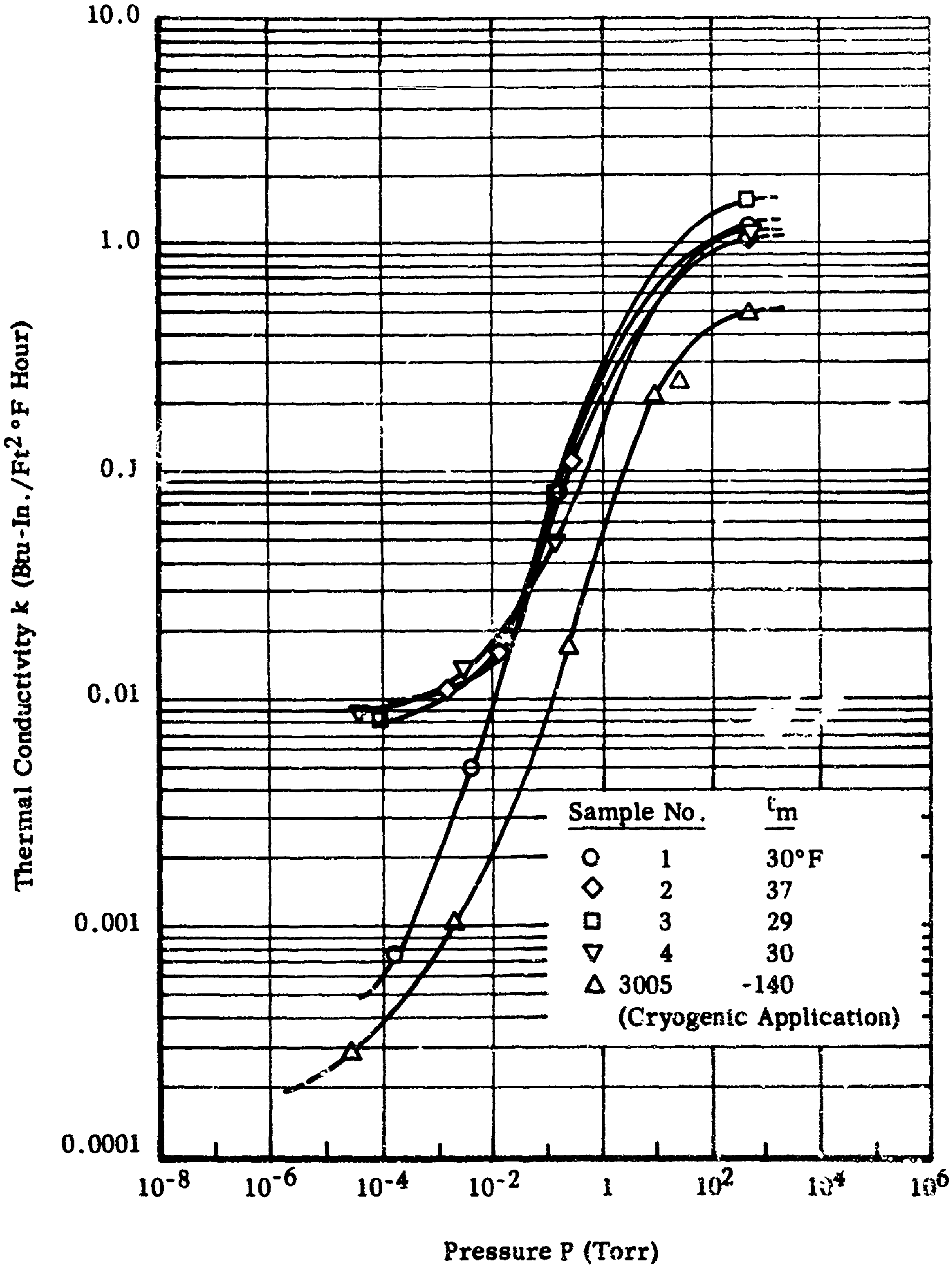

FIGURE 21. EFFECT OF HELIUM GAS PRESSURE ON THERMAL CONDUCTIVITY

TABLE V

RESULTS OF INSULATION SCREENING TESTS

Sample No.	Thickness (in)	Pressure (mm Hg)	Temperature Warm Plate (^oF)	Temperature Cold Plate (^oF)	ΔT	Heat Flux (Btu/sq ft hr)	Apparent Thermal Conductivity (Btu in/sq ft hr ^oF)	Apparent Conductance (Btu/sq ft hr ^oF)
1	0.127	2×10^{-4}	93	-34	127	0.75	7.5×10^{-4}	5.9×10^{-3}
	± 0.012	5×10^{-3}	93	-33	126	5.4	5.4×10^{-3}	4.3×10^{-2}
		0.2	90	-29	119	84	9.0×10^{-2}	7.1×10^{-1}
		760	56.5	-15.5	72	740	$1.3 {}^{+.15}_{-.09}$	$10.2 {}^{+1.1}_{-0.7}$
2	0.079	2×10^{-3}	108	-30	138	20	1.1×10^{-2}	1.4×10^{-1}
	± 0.021	2×10^{-2}	105	-31	136	28	1.6×10^{-2}	2.0×10^{-1}
		5×10^{-1}	109	-26	135	190	11×10^{-2}	1.4
		770	46	-10	56	765	1.1	14
3	0.089	1×10^{-4}	94	-35	129	12	0.83×10^{-2}	9.3×10^{-2}
	± 0.009	2.5×10^{-2}	92	-35	127	26	1.8×10^{-2}	2.0×10^{-1}
		2.0×10^{-1}	94	-37	131	114	8×10^{-2}	9.0×10^{-1}
		770	71	+ 1	70	1260	1.6	18
4	0.087	6×10^{-5}	95	-35	130	13	8.7×10^{-3}	1.0×10^{-1}
	+ 0.012	5×10^{-3}	94	-34	128	19	1.3×10^{-2}	1.5×10^{-1}
	- 0.002	2×10^{-1}	92	-34	126	76	4.9×10^{-2}	5.6×10^{-1}
		760	93	-20	113	1800	1.2	14

radiation) the coatings least affected are those made with a silicone or a potassium silicate binder and pigmented with zinc oxide.[16] However, for short duration exposures titanium dioxide pigments do not degrade appreciably.

Studies were recently initiated by NASA to determine the ϵ and α/ϵ characteristics of coated flexible space suit materials. Two of the organizations presently participating in this program were contacted and information and samples of candidate coatings were provided for screening tests.

1. Available Materials

Four candidate flexible coatings with low α/ϵ properties were chosen for application to flexible space suit materials (table VI). The sample designated S-13 silicone polymer with zinc oxide pigment is a formulation reported in reference 16. Samples Nos. 2 and 3 were provided by Dr. Norma Searle of American Cyanamid Co. in Stamford, Connecticut. The fourth sample tested was an epoxy resin with titanium dioxide pigment which is a standard formulation by the Finch Paint & Chemical Co., of Torrance, California. All samples of material were applied to 3 oz and 6 oz high temperature nylon cloth Nomex HT-1 by the techniques recommended by the persons responsible for their formulation.

2. Test Program

To establish the thermal performance characteristics of these samples, two tests were performed on each sample.

a. Room Temperature Emittance

Emittance of each sample was measured using the emissometer shown in figure 22. This instrument uses the receiver disc principle. A thin circular blackened disc about 2-1/2 inches in diameter is placed closely adjacent and parallel to a circular sample in an evacuated space. The back side of the receiver disc (also blackened) is surrounded by a black cavity held at a temperature that is low with respect to that of the sample. The receiver disc exchanges heat with the sample on one side and with the black cavity on the other, principally by radiative heat transfer. The geometry is such that the heat transfer between the sample and the receiver is essentially that between two infinite parallel planes. Radiative transfer between the side of the disc and the black cavity is essentially that between two black bodies. From measurement of the sample temperature, the cavity temperature, and the disc temperature, the emissivity of the sample can be determined.

The sample is mounted on the lower surface of the sample holder block and its temperature is maintained at a desired fixed level to within $\pm$ 0.25^{o}F by means of a controlled heater. The cavity temperature is maintained at a desired low temperature (e.g., liquid nitrogen temperature) while the receiver disc temperature is measured with a thermocouple. The apparatus can be used for comparative measurements without extensive calibration.

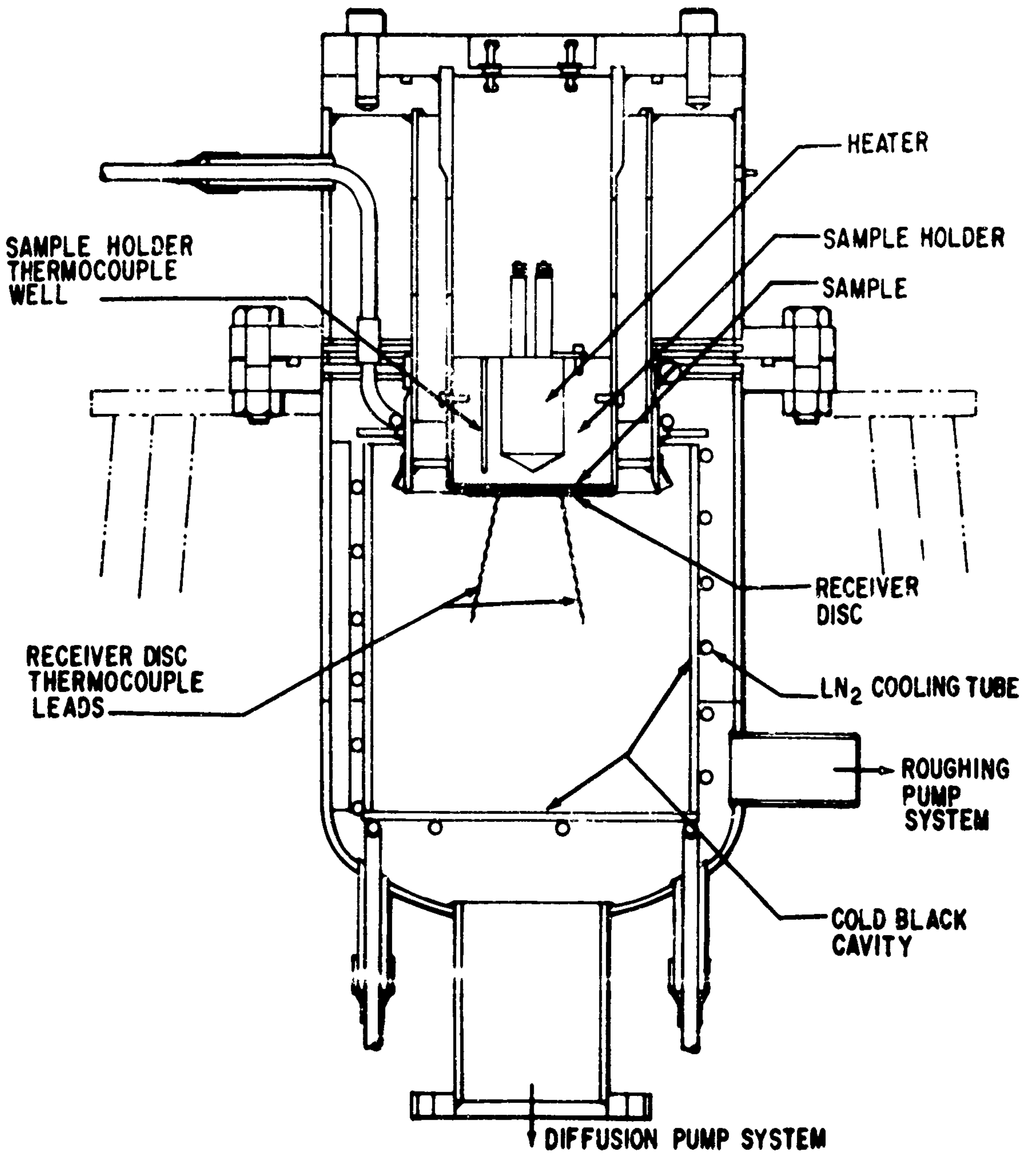

FIGURE 22. EMISSOMETER

TABLE VI

SUMMARY OF SOLAR ABSORPTANCE AND EMITTANCE FOR FLEXIBLE SPACE SUIT OUTER GARMENT MATERIALS

Coating	Coating Thickness (in)	Weight of Nomex Material (oz)	Solar Absorptance α	Room Temperature Emittance ϵ	Ratio α/ϵ
S-13 silicone polymer with ZnO pigment	0.004-0.005	6	0.16	0.73	0.22
	0.004-0.005	3	0.16	0.70	0.23
PDL-1-3066 melemine modified polyvinyl butyral resin with TiO_2 pigment	0.001-0.002	6	0.21	0.82	0.26
	0.001	3	0.20	0.82	0.24
PDL-1-3067 thermosetting epoxy acrylic resin with TiO_2 pigment	0.002-0.003	6	0.19	0.78	0.24
	0.002-0.003	3	0.19	0.83	0.23
Cat-a-lac W-443-1-500 epoxy resin with TiO_2 pigment	0.002-0.003	6	0.21	0.89	0.24
	0.003-0.004	3	0.21	0.91	0.23
Uncoated samples	0.012	6	0.38	0.80	0.47
		6	0.34		0.43
	0.006	3	0.35	0.86	0.40
		3	0.36		0.42

Results of these emittance measurements are given in table VI. Also summarized in table VI are the room temperature emittances for uncoated samples of the base material.

b. Absorptance Tests

Coated and uncoated samples were also measured for their solar absorptance. In these tests a Beckman DK spectrophotometer with an integrating sphere attachment was used to measure the spectral reflectance of samples in the wavelength region from 0.2 to 3.0 microns. Measurements were made with freshly prepared MgO as the reflectance standard. An IBM 1041 data reduction program was used to compute solar absorptance from the measured spectral reflectance and the known reflectance of MgO. Results of these measurements are summarized in table VI. Included in this table are the corresponding measured values of room temperature total hemispherical emittance for coated and uncoated materials. The ratio of absorptance to emittance (α/ϵ) was calculated and is also included in this table.

The S-13 silicone polymer with the ZnO pigment exhibited the lowest value of solar absorptance but not the lowest value of room temperature emittance. However, it did exhibit the lowest value of the ratio α/ϵ. The 6 oz Nomex material with S-13 silicone polymer with ZnO pigment was used in the space suit section which was tested in a simulated 300 nautical mile orbit.

C. RADIATION DAMAGE TO SPACE SUIT MATERIALS

A study was made of the effects of the space radiation environment at altitudes between 300 and 23,000 nautical miles on typical materials which may be used in systems for thermal control of space suits.

1. Ultraviolet Radiation

At all altitudes, solar ultraviolet radiation will degrade the performance of high α/ϵ surface coatings, mainly by increasing α.[18] However, the magnitude of this effect and its time and temperature dependence vary greatly among different coating materials, and a careful selection of pigments, polymer films, and other vehicles will be necessary.

Coatings of high-purity zinc oxide or zinc sulphide dispersed in a silicone resin have shown particularly low rates of degradation. In favorable cases, the increase in solar absorptance is reported to be less than 0.02 after 4200 equivalent sun-hours ultraviolet radiation.[16] Other pigment and vehicle combinations with relatively stable α when subjected to simulation tests include TiO_2/silicone and Li-Al-SiO_3/Na_2 SiO_3.[17] However, comparisons of simulation results with data obtained during space flights have generally poor agreement,[6] so caution must be exercised in predicting the ultraviolet stability of any given coating.

2. Ionizing Radiation

The low-energy components of the several space radiation fluxes are of primary interest in evaluating damage to space suit materials. This is because the high-energy protons and electrons will penetrate the [illegible] injure or kill its occupant long before they will noticeably af[illegible] polymers, pigments, or metals.

At altitudes below the magnetopause (about 34,000 nautical miles) the solar wind is deflected away from the earth.[6] Galactic cosmic rays have such a low flux that damage from this source will be negligible.[9] The two remaining sources of ionizing radiation are solar flares and the Van Allen belts. At an altitude of 300 nautical miles, an astronaut will be exposed to the lower fringes of the radiation belts. In the worst case, this orbit corresponds to a distance of 1.16 earth radii above the magnetic dipole axis. In this region, for exposures of several weeks, the surface doses due to low-energy electrons and protons are estimated to be well below the levels required for noticeable changes in optical properties of coatings (10^6 - 10^8 rads).

Although limited information is available on the low-energy component of solar flares, it is unlikely that surface doses from a major flare will exceed 10^5 rads.[9] In such a case, the astronaut is likely to receive a dangerous body surface dose of about 1000 rads if he is protected by nothing more than a light suit (0.5 gm/cm^2). The low probability of a major flare, coupled with the likelihood of obtaining at least a 30 minute warning by microwave monitoring on earth and transmission of the warning to the astronaut, would reduce this hazard to one which has to be handled in terms of the space vehicle rather than an extravehicular protection system.

In summary, the effects of ultraviolet radiation are expected to be more serious than those caused by ionizing radiation when the astronaut is not injured or killed by the radiation dose.

SECTION VII
ORBIT SIMULATION

On the basis of results of screening tests, we designed an experiment to test the feasibility of using a helium-filled evacuated insulation as a method for controlling the thermal environment of an astronaut within a flexible space suit. For the test program, we used a cylindrical calorimeter to simulate a short section of an astronaut's arm. On this calorimeter we tested two insulations; one was evacuated and the other was filled with helium. Each assembled space suit section was tested in an ADL space simulation chamber which was equipped with a solar simulator and a planet infrared radiation simulator. Tests were made for a 300 nautical mile orbit at the equilibrium conditions encountered when the space suit section is located on the earth-sun line and when it is located in the earth's umbra. The space suit section was not subjected to alternate solar radiation and then shade as would be encountered in an actual 300 nautical mile noon orbit because the equilibrium conditions achievable after long periods in either sunlight or in the earth's umbra provide the extreme limits to the orbit environment. Second, an exact simulation of the earth orbit environment requires that the space suit section be rotated and that the planet simulation also be rotated while the model proceeds on its 88-minute earth orbit. Such refinements in simulation are beyond the limits of the present space chamber.

A. FACILITIES

1. Space Chamber

The space simulation chamber (figure 23) is a cylindrical vessel 5 ft in diameter and 7-1/2 ft long, mounted vertically. The top of the chamber is removable to permit access to tests within the chamber. The main chamber opening is sealed at a flange near the top. In addition, there is an 8-inch window for observing experiments in the chamber.

The chamber contains two copper baffles which completely enclose the test area of the chamber. One baffle is mounted in the lower section of the chamber and the second baffle is attached to the removable top. These baffles contain integrally mounted coils through which is circulated liquid nitrogen for control of their temperature. The interior surface of the chamber baffles is coated with 3M velvet black which has an emittance of approximately 0.93 at room temperature. The purpose of this coating is to provide a highly absorptive surface and to prevent reflection of solar energy.

The chamber is equipped with a 6-inch diffusion pump that reaches pressures of 10^{-6} torr. The facility is also equipped with an automatic liquid nitrogen filling system which always maintains the inner shrouds of the chamber at temperatures of approximately 139°R.

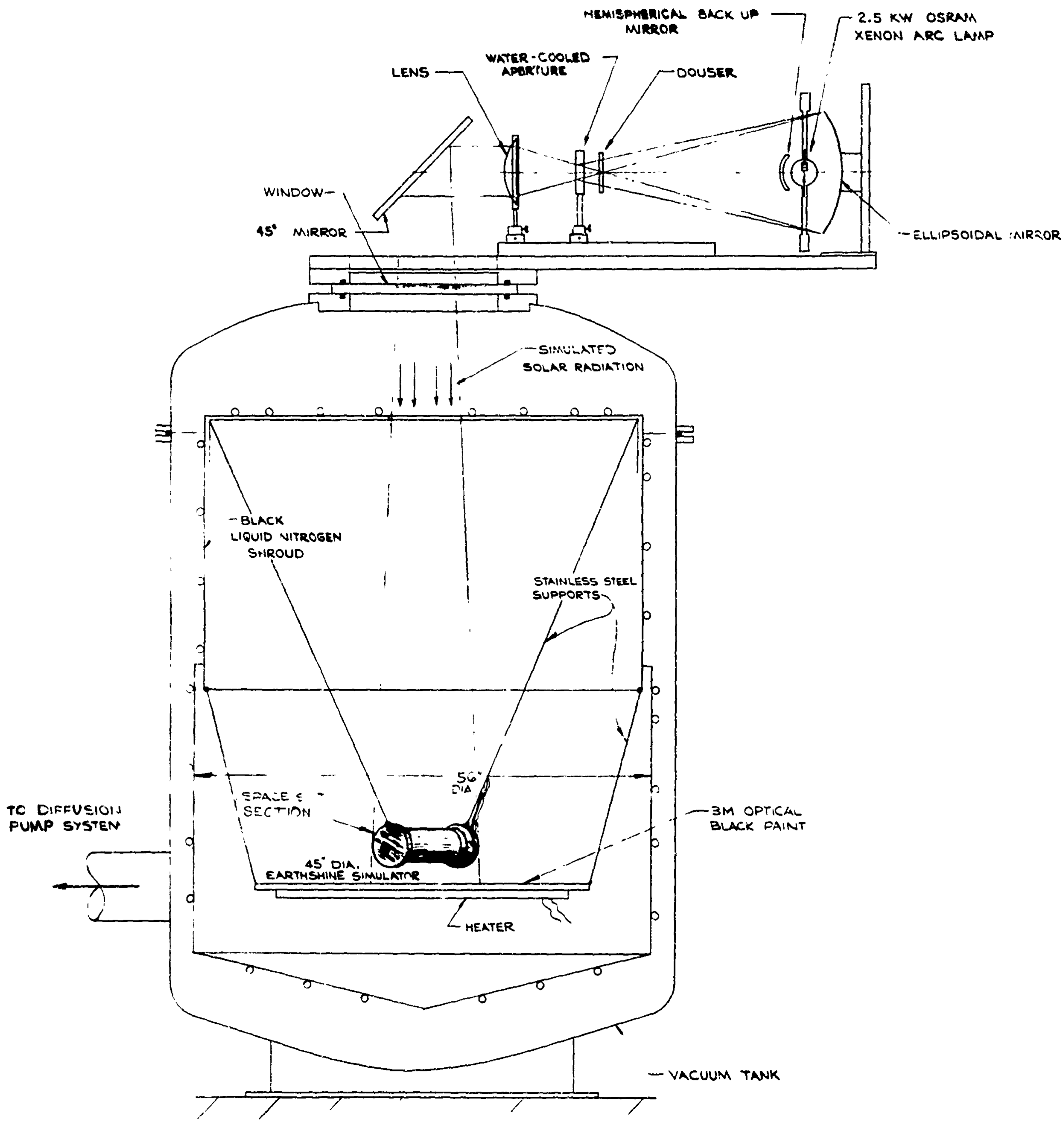

FIGURE 23 SPACE CHAMBER SCHEMATIC

2. Solar Simulation

A solar simulator was fabricated which utilizes a 2.5 kw Osram [illegible] as the radiant source. Radiation from this lamp is collected with [illegible] ellipsoidal mirror and focused on a water-cooled aperture. This ap[illegible] is placed at the focal point of an 8-inch diameter, 10-inch focal le[illegible] lens. This lens provides a nearly collimated beam of radiant energy. The beam is directed downward into the chamber by a 45-degree front surfaced mirror located on the top of the space chamber. Radiation enters the chamber through a 3/4-inch thick Pyrex window. Radiant output of the lamp is controlled by varying the current and voltage at the lamp terminals.

The solar beam was adjusted to a diameter of 10 inches at the surface of the space suit section, the lamp current was increased until there was a solar intensity of approximately 442 Btu/sq ft hr throughout the 10-inch beam. Measurements were made in the center of the beam and on a circle 6 inches in diameter. Measurements indicated that the radiant intensity distribution was 442 $\pm$ 10% Btu/sq ft hr throughout this area. Measurements were made with an eight-junction Eppley thermopile with a sensing element 3/16 inch in diameter. This instrument has a flat spectral response in the spectral range of the simulated solar beam. The solar beam was estimated to have a half angle divergence of 5 degrees.

The spectral distribution of the simulated solar energy in the chamber was estimated to be similar to that shown in figure 24. For comparison, the relative intensity of solar energy is included. The sharp cut-off in simulated solar energy at a wavelength approximately at 0.3 micron is attributed to the cut-off characteristics of the Pyrex lens of the solar simulator and the Pyrex window in the space chamber. In comparison to the solar spectrum, the xenon lamp has an excess of radiant energy in the region from 0.8 to 1.0 micron.

From the above it can be seen that the solar simulator, although not faithfully reproducing the spectral distribution of the solar energy, does, however, provide an incident heat flux equivalent to one solar constant.

3. Planet Simulation

Earth radiation was simulated by a high emittance electrically heated plate placed 5 inches from the centerline of the space suit section. To simulate the long wavelength earth radiation to the space suit section when it was located in the earth's umbra, the earthshine panel design temperature was 432°R. For combined earth radiation and solar albedo, we simulated absorbed heat flux. For space suit surface properties of $\alpha_s = 0.16$ and $\epsilon_o = 0.73$, the design equilibrium temperature of the earthshine panel is 510°R to simulate the absorbed radiation when the space suit section is located on the earth-sun line.

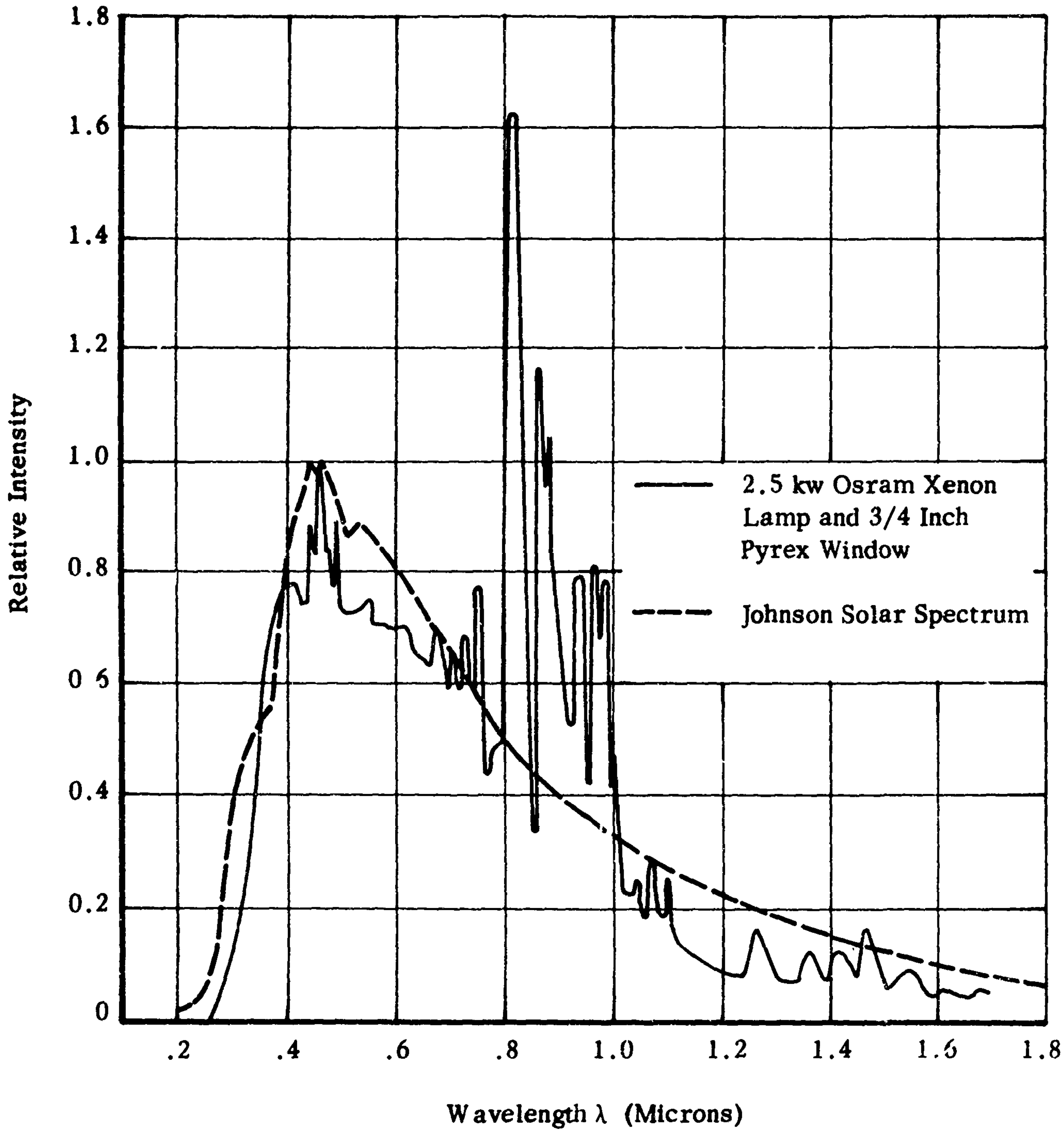

FIGURE 24. RELATIVE SPECTRAL INTENSITY OF SIMULATED SOLAR ENERGY

B. SPACE SUIT SECTION

1. Basic Configuration

A cylindrical section representative of an arm section of a space suit was chosen for test. The size of the section was determined [illegible] by the maximum diameter of the solar beam in our test chamber. In addition, space suit components were available which could be readily adapted for our space chamber tests.

In addition to simulating the external environment of a space suit section, we also simulated the internal environment--i.e., the metabolic heating rate of the astronaut and the various associated internal subsystem heating rates--by placing in the space suit section two half-cylinder aluminum calorimeters, each equipped with an electrical heater (figure 25). The calorimeters were 3-1/2 inches in diameter and 6 inches long. The heater inside each calorimeter simulated the metabolic heating rate per unit area of the astronaut. Over this two-section cylindrical calorimeter was a gas-tight bladder that formed the enclosure for the astronaut's environment. The bladder was made from neoprene-coated rip-stop-nylon cloth and was anchored to the bulkheads of the calorimeter assembly by a molded neoprene flange.

The outer wall of the inner bladder was equipped with eight thermocouples equally spaced circumferentially in a plane at the middle of the calorimeter assembly. These thermocouples were made from No. 40 copper-constantan (0.003-inch diameter) and were used to measure the circumferential temperature distribution on the inner wall of the space suit.

Figure 26 is a composite photograph of the space suit section during various stages of assembly.

2. Insulations Tested

The two insulations tested were an evacuated multilayer insulation and the same insulation filled with helium. To insure that the evacuated insulation reached a pressure at which gas conduction is negligible, the insulation had its ends open to the low vacuum of the space chamber. This was done by wrapping the requisite layers of insulation on the bladder.

For the helium-fillable insulation, a gas-tight structure was fabricated from the requisite number of insulation components (figure 25). While each of these insulations was installed on the bladder, the bladder was inflated to a pressure of 8 inches of mercury. After the insulation was applied, the outer layer of the space suit was wrapped around the insulation and laced in position. This procedure insured that the insulation had negligible mechanical loading.

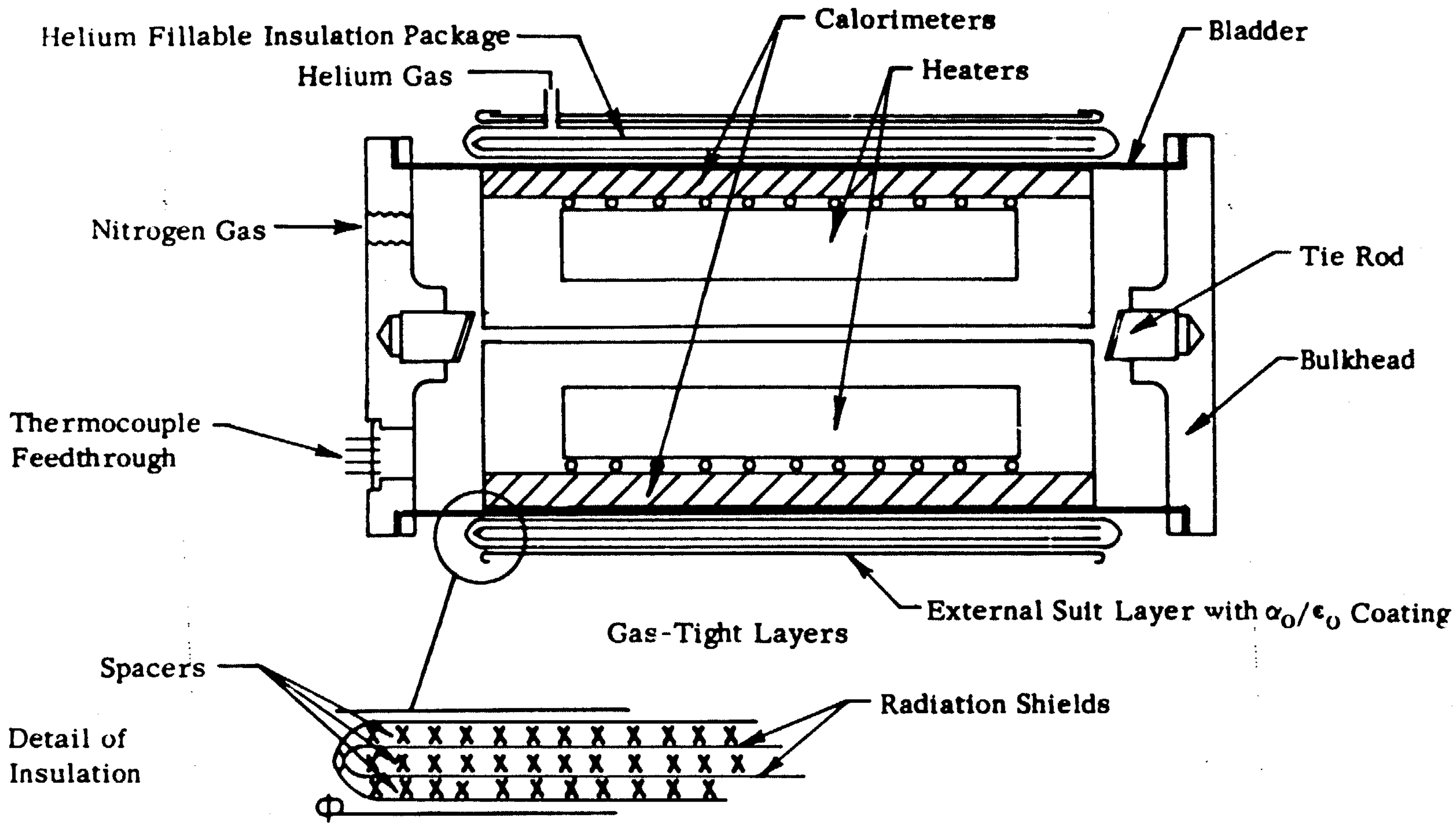

FIGURE 25. SECTION OF SPACE SUIT

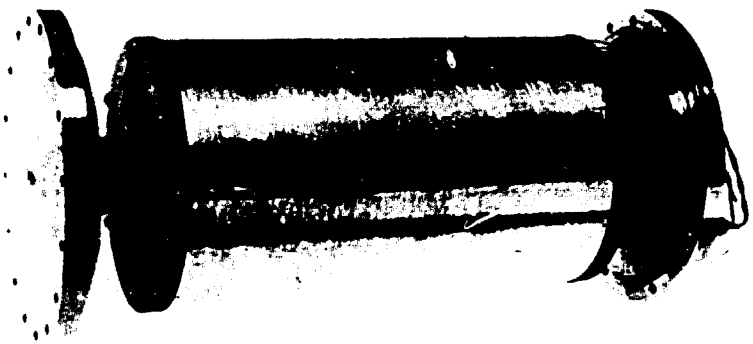

Calorimeter

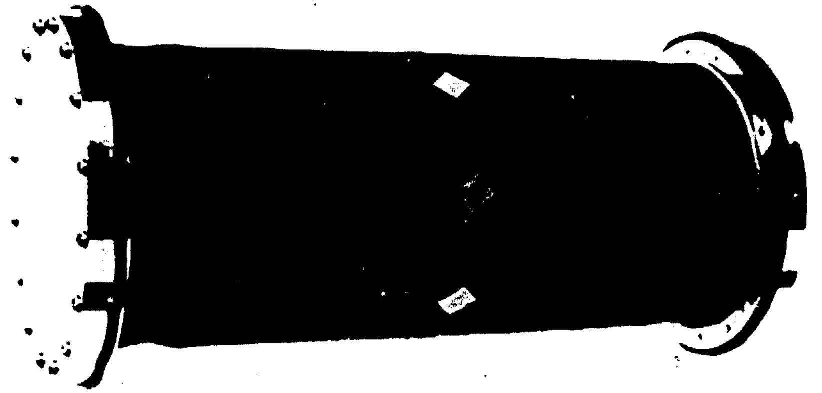

Instrumented Bladder

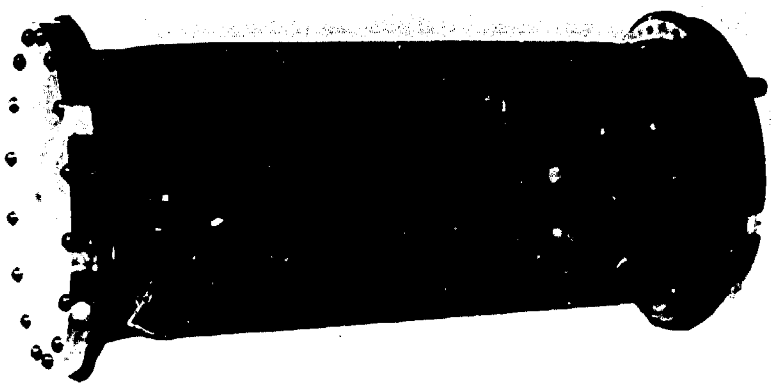

Bladder

Insulation and HT-1 Nomex Cover
No α_0 / ϵ_0 Coating

FIGURE 26. SPACE SUIT SECTION IN VARIOUS PHASES OF ASSEMBLY

The outer layer of the space suit with either insulation was covered with 6-oz Nomex and was equipped with eight No. 40 copper-constantan thermocouples which, when the outer cover was laced on the outside of the insulation, were located radially above the eight inner thermocouples. The external thermocouples measured the circumferential temperature distributions in the outer layer of the space suit.

The space suit section was then given a 0.005-inch thick α_o/ϵ_o surface coating of S-13 formulation of zinc oxide in silicone polymer. The assembled space suit section shown in figure 27 is suspended in the space simulation chamber above the earthshine panel and the solar simulator is in operation.

3. Auxiliary Instrumentation

In addition to the eight thermocouples on the inner wall and on the outer wall of the space suit, each calorimeter contained two thermocouples for monitoring its temperature. These thermocouples were led out of the inner wall of the calorimeter through a feedthrough, and all thermocouples were led out of the chamber through chamber-wall thermocouple feedthroughs. All thermocouples were connected to a thermoelectric ice reference junction. Millivolt outputs from the 16 thermocouples on the space suit wer read out on a 16-point recorder, while the calorimeter thermocouples and the thermocouples on the earthshine panel were read by means of a potentiometer.

Pressures, within the space suit calorimeter and within the insulation when filled with helium, were separately measured by differential mercury manometers which indicated the pressure differential between the space suit calorimeter interior and the pressure of the space chamber. Figure 28 is a schematic diagram of the instrumentation used in the test program.

C. TEST PROGRAM

Each of the two insulations was tested in the earth umbra and then on the earth-sun line. The sequence of testing was as follows:

1. The insulation which could be evacuated was installed on the calorimeter bladder and then placed in the chamber. The chamber was pumped down, the calorimeter was filled with nitrogen at 8 inches of mercury, and the earthshine panel was heated to a temperature of $432^{\circ}R$. These conditions simulate the earth umbra orbit position. A range of metabolic activity was simulated by alternately increasing the power input to the calorimeters and waiting for equilibrium conditions.

2. The solar simulator was then turned on and the earthshine panel was heated to a temperature of $513^{\circ}R$. These conditions simulate the earth-sun line orbit position. A range of metabolic activity was again simulated. At the conclusion of the tests

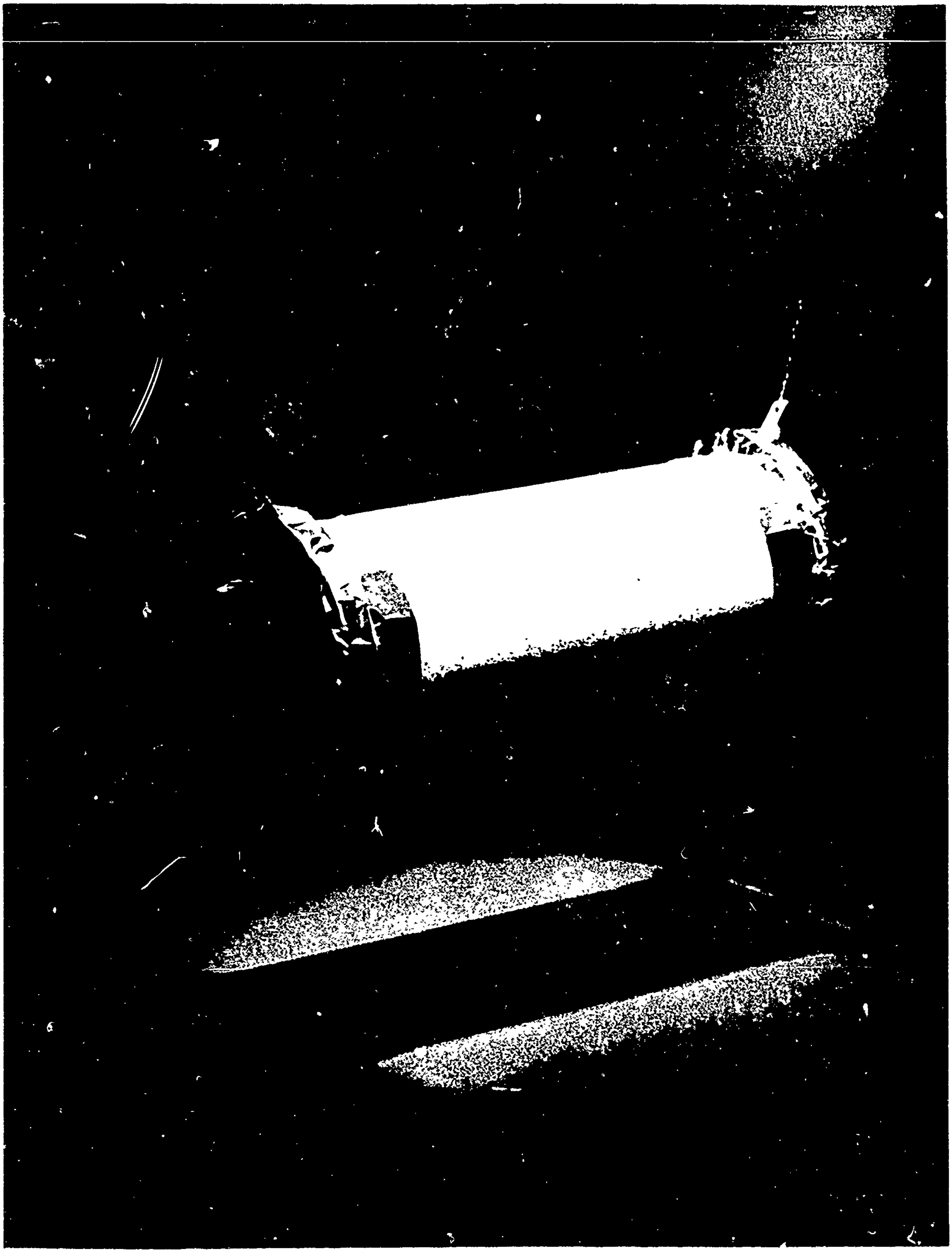

FIGURE 27. SPACE SUIT SECTION IN THE SOLAR BEAM

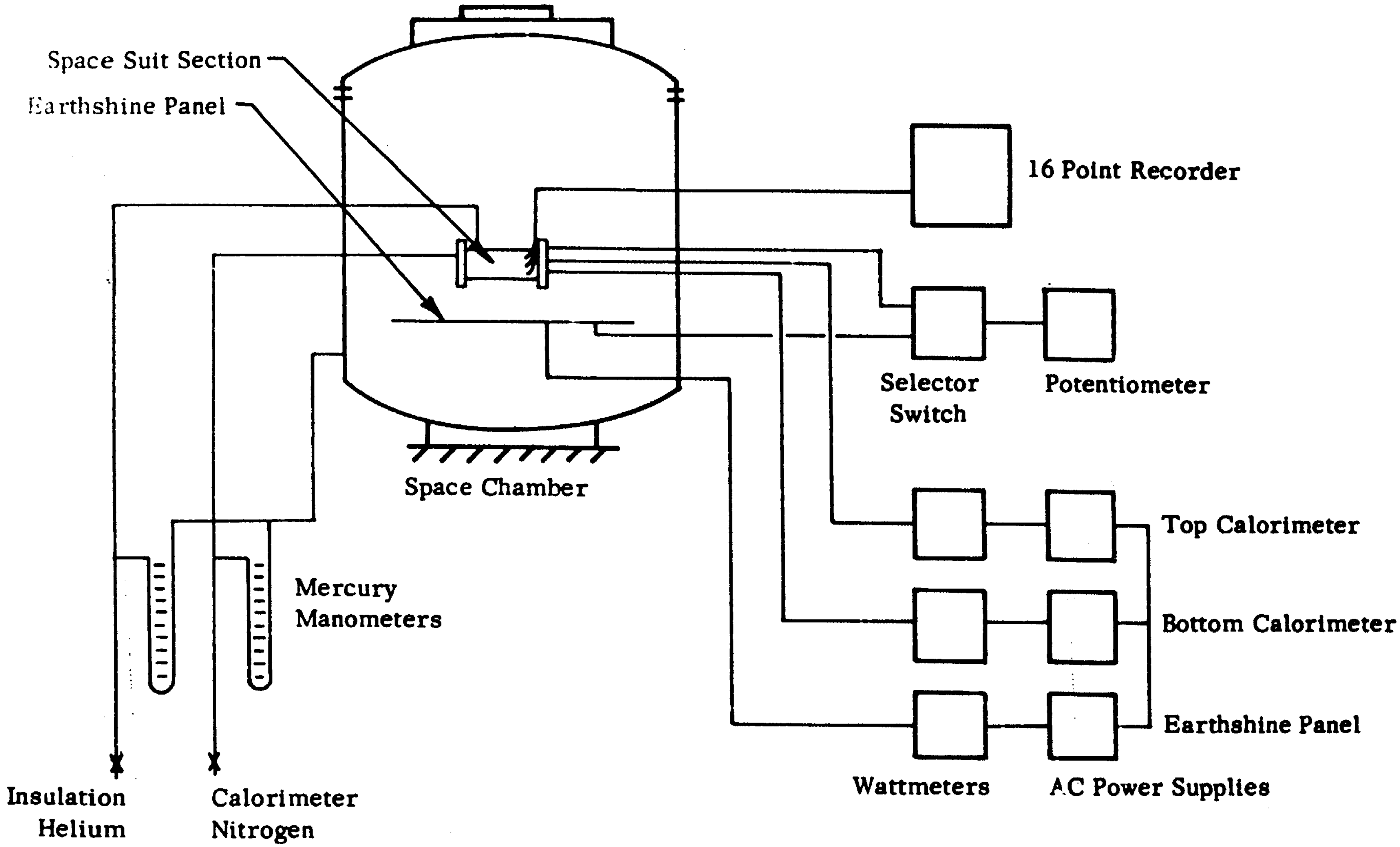

FIGURE 28. SCHEMATIC DIAGRAM OF INSTRUMENTATION

with the evacuated insulation, the space chamber was opened and the space suit section was removed and the evacuated insulation was replaced with a helium-fillable insulation.

3. The space suit section with helium-fillable insulation was placed in the chamber. The chamber was pumped down, the calorimeter was filled with nitrogen at 8 inches of mercury, the insulation was filled with helium at a pressure of 6 inches of mercury, and the umbra orbit position was again simulated.

4. At the conclusion of tests in the earth umbra orbit position, the solar simulator was turned on and the earthshine panel was heated to 513°F to simulate the earth-sun line orbit position.

For simulation of conditions in the earth umbra, the earthshine panel was maintained in the temperature range of 450-455°R. For simulation of the environment on the earth-sun line, the model was irradiated with a flux intensity of 442 $\pm$ 10% Btu/sq ft hr by the solar simulator. The absorbed radiant flux from the combined earthshine and albedo was simulated by maintaining the earthshine panel in the temperature range of 508 to 521°R. For all orbit conditions simulated, the walls of the space chamber were maintained at 139°R (liquid nitrogen temperature) to simulate deep space.

The space suit section was suspended in the test chamber and located over the center of the earthshine panel as indicated in figure 23. The chamber was evacuated to pressures in the range of 10^{-4} torr for all tests. Electrical power was applied to each of the two calorimeters which simulated the astronaut's metabolic rate. The two calorimeters were oriented so that their dividing line was parallel with the earthshine panel. Thus, one calorimeter faced the earthshine panel and the other faced either deep space or the solar simulation beam, depending on the orbit being simulated.

For each power input to the calorimeters, temperatures were recorded at half-hour intervals until we thought that equilibrium temperatures had been achieved. It often took as long as three hours for the temperature change in each calorimeter to become less than 2°F per hour, particularly during tests with the evacuated insulation. At equilibrium, calorimeter temperatures were measured and the time was noted on the printout record of the 16 thermocouples located circumferentially on the inner and outer walls of the space suit. Power input to the calorimeters was then increased and the calorimeter temperatures were monitored until equilibrium conditions were again achieved. Calorimeter power input was increased stepwise until at least three equilibrium conditions had been achieved for each orbit position and insulation.

As a result of the long time constant for the insulated calorimeter system, good equilibrium conditions were not always achieved during the test period. To correct this lack of equilibrium, the calorimeter temperatures were plotted as a function of time and a smooth curve was extrapolated through them to what was believed to be the final equilibrium temperature. This final equilibrium temperature correction seldom exceeded the last measured equilibrium temperature by more than 1 or 2°F.

Pressures within the bladder which surrounds the calorimeter were maintained at 8.0 inches of mercury for all tests. For tests when helium was used to fill the insulation space, the helium was maintained at a pressure of 6 inches of mercury.

Output of the solar simulator was maintained at a constant level by maintaining the lamp input in the range of 1.85 to 1.90 kw.

D. TEST RESULTS

1. Equilibrium Temperatures

Calorimeter equilibrium temperatures were measured for each insulation configuration and for the two orbit positions. The object of these tests was to determine the maximum metabolic rate possible before the astronaut experiences uncomfortably warm skin temperatures. We assume that the temperature of the calorimeters is indicative of the astronaut's skin temperature.

Summarized in figure 29 are the calorimeter equilibrium temperatures for the space suit section in the earth umbra, for both the evacuated insulation and for the helium-fillable insulation. Indicated on this figure is the range of the comfort zone. For each insulation there is a difference in the equilibrium temperature between the two calorimeters in the space suit section. The orientation of each calorimeter is indicated. The calorimeter facing the earth always indicated a slightly higher temperature than did the calorimeter facing either the space or the sun.

Figure 29 shows that there is a substantial increase in metabolic range when the evacuated insulation is filled with helium. The maximum metabolic rate possible before the comfort zone is exceeded is approximately 600 Btu/hr, for the evacuated insulation. For the helium-fillable insulation the comfort zone temperature is not exceeded until the astronaut is working at a metabolic rate of almost 2200 Btu/hr. Figure 29 indicates that by filling the insulation with helium a wide degree of control of the heat transfer rate through the insulation is possible.

Calorimeter equilibrium temperatures for the space suit section on the earth-sun line are shown in figure 30 for both the evacuated and the helium-fillable insulation. Again the maximum metabolic rate before the comfort zone is exceeded for the evacuated insulation is approximately 600 Btu/hr. When the insulation is filled with helium, the heat transfer through the insulation is again increased and there is an increase in metabolic rate to approximately 1600 Btu/hr before intolerable temperatures are reached.

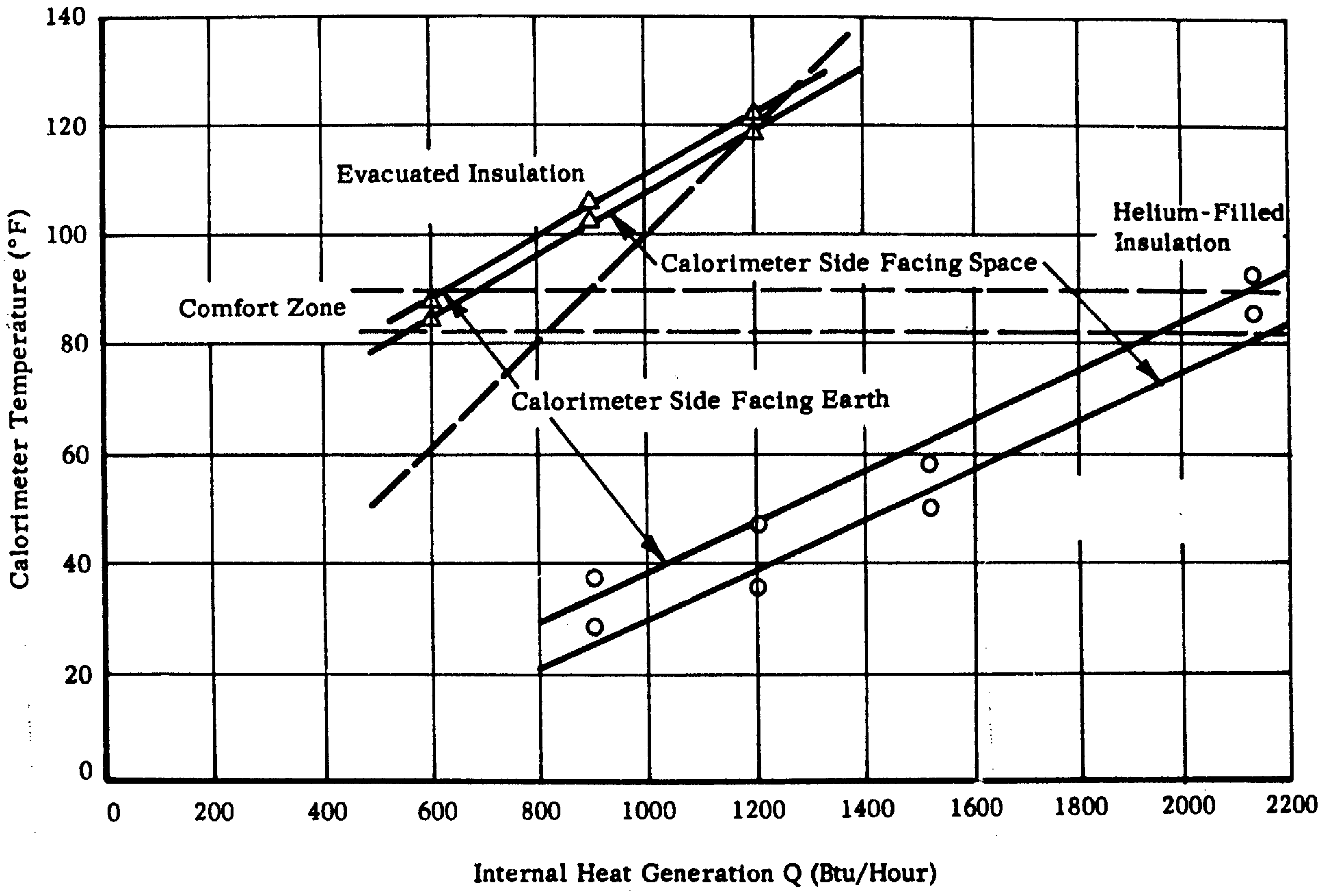

FIGURE 29. CALORIMETER EQUILIBRIUM TEMPERATURES - SPACE SUIT SECTION IN THE EARTH UMBRA

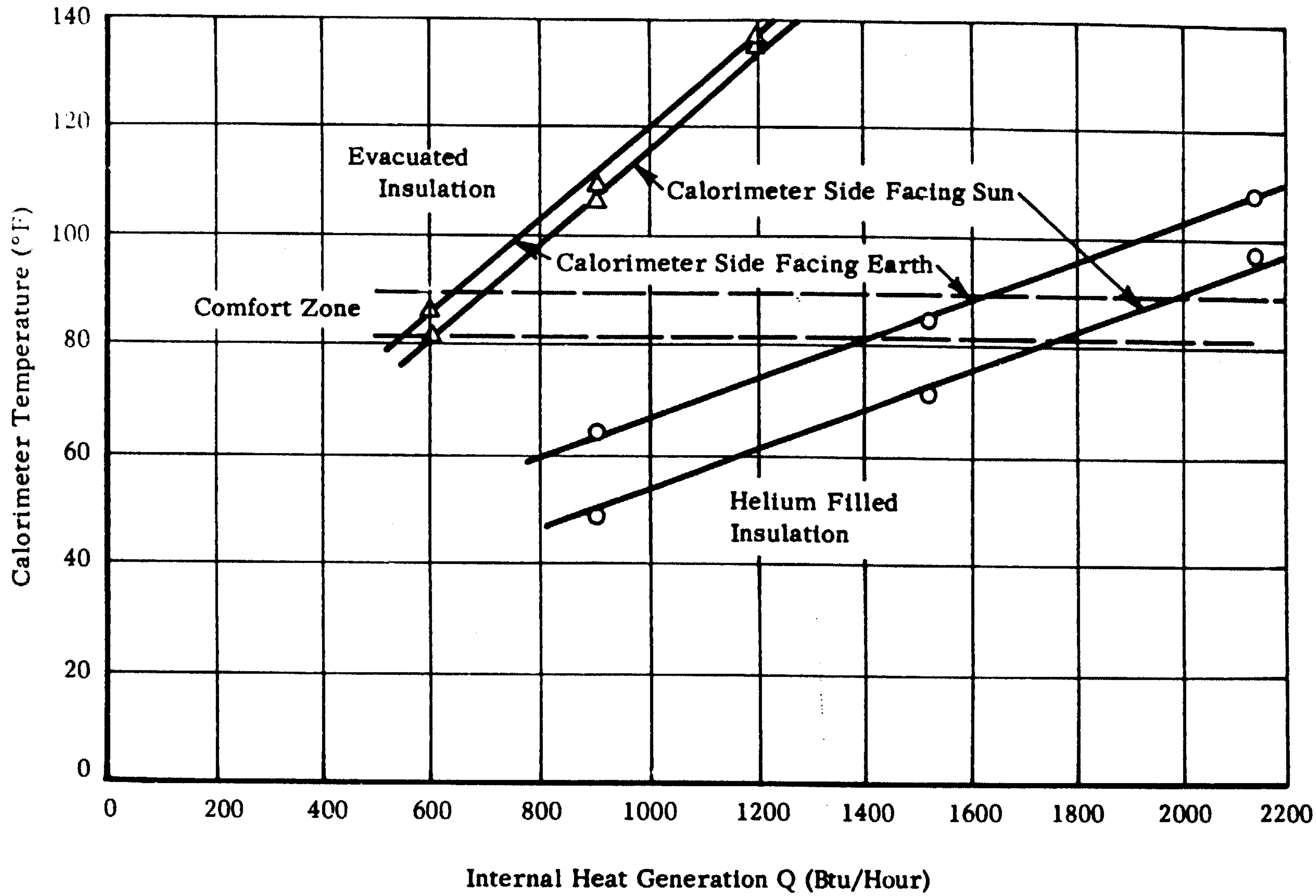

FIGURE 30. CALORIMETER EQUILIBRIUM TEMPERATURES - SPACE SUIT SECTION ON THE EARTH-SUN LINE

There are some discrepancies in the calorimeter equilibrium temperature data indicated on figures 29 and 30. For the space suit section in either orbit, the data for both the helium-fillable and evacuated insulations, when extrapolated to a metabolic rate of zero, should have the same equilibrium temperature for the orbit. Data for the space suit section in the earth umbra (figure 29) do not indicate this equality of temperature while data for the space suit section on the earth-sun line (figure 30) do extrapolate to approximately the same equilibrium temperatures at zero metabolic rate.

The slopes of the temperature curves of figures 29 and 30 are proportional to the conductances of the insulations. Therefore, one might expect that the slopes of the helium-fillable insulation should be the same and should be independent of the orbit the space suit section is in. Likewise, the slopes of the evacuated insulation should be the same. By comparing the slopes of the temperature curves in figures 29 and 30, one can see that for the helium-fillable insulation, the slopes are approximately the same whereas the slopes for the evacuated insulation are different.

On the basis of the slopes of the temperature curves and the extrapolation of the data to zero metabolic rate, it appears that the data for the evacuated insulation for the model in the earth umbra (shown in figure 29) are subject to some uncertainty. On figure 29 is a dashed line which indicates the location of where we think the data should fall. One explanation for this discrepancy is that the evacuated insulation data points were the first taken during the test program and they were initiated shortly after the model was evacuated in the chamber. There is a possibility that some residual gas remained within the insulation which led to a higher conductance and, therefore, caused the slope of the line on figure 29 to be less than is indicated by the dashed line.

However, despite the apparent discrepancy in the evacuated insulation data, the validity of the increase in conductance and the associated increase in the metabolic rate when the insulation is filled with helium still holds.

2. Azimuthal Temperature Distribution

The azimuthal temperature distributions on the inner and outer walls of the space suit section were recorded continuously throughout the whole test program. Summarized on figures 31 through 34 are the temperature distributions for the space suit section for selected equilibrium conditions. These selected equilibrium conditions correspond to the points on figures 29 and 30 where the calorimeter equilibrium curves bisect the comfort zone. Inasmuch as we have no data for azimuthal temperatures where the curves exactly bisect the comfort zone, azimuthal temperature distribution data are reported which are as near as possible to the comfort zone.

Figure 31 shows the temperature distribution for the space suit section

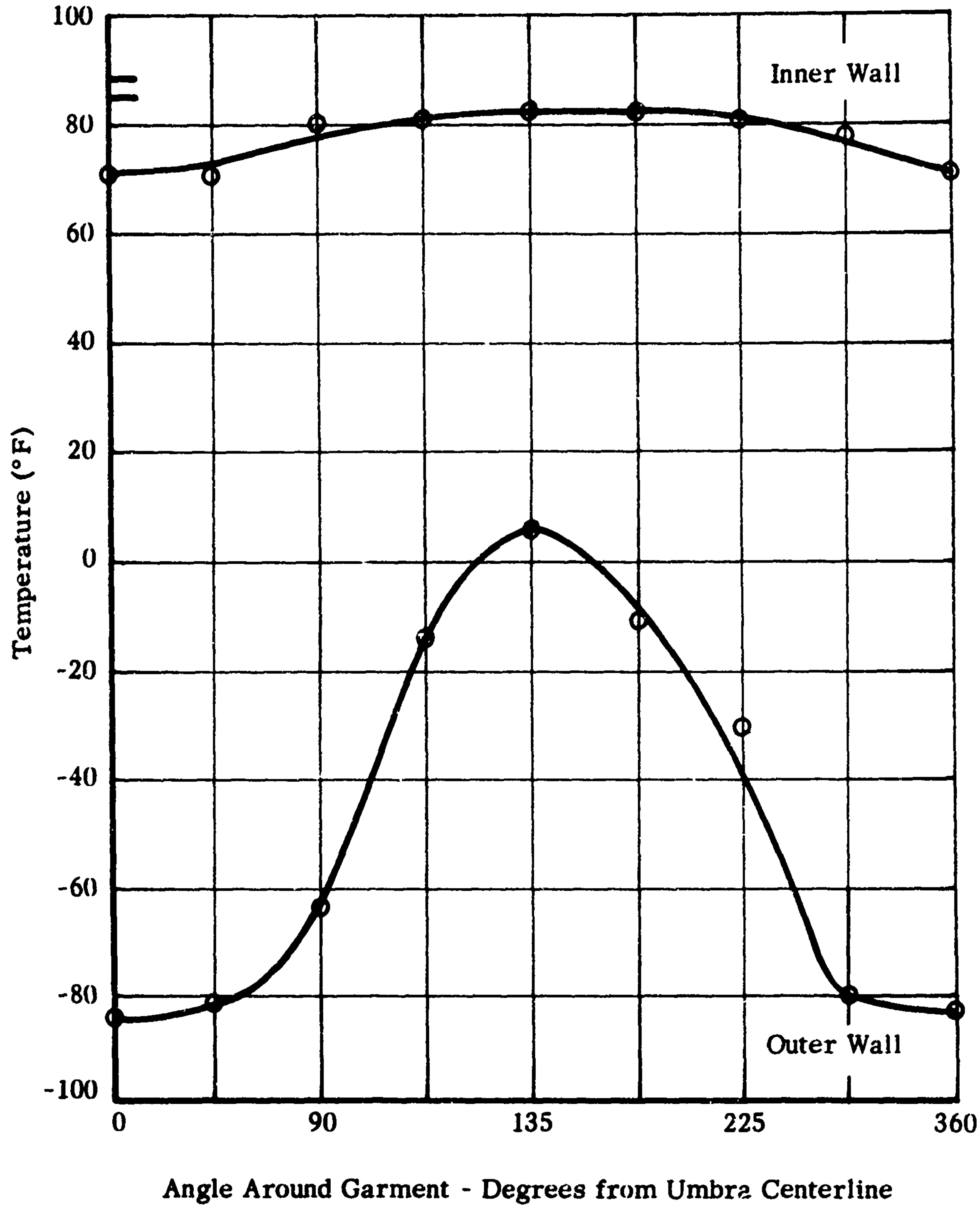

FIGURE 31. AZIMUTHAL TEMPERATURE DISTRIBUTIONS--SPACE SUIT SECTION IN THE EARTH UMBRA, EVACUATED INSULATION--Heating Rate = 600 Btu/Hour, Calorimeter Equilibrium Temperature = 85-88°F

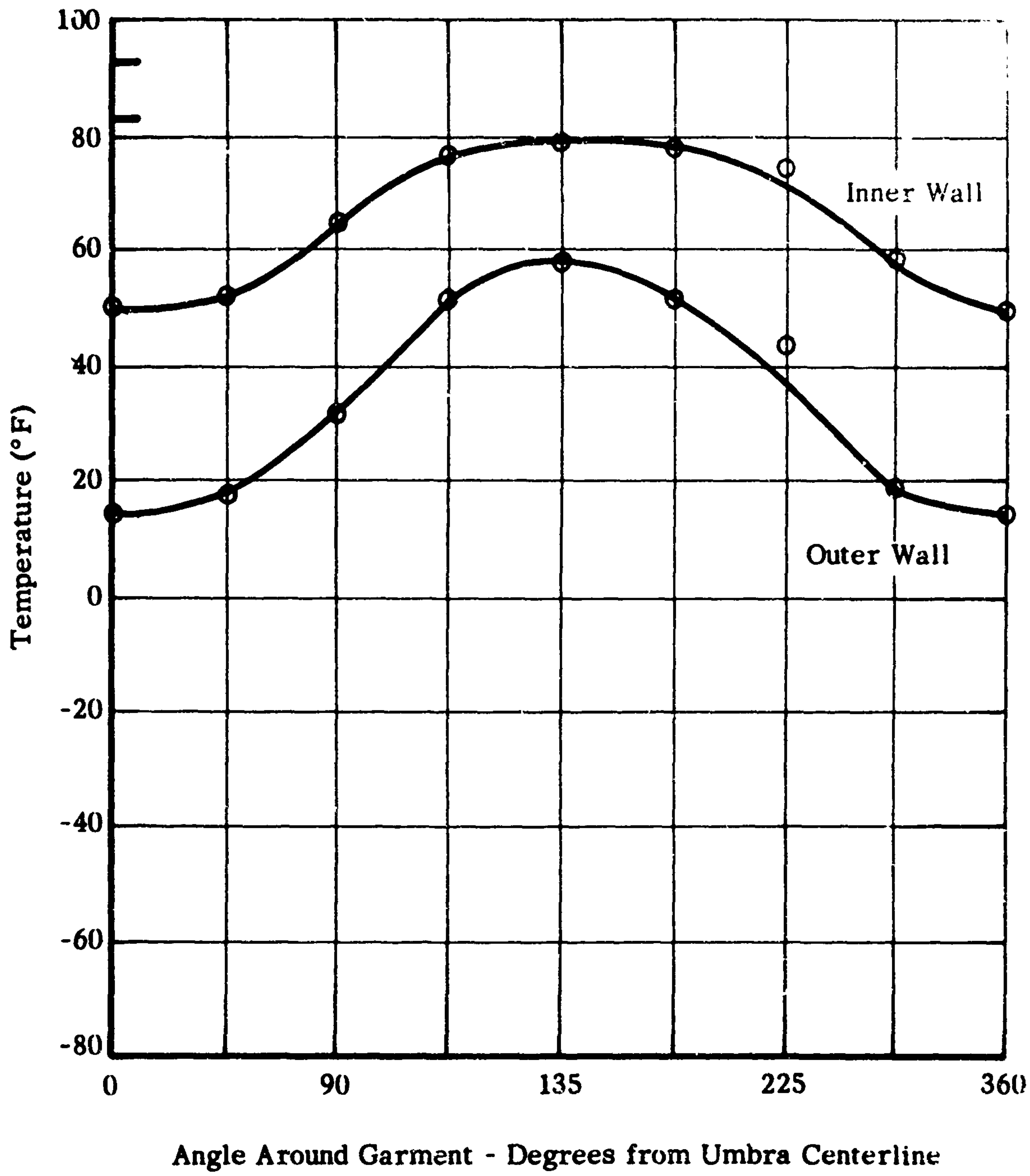

FIGURE 32. AZIMUTHAL TEMPERATURE DISTRIBUTIONS--SPACE SUIT SECTION IN THE EARTH UMBRA, HELIUM-FILLED INSULATION--Heating Rate = 2140 Btu/Hour, Calorimeter Equilibrium Temperature = 83-93°F

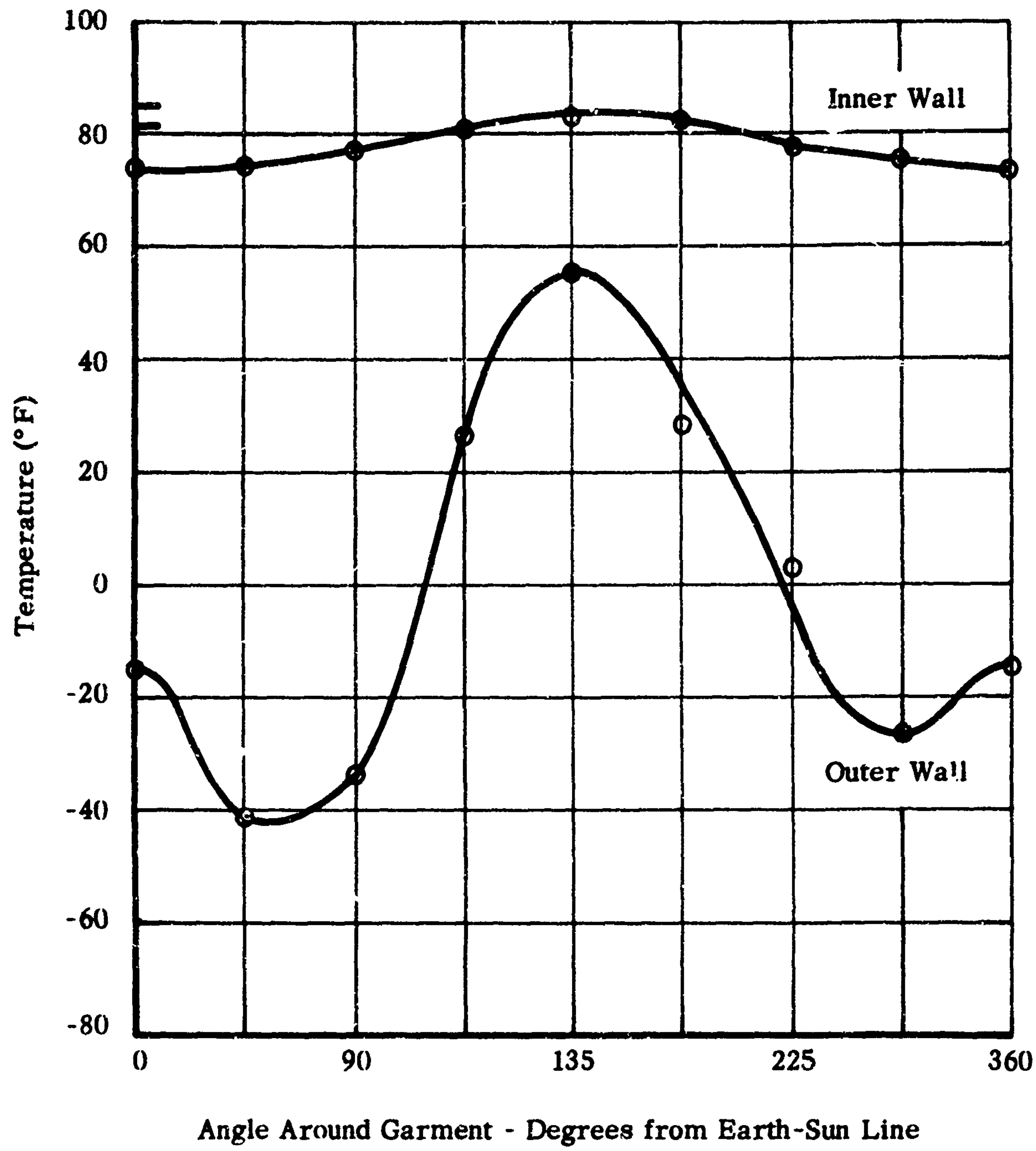

FIGURE 33. AZIMUTHAL TEMPERATURE DISTRIBUTIONS--SPACE SUIT SECTION ON THE EARTH-SUN LINE, EVACUATED INSULATION--Heating Rate = 680 Btu/Hour, Calorimeter Equilibrium Temperature = 81-85°F

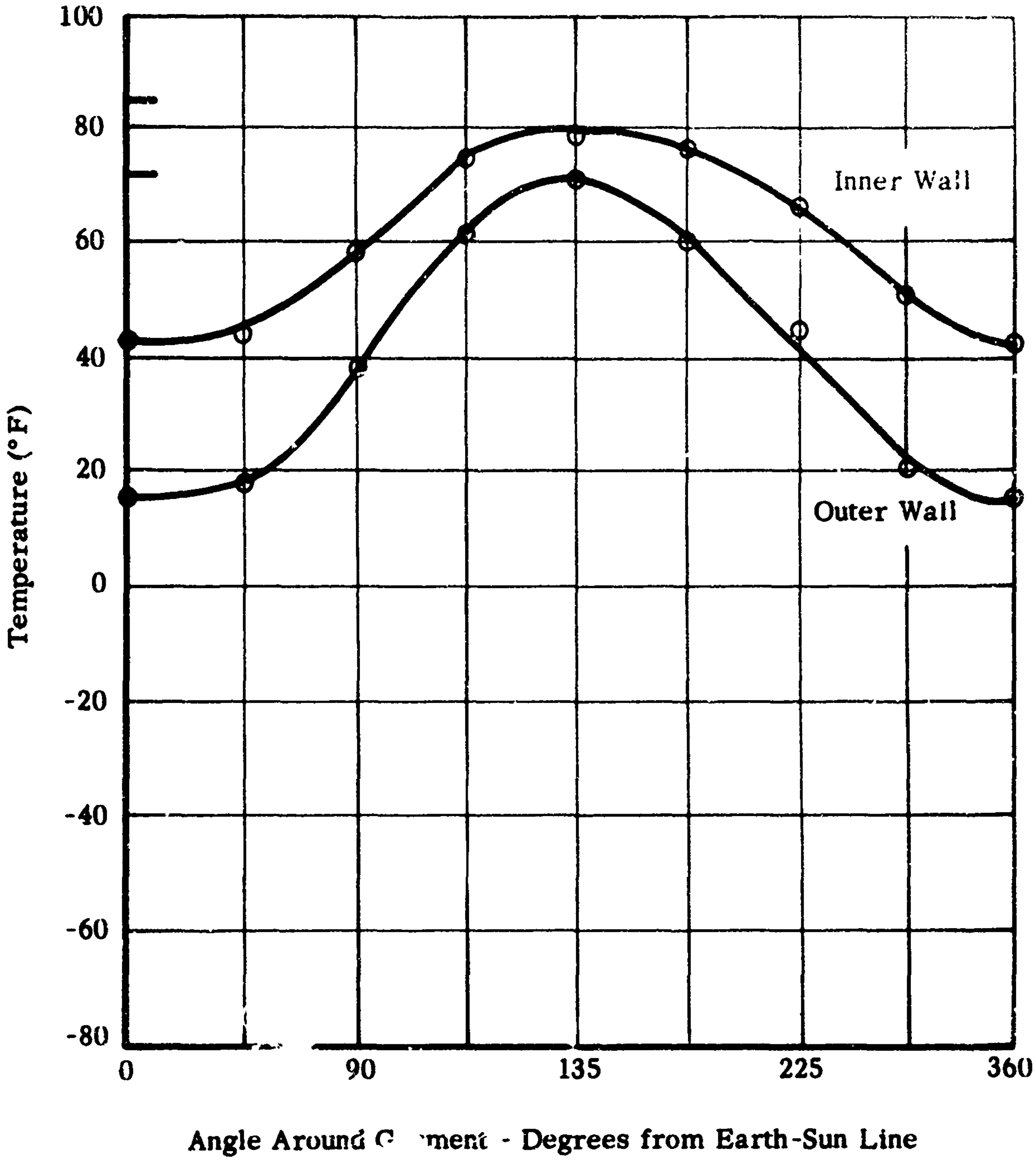

FIGURE 34. AZIMUTHAL TEMPERATURE DISTRIBUTIONS--SPACE SUIT SECTION ON THE EARTH-SUN LINE, HELIUM-FILLED INSULATION--Heating Rate = 1520 Btu/Hour, Calorimeter Equilibrium Temperature = 72-85°F

in the earth umbra and with evacuated insulation. Figure 32 indicates what happens to the temperature distribution around the suit section when helium is introduced into the insulation. Figure 33 shows the azimuthal temperature distribution for the section on the earth-sun line with evacuated insulation, and figure 34 shows the same insulation in the same orbit but with the insulation filled with helium.

The equilibrium temperatures on the exterior surface of the space suit show the general shape of the predicted external temperatures shown in figures 12 and 13. However, any direct comparison between predicted and measured temperature distributions is meaningless because the temperatures measured are subject to a high degree of uncertainty. Although the thermocouple wires were small (0.003 inch diameter), thermal conduction losses along the wires might indicate lower temperatures than were actually achieved on the surface.

3. Effective Range of k/δ

Point by point conductances around the space suit model were calculated by assuming that the heat flux per unit area through the space suit was constant and using the measured temperature differences from figures 31 through 34. Average conductances were then calculated for each insulation under the two orbit conditions. Summarized in table VII are the average conductances for these four conditions. The ratio of conductance for the helium-fillable and the evacuated insulations in both the umbra and on the earth-sun line are also given.

A second over-all conductance was calculated (table VII) which, in addition, accounts for the conductance of the gas layer between the inside of the space suit and the calorimeters. These conductances were calculated from the temperature difference between the outer wall and the inner calorimeter temperature. The ratio of conductance from the helium-fillable to the evacuated insulation is also given in table VII.

TABLE VII

INSULATION CONDUCTANCE DERIVED FROM DATA IN FIGURES 31-34

Orbit Position	Insulation Type	Internal Heat Rate (Btu/hr)	Insulation Average Conductance (Btu/sq ft hr ^{o}F)	Ratio of He Fillable to Evacuated Insulation	Calorimeter-to-Outer-Wall Average Conductance (Btu/sq ft hr ^{o}F)	Ratio of He Fillable to Evacuated Insulation
Earth Umbra	Evacuated	600	0.26	13.8	0.24	8.8
	He Fillable	2140	3.6		2.1	
Earth-Sun Line	Evacuated	600	0.48	9.2	0.45	5.6
	He Fillable	1520	4.4		2.5	

APPENDIX

HEAT BALANCE EQUATIONS AND SOLUTION TECHNIQUES FOR AN ASTRONAUT WITH A SOLAR PARASOL IN EARTH ORBITS

In this analysis we are concerned with (1) the average temperature of the external surface of an astronaut in orbit and (2) the azimuthal temperature distribution on the external surface of an astronaut at selected locations in earth orbits. The heat balance equations are the same for both of these conditions but the method of solution differs. Summarized in this section are derivation of generalized heat balance equations for the astronaut with a solar parasol, the simplification of the equations for the case with no solar parasol, and the methods of solution for average orbit temperatures for temperature distributions for selected orbit positions.

A. ASSUMPTIONS

The following assumptions were made:

1. The internal heat generated by the astronaut is uniformly distributed at the surface of the astronaut.

2. The astronaut is represented by a cylinder which has a length-to-diameter ratio (L/D) of 5.5 and a total area (A_o) of 25.5 ft^2.

3. For the astronaut in selected orbit positions, the lateral conductivity of the space suit is zero.

4. For the average temperature in orbit, the space suit is isothermal.

5. The astronaut and his space suit have negligible heat storage capacity.

6. Reflection at all surfaces is diffuse reflection.

7. Astronaut and parasol are separated sufficiently so that view factor blockage is negligible.

8. Earthshine and albedo reflected by the astronaut onto the parasol is negligible.

9. $\alpha = \epsilon$ for long wavelength radiation corresponding to earth, parasol, and astronaut temperatures.

B. ANALYSIS

The heat balance equations for the astronaut and the solar parasol are based on the scheme shown in figure 35.

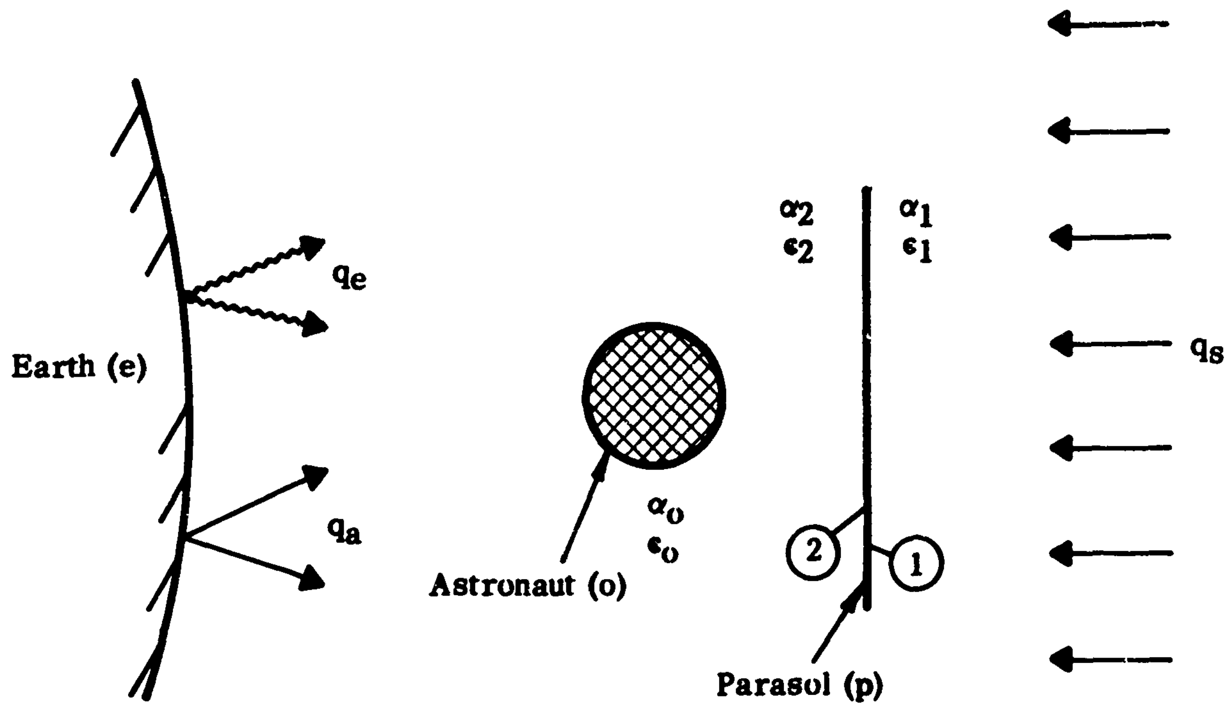

FIGURE 35. ANALYSIS MODEL

Heat Balance on Astronaut (1)

$A_o \epsilon_o \sigma T_o^4 =$ (emitted radiation)

$A_o \epsilon_o \sigma T_o^4 =$	$\alpha_o q_s F_{s-o} A_o$	solar
(emitted radiation)	$\alpha_o q_a F_{a-o} A_o$	albedo
	$\epsilon_o q_e F_{e-o} A_o$	earthshine
	$\epsilon_o \epsilon_2 \sigma T_p^4 F_{p-o} A_p$	direct radiation from parasol
	$\epsilon_o (1-\epsilon_2) q_e F_{e-p_2} F_{p-o} A_p$	earthshine reflected by parasol
	$\alpha_o (1-\alpha_2) q_a F_{a-p_2} F_{p-o} A_p$	albedo reflected by parasol
	$(1-\epsilon_2) \epsilon_o^2 \sigma T_o^4 F_{o-p} F_{p-o} A_p$	space suit seeing itself in the parasol
	Q	internal heat generation

Heat Balance on Parasol (2)

$A_p (\epsilon_1 + \epsilon_2) \sigma T_p^4 =$	$\alpha_1 q_s F_{s-p} A_p$	solar
(emitted radiation)	$(\alpha_1 F_{a-p_1} + \alpha_2 F_{a-p_2}) q_a A_p$	albedo
	$(\epsilon_1 F_{e-p_1} + \epsilon_2 F_{e-p_2}) q_e A_p$	earthshine
	$\epsilon_2 \epsilon_o \sigma T_o^4 F_{o-p} A_o$	direct radiation from astronaut
	$(1-\epsilon_o) \epsilon_2^2 \sigma T_p^4 F_{p-o} F_{o-p} A_o$	parasol seeing itself in the astronaut

For the case with no parasol, equation 1 reduces to

$$\sigma T_o^4 = \frac{Q}{A_o \epsilon_o} + \frac{\alpha_o}{\epsilon_o} (q_s F_{s-o} + q_a F_{a-o}) + q_e F_{e-o} \qquad (3)$$

Solutions for simultaneous equations 1 and 2 or equation 3 requires that the view factors be evaluated for the particular orbit or orbit position. The following constants were used:

$$q_s = 442 \text{ Btu/ft}^2 \text{ hr}$$

$$q_a = 0.4 \times q_s = 177 \text{ Btu/ft}^2 \text{ hr}$$

$$q_e = 66.4 \text{ Btu/ft}^2 \text{ hr}$$

$$A_o = 25.5 \text{ ft}^2$$

$$A_p = 11.1 \text{ ft}^2$$

C. SOLUTION FOR AVERAGE TEMPERATURE OF ASTRONAUT DURING AN ORBIT

The average temperature which an astronaut achieves during an orbit was determined by calculating the average view factor for each geometrical shape and each class of radiant energy from equation 4,

$$\bar{F} = \frac{\sum (F_n)_\theta}{n_{\text{orbit increments}}} \tag{4}$$

and applying these average view factors to equations 1 and 2 or equation 3. View factors for albedo and earthshine for various geometrical shapes in earth orbits are tabulated in reference 19 for orbit increments of 30 degrees. In our analysis we used orbit increments of 30 degrees.

For the cylindrical astronaut, the average view factor accounts for the proportion of radiant energy falling on the cylindrical sides and on the two ends of the astronaut. For cylinder with an L/D = 5.5, the average view factor is given by equati .

$$\bar{F}_{cyl} = \frac{1}{6} (\bar{F}_{sides} + 0.5 \bar{F}_{ends}) \tag{5}$$

D. SOLUTION FOR AVERAGE TEMPERATURE ON THE EXTERNAL SURFACE AT SELECTED ORBIT POSITIONS

In this solution, the view factor for each geometrical shape and each class of radiant energy is determined for the particular orbit position. These view factors are applied to equations 1, 2, and 5 (for the case of an astronaut with a parasol) or to equations 5 and 3 (for the astronaut without a parasol) in order to determine the average temperature.

E. SOLUTION FOR AZIMUTHAL TEMPERATURE DISTRIBUTION ON THE EXTERNAL SURFACE AT SELECTED ORBIT POSITIONS - NO SOLAR PARASOL

In this solution view factors are determined for azimuthally located differential areas on the cylinder in the selected orbit position. These view factors were applied to equation 3 to determine the temperature of each differential area.

REFERENCES

1. J. D. Bowen, X-20A Full-Pressure Suit Quantitative Performance, Technical Documentary Report No. AMRL-TDR-64-36 (AD No. 603701), Aerospace Medical Research Laboratories, Wright-Patterson Air Force Base, Ohio, May 1964.

2. Study of the Thermal Processes for Man-in-Space, Prepared by Airesearch Manufacturing Co. under Contract No. NASw-1015, NASA Contract Report NASA CR-216, National Aeronautics and Space Administration, Washington, D. C., April 1965.

3. I. Streimer, D. P. W. Turner, et al., "An Investigation of the Effects of Pressure Suit Wearing on Work Output Characteristics", Aerospace Medicine, 35, 8, pp 747-751, August 1964.

4. T. F. Irvine and K. R. Cramer, Thermal Analysis of Space Suits in Orbit, Technical Note WADD-TN-60-145, Wright Air Development Division, Wright-Patterson Air Force Base, Ohio, May 1960.

5. H. Friedman, "Sun's Ionizing Radiations" in Physics of the Upper Atmosphere, J. A. Ratcliffe, Editor, Academic Press, New York, N. Y., 1960.

6. R. Jastrow and A. G. W. Cameron, "Space: Highlights of Recent Research", Science, 145, p 1129, 1964.

7. C. E. McIlwain, "The Radiation Belts, Natural and Artificial", Science, 142, p 355, 1963.

8. P. Morrison, "The Origin of Cosmic Rays", in Encyclopedia of Physics, S. Flugge, Editor, XLV/1, 1961.

9. T. Foelsche, "Radiation Doses in Interplanetary Flight", in Advances in the Astronautical Sciences, E. Burgen, Editor, 13, p 90, 1963.

10. P. S. Freier and W. R. Webber, "Exponential Rigidity Spectrum for Solar-Flare Cosmic Rays", J. Geophys. Res., 68, p 1605, 1963.

11. "Aspects of the Meteoroid Hazards", MDW6-63-2, Working Group of the George C. Marshall Space Flight Center, Huntsville, Alabama, April 1963.

12. W. M. Alexander, "The Mission of Mariner II: Preliminary Results, Cosmic Dust", Science, 138, p 1095, 1962.

13. P. E. Glaser, "Thermal Control of Space Vehicles", Aero/Space Engineering, 19, p 52, May 1960.

REFERENCES (cont'd)

14. R. B. Hinckley, et al., "Liquid Propellant Losses during Space Flight", Final Report No. 65008-00-04, Contract No. NASw-615, Arthur D. Little, Inc., Cambridge, Mass., October 1963.

15. P. E. Glaser, "Heat Transfer Mechanisms in Evacuated Powder Insulations", International Developments in Heat Transfer, Part IV, 829, ASME, New York, 1961.

16. G. A. Zerlaut, Y. Harada, and E. H. Tompkins, "Ultraviolet Irradiation in Vacuum of White Spacecraft Coatings", p 391-420, Symposium on Thermal Radiation of Solids, Edited by S. Katzoff, NASA SP-55, ML TDR-64-159, Scientific and Technical Information Division, National Aeronautics and Space Administration, Washington, D. C., 1965.

17. R. L. Olson, L. A. McKellar, and J. V. Stewart, "The Effects of Ultraviolet Radiation on Low α_s/ϵ Surfaces", p 421-432, Symposium on Thermal Radiation of Solids, Edited by S. Katzoff, NASA SP-55, ML TDR-64-159, Scientific and Technical Information Division, National Aeronautics and Space Administration, Washington, D. C., 1965.

18. A. L. Alexander, "Thermal Control in Space Vehicles", Science, 143, p 654, 1964.

19. J. A. Stevenson and J. C. Grafton, Radiation Heat Transfer Analysis for Space Vehicles, ASD Technical Report 61-119, Part I, Aeronautical Systems Division, Wright-Patterson Air Force Base, Ohio, December 1961.

Security Classification

DOCUMENT CONTROL DATA - R&D

(Security classification of title, body of abstract and indexing annotation must be entered when the overall report is classified)

1 ORIGINATING ACTIVITY *(Corporate author)*

Arthur D. Little, Inc.
Acorn Park
Cambridge, Mass. 02140

2a REPORT SECURITY CLASSIFICATION: UNCLASSIFIED

2b GROUP: N/A

3 REPORT TITLE

STUDY AND DEVELOPMENT OF MATERIALS AND TECHNIQUES FOR PASSIVE THERMAL CONTROL OF FLEXIBLE EXTRAVEHICULAR SPACE GARMENTS

4 DESCRIPTIVE NOTES *(Type of report and inclusive dates)*

Final Report, July 1964 - June 1965

5 AUTHOR(S) *(Last name, first name, initial)*

Richardson, David L.

6 REPORT DATE	7a TOTAL NO OF PAGES	7b NO OF REFS
September 1965	82	19

8a CONTRACT OR GRANT NO. AF 33(615)-1904

b PROJECT NO 6373

c Task No. 637302

d

9a ORIGINATOR'S REPORT NUMBER(S)

9b OTHER REPORT NO(S) *(Any other numbers that may be assigned this report)*

AMRL-TR-65-156

10 AVAILABILITY/LIMITATION NOTICES

Qualified requesters may obtain copies of this report from DDC.
Available, for sale to the public, from the Clearinghouse for Federal Scientific and Technical Information, CFSTI (formerly OTS), Sills Bldg, Springfield, Virginia 22151.

11 SUPPLEMENTARY NOTES

12 SPONSORING MILITARY ACTIVITY

Aerospace Medical Research Laboratories, Aerospace Medical Division, Air Force Systems Command, Wright-Patterson AFB, Ohio

13 ABSTRACT

This program encompassed an analytical and experimental investigation of the application of passive thermal control techniques to extravehicular flexible space garments in 300 nautical mile earth orbits. Results indicate that passive thermal control by varying the absorptance and emittance of the outer surface of the garment is not possible when internal heat generated is in excess of 1500 Btu/hr. For all conditions, the suit's solar absorptance should be as small as possible and its emittance as large as possible. By controlling the conductance of the space suit wall, internal heating rates to 2000 Btu/hr are achievable when the space suit has an absorptance of 0.17 and an emittance of 0.85. A solar parasol with selected radiating properties on each side allows for higher internal heating rates. Experiments were made in a simulated noon orbit with a cylindrical section of a space suit which was first tested with an evacuated insulation and then with a helium-fillable insulation. The range of average conductance for these insulations was 0.3 to 4.0 Btu/sq ft hr ^{o}F. A range of internal heat generation from 600 to 2100 Btu/hr was achieved when the evacuated insulation was filled with helium.

DD FORM 1 JAN 64 1473

AF-WP-B-AUG 64 400

Security Classification

14 KEY WORDS	LINK A		LINK B		LINK C	
	ROLE	WT	ROLE	WT	ROLE	WT
Extravehicular Space Garments Passive Thermal Control 300 n.m. Earth Orbit Helium-Filled Insulation Evacuated Insulation						

INSTRUCTIONS

1. ORIGINATING ACTIVITY: Enter the name and address of the contractor, subcontractor, grantee, Department of Defense activity or other organization *(corporate author)* issuing the report.

2a. REPORT SECURITY CLASSIFICATION: Enter the overall security classification of the report. Indicate whether "Restricted Data" is included. Marking is to be in accordance with appropriate security regulations.

2b. GROUP: Automatic downgrading is specified in DoD Directive 5200.10 and Armed Forces Industrial Manual. Enter the group number. Also, when applicable, show that optional markings have been used for Group 3 and Group 4 as authorized.

3. REPORT TITLE: Enter the complete report title in all capital letters. Titles in all cases should be unclassified. If a meaningful title cannot be selected without classification, show title classification in all capitals in parenthesis immediately following the title.

4. DESCRIPTIVE NOTES: If appropriate, enter the type of report, e.g., interim, progress, summary, annual, or final. Give the inclusive dates when a specific reporting period is covered.

5. AUTHOR(S): Enter the name(s) of author(s) as shown on or in the report. Enter last name, first name, middle initial. If military, show rank and branch of service. The name of the principal author is an absolute minimum requirement.

6. REPORT DATE: Enter the date of the report as day, month, year; or month, year. If more than one date appears on the report, use date of publication.

7a. TOTAL NUMBER OF PAGES: The total page count should follow normal pagination procedures, i.e., enter the number of pages containing information.

7b. NUMBER OF REFERENCES: Enter the total number of references cited in the report.

8a. CONTRACT OR GRANT NUMBER: If appropriate, enter the applicable number of the contract or grant under which the report was written.

8b, 8c, & 8d. PROJECT NUMBER: Enter the appropriate military department identification, such as project number, subproject number, system numbers, task number, etc.

9a. ORIGINATOR'S REPORT NUMBER(S): Enter the official report number by which the document will be identified and controlled by the originating activity. This number must be unique to this report.

9b. OTHER REPORT NUMBER(S): If the report has been assigned any other report numbers *(either by the originator or by the sponsor)*, also enter this number(s).

10. AVAILABILITY/LIMITATION NOTICES: Enter any limitations on further dissemination of the report, other than those imposed by security classification, using standard statements such as:

(1) "Qualified requesters may obtain copies of this report from DDC."

(2) "Foreign announcement and dissemination of this report by DDC is not authorized."

(3) "U. S. Government agencies may obtain copies of this report directly from DDC. Other qualified DDC users shall request through ________________."

(4) "U. S. military agencies may obtain copies of this report directly from DDC. Other qualified users shall request through ________________."

(5) "All distribution of this report is controlled. Qualified DDC users shall request through ________________."

If the report has been furnished to the Office of Technical Services, Department of Commerce, for sale to the public, indicate this fact and enter the price, if known.

11. SUPPLEMENTARY NOTES: Use for additional explanatory notes.

12. SPONSORING MILITARY ACTIVITY: Enter the name of the departmental project office or laboratory sponsoring *(paying for)* the research and development. Include address.

13 ABSTRACT: Enter an abstract giving a brief and factual summary of the document indicative of the report, even though it may also appear elsewhere in the body of the technical report. If additional space is required, a continuation sheet shall be attached.

It is highly desirable that the abstract of classified reports be unclassified. Each paragraph of the abstract shall end with an indication of the military security classification of the information in the paragraph, represented as *(TS), (S), (C), or (U)*

There is no limitation on the length of the abstract. However, the suggested length is from 150 to 225 words.

14. KEY WORDS: Key words are technically meaningful terms or short phrases that characterize a report and may be used as index entries for cataloging the report. Key words must be selected so that no security classification is required. Identifiers, such as equipment model designation, trade name, military project code name, geographic location, may be used as key words but will be followed by an indication of technical context. The assignment of links, rules, and weights is optional.